UNIVERSITÀ DEGLI STUDI DI FIRENZE
DIPARTIMENTO DI INGEGNERIA DELL'INFORMAZIONE (DINFO)
CORSO DI DOTTORATO IN INGEGNERIA DELL'INFORMAZIONE

CURRICULUM: ELETTRONICA, ELETTROMAGNETISMO ED ELETTROTECNICA

DEVELOPMENT OF AN ULTRASONIC SYSTEM FOR THE IDENTIFICATION AND AUTHENTICATION OF COPPER CANISTERS FOR SPENT NUCLEAR FUEL

Candidate
Chiara Clementi

Supervisors
Prof. Lorenzo Capineri
Ing. François Littmann
PhD Coordinator
Prof. Fabio Schoen

PhD CYCLE XXXII, 2016-2019

Università degli Studi di Firenze, Dipartimento di Ingegneria dell'Informazione (DINFO).

A Enrica e Gabriele

Acknowledgements

First of all, I would like to sincerely thank my supervisors, Prof. Lorenzo Capineri and Ing. François Littmann, for their encouragement, insightful comments and expertise that greatly assisted my researches. I would like also to show my gratitude to my colleagues of the Seal and Identification Laboratory (SILab) who provided great help during my stay at the JRC. They collaborated on my research, always showing patience, motivation and enthusiasm. I thank also the colleagues of the Ultrasound and Non-Destructive Laboratory (USCNDLab) of the University of Florence, for the useful comments that greatly improved my work. Furthermore, I thank all the friends I met during my stay at the JRC. They shared beautiful moments with me, enriching my lifetime and making me feel at home. Last but not least, I thank my family and my dearest friends in Florence for the unfailing support and continuous encouragement that provided me throughout these years of study, staying always close to me even if far away. This accomplishment would not have been possible without them.
Thank you.

Contents

Chapter 1

Introduction

The final disposal of copper canisters for spent nuclear fuel in long-term geological repositories has introduced the need to develop new safeguards measures and techniques to keep the Continuity of Knowledge (CoK) of the fuel from the encapsulation plant to the final repository. For this purpose, the ultrasonic method has been proposed as an innovative solution for the identification and authentication of copper canisters. This thesis deals with the development of the method by simulations and experimental tests with the aim of providing an ultrasonic acquisition system suitable for the implementation in the field. In this chapter, the objective of the research and the main contributions are illustrated. [1]

[1]This work was supported by the Joint Research Centre (JRC) of the European Commission. The research is the result of a fruitful collaboration between the JRC and the University of Florence.

1.1 Objective

Several countries in Europe are planning to store nuclear spent fuel in long-term geological repositories. In Sweden, the Swedish Nuclear Fuel and Waste Management Co. (SKB) developed a multi-barrier system to preserve the fuel for thousands of years. The spent nuclear fuel will be encapsulated in copper canisters with cast iron inserts and then transported to the geological repository for the final deposition in tunnels, excavated 500 m underground. The analysis of threats and diversion strategies for a geological repository stressed the importance of keeping the Continuity of Knowledge (CoK) of spent fuel during transport from the encapsulation plant to the final repository. As reported in [1], the CoK "refers to the process of using surveillance, containment and monitoring measures to maintain already verified safeguards information by detecting any efforts to alter an item's properties which are relevant to safeguards". In particular, the International Atomic Energy Agency (IAEA) and the European Atomic Energy Community (EURATOM) recommended the use of canister identification to support the CoK, the traceability, of the fuel [2]. Traditional tagging methods could potentially provide a unique identity for each canister but none of them is applicable in practice. For example, the external engraving of the canisters' surface is a simple identification method but may trigger a corrosion process, affecting the long-term integrity of the canister. Therefore, alternative solutions should be developed to cover the lack of suitable techniques. In 2015, the Swedish Radiation Safety Authority (SSM) asked the Joint Research Centre (JRC) of the European Commission for a feasibility study on copper canisters' identification by ultrasound. Therefore, the Seals and Identification Laboratory (SILab) of the JRC in Ispra (VA), in collaboration with the Ultrasound and Non-Destructive Laboratory (USCNDLab) of the University of Florence, has developed a new approach for the identification and authentication of copper canisters: the ultrasonic method.

This thesis reports the development and the experimental validation of the ultrasonic method with the aim of providing an innovative ultrasonic system for the acquisition of identification and authentication fingerprints. The proposed solution not only gives a unique identity to each copper canister (identification fingerprint), but also ensures security against falsification attempts (authentication fingerprint).

The researches carried out in this thesis are the outcome of a multidisciplinary approach, including different domains such as mechanics, electronics, nuclear

security and safeguards. The greater part of the experimental tests reported in this thesis have been carried out at the laboratory of the SILab in Ispra (Italy) and at the SKB's Canister laboratory in Oskarshamn (Sweden).

Following this brief introduction, the manuscript is organized as follows:

- Chapter 2: the Swedish system for final disposal is illustrated and the safeguards approach for a geological repository is discussed. In addition, several technical requirements of a tagging system for copper canisters are reported.

- Chapter 3: traditional tagging techniques are described and compared to verify to what extent each method could be potentially used for the identification and authentication of copper canisters.

- Chapter 4: an introduction on the design and manufacturing of copper canisters is presented, paying particular attention on the Friction Stir Welding process. Mechanical and acoustic properties of canisters are then described in details and results of the optical inspection of the internal gap between lid and tube after welding are reported.

- Chapter 5: the ultrasonic method is illustrated starting from the identification concept. Following preliminary studies on Flat Bottom Holes, a discussion on the design and position of chamfers (notches) to realize unique codes is addressed. In the end, results of the experimental test carried out on a laboratory mock-up with chamfers are reported.

- Chapter 6: the authentication concept is presented and validated by experimental tests at the SKB's Canister Laboratory on real copper lids already welded. Two ultrasonic acquisition system prototypes have been developed for tests and their mechanical and electronic features are illustrated.

- Chapter 7: the angular matching between the identification and authentication fingerprints is detailed and the development and the test of a new ultrasonic acquisition system prototype, based on a single probe and a beam splitter, are

reported. The Seals Fingerprint Acquisition Device (SFAD) is then proposed to optimize the acquisition system for the implementation in the field.

- Chapter 8: conclusive remarks are discussed and new causes of reflection are introduced for the future work.

1.2 Contributions

This research activity has led to several publications in international conferences and journals.

International Journals

1. C. Clementi, F. Littmann, L. Capineri, C. Andersson, U. Ronneteg, "Ultrasonic Identification Methods of Copper Canisters for Final Geological Repository", ESARDA BULLETIN, No. 54, pp 75-81, June 2017.

2. C. Clementi, L. Capineri, F. Littmann, "Innovative Method to Authenticate Copper Canisters Used for Spent Nuclear Fuel Based on the Ultrasonic Investigation of the Friction Stir Weld", IEEE Access, Volume 5, Issue 1, December 2017. DOI: 10.1109/ACCESS.2017.2694878.

3. C. Clementi, F. Littmann, L. Capineri, "Comparison of Tagging Technologies for Safeguards of Copper Canisters for Nuclear Spent Fuel", Sensors- Open Access Journal from MDPI, Volume 18, Issue 4, March 2018. DOI: 10.3390/s18040929.

4. C. Clementi, F. Littmann, L. Capineri, "Ultrasonic Investigation of the Welding Area of Copper Canisters for Spent Nuclear Fuel", ESARDA BULLETIN, No. 56, pp 19-27, June 2018.

5. C. Clementi, L. Capineri, F. Littmann, "Identification of copper canisters for spent nuclear fuel: the ultrasonic method", ESARDA BULLETIN, No. 58, pp 55-62, June 2019.

Submitted

1. C. Clementi, F. Littmann, L. Capineri, “Identification and Authentication of Copper Canisters for Spent Nuclear Fuel by a Portable Ultrasonic System”, IEEE Transactions on Ultrasonics, Ferroelectrics, and Frequency Control", (under minor revision).

International Conferences and Workshops

1. C. Clementi, M. Calzolai, L. Capineri, F. Littmann, “Ultrasonic identification of copper canisters to be used for long term geological repository”, 2016 IEEE International Ultrasonics Symposium, September 2016, Tours, France.

2. F. Littmann, C. Clementi, L. Capineri, “Ultrasonic Identification & Authentication of Copper Canisters”, INMM 59th Annual Meeting, 16-20 July 2017, Indian Wells, California USA.

3. C. Clementi, L. Capineri, F. Littmann, “An Authentication and Identification System of Copper Containers for Spent Nuclear Fuel by means of an Ultrasonic Probe with a Beam Splitter”, 2017 IEEE International Ultrasonics Symposium, 6-9 September 2017, Washington, D.C., USA.

4. C. Clementi, L. Capineri, F. Littmann, “Ultrasonic method to keep the Continuity of Knowledge of spent nuclear fuel from the Encapsulation Plant to the Geological Repository”, IAEA International Conference on the Management of Spent Fuel from Nuclear Power Reactors, 24-28 June 2019, Vienna, Austria.

5. C. Clementi, F. Littmann, L. Capineri, “Development of an Innovative Ultrasonic Reader for the Authentication and Identification of Copper Canisters for Spent Nuclear Fuel”, 2019 IEEE International Ultrasonics Symposium, 6-9 October 2019, Glasgow, Scotland (UK).

Chapter 2

The storage of nuclear spent fuel in geological repositories

This chapter reports the description of the Swedish method for the final disposal of spent nuclear fuel in a long-term geological repository. The integrated safeguards approach for encapsulation plants and geological repositories is reported, focusing on the importance of having robust Containment and Surveillance (C/S) measures to keep the traceability of the fuel during transport. In the last part, the most important requirements for a tagging system for copper canisters are listed.[1]

[1]Part of the work presented in this chapter has been published as "Comparison of Tagging Technologies for Safeguards of Copper Canisters for Nuclear Spent Fuel", in *Sensors - Open Access Journal, Volume 8, Issue 4, 2018* [3].

2.1 The Swedish system for final disposal

The spent nuclear fuel coming from nuclear power plants is still highly radioactive and continues to generate high heat levels for years. Therefore, after removal from the reactor core, the fuel needs to be safely managed in two alternative ways: reprocessing (when the fuel is seen as a potential future energy source) or direct storage. Storage options include nuclear ponds or dry storages. However, the need to keep long-lived radioactive wastes (including spent nuclear fuel) contained and isolated from humans and the environment for a very long time, has led to the idea of a long-term disposal underground. Several countries have already invested many years and resources toward developing a 'multi-barrier' system for the final disposal of spent nuclear fuel in a geological repository [4]. Among them, Sweden is one of the countries in which this process is most advanced. The Swedish Nuclear Fuel and Waste Management Company (SKB) has developed a method called "KBS-3" for the final disposal of the spent nuclear fuel at a depth of about 500 meters underground in the Swedish bedrock. A picture of the geological repository designed by SKB is shown in Figure 1. The final repository will be designed so that it does not require maintenance or supervision.

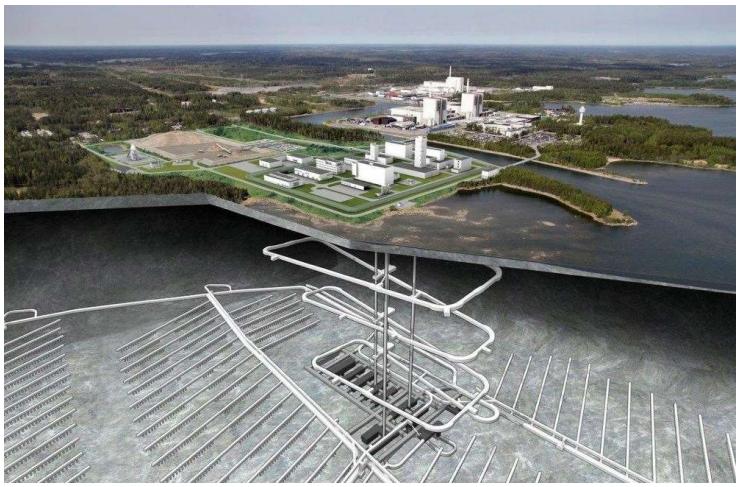

Figure 1 Design of the geological repository proposed for Sweden with its 66 km of tunnels. Source: SKB.

According to the Swedish system (Figure 2), after a storage period at the Central Interim Storage Facility (Clab) in Oskarshamn (Sweden), spent fuel assemblies will be lifted from pools, dried and moved to the encapsulation plant (that will be built

next to the Clab). There, fuel assemblies will be inserted in canisters with an external shell made of copper and an insert of cast iron. After the encapsulation, a copper lid will be welded onto the copper tube by Friction Stir Welding (FSW). After closure, in order to guarantee the canister properties, different inspections will be carried out in accordance with standards and procedures developed by SKB. Inspections consist of Non-destructive Testing (NDT) such as ultrasonic testing, radiography, eddy current testing and visual testing. After the check of the weld, canisters will be shielded by transport casks (KTB) and transported to the geological repository located in Forsmark (Sweden), about 360 km north of the encapsulation plant.

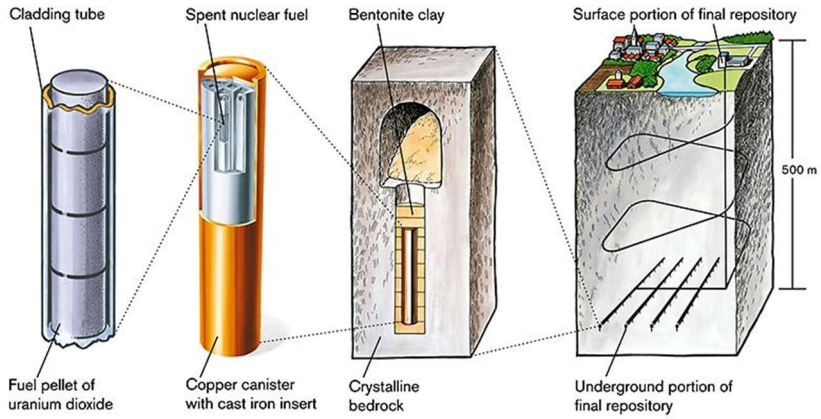

Figure 2 KBS-3 method for final disposal of spent nuclear fuel based on three protective barriers: copper canisters, bentonite clay and the Swedish bedrock. Source: SKB.

A special ship will transfer transport casks containing filled copper canisters from the encapsulation plant to the geological repository (Figure 3). Transport casks will be temporarily stored at surface level in a terminal building before being transferred underground to the Central Area. Copper canisters will be then loaded on a deposition machine and transported to the deposition hole. Once placed in tunnels, canisters will be surrounded by a particular kind of bentonite clay that swells when it comes in contact with groundwater. In this way, copper can endure the anoxic conditions deep inside the bedrock and will not corrode. Around 6,000 canisters will be deposited in the Swedish repository, with an average of one canister per day during roughly 45 years [5]. The long-term storage of spent nuclear fuel in geological repositories has introduced the need to adapt and expand conventional safeguards approaches based on nuclear material accountancy (NMA) and Containment and Surveillance (C/S)

measures, in order to guarantee a high security level throughout all the disposal process [6].

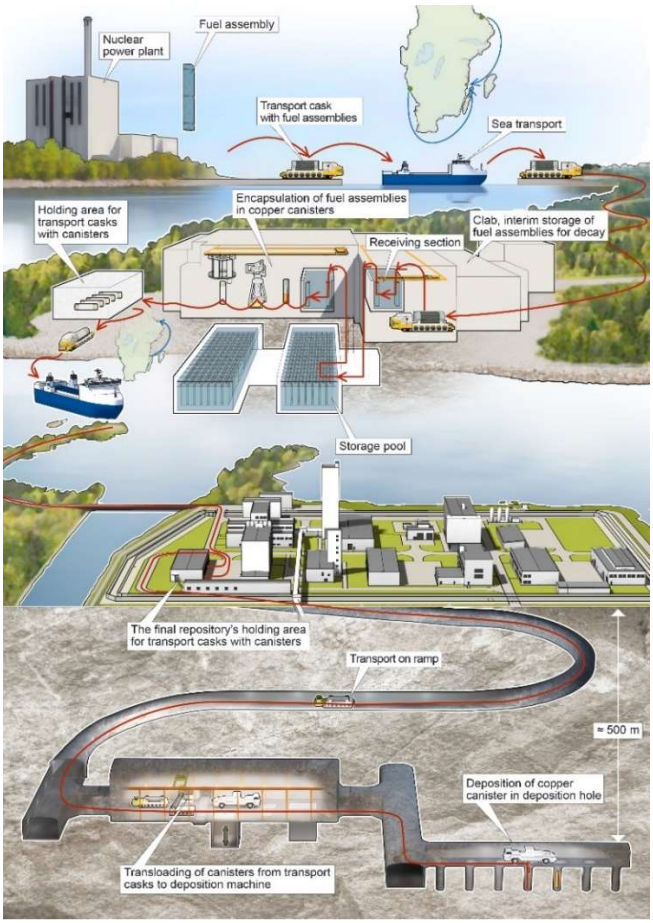

Figure 3 Path of spent nuclear fuel from nuclear power plants to the geological repository, according to the Swedish KBS-3 method for final disposal. Source: SKB.

2.2 Safeguards aspects for a geological repository

The Swedish KBS-3 method for final disposal has introduced new challenges in the safeguards approach. Throughout all the handling process of canisters, Containment and Surveillance (C/S) measures must be implemented in order to maintain the Continuity of Knowledge (CoK) of the fuel. As reported in [7], the CoK is defined as the outcome of 'a system of data or information regarding an item or activity that is uninterrupted and authentic and provides the International Atomic Energy Agency

(IAEA) and the European Atomic Energy Community (EURATOM) with adequate insight to draw conclusions that nuclear material is not being diverted from peaceful purposes'. In this thesis, the Continuity of Knowledge of the fuel will be considered as the traceability of the fuel. The IAEA and the EURATOM recommend the implementation of an integrated safeguards in order to reduce the possibility of traceability losses. The idea of integration can be resumed with the "3S concept" that shows the relationship between Safety, Security and Safeguards [8]. A graphic representation of the 3S concept is illustrated in Figure 4.

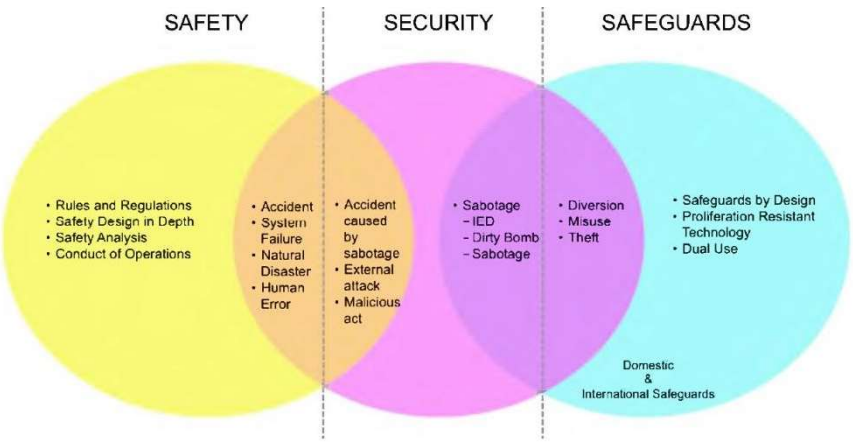

Figure 4 The "3S Concept" for harmonizing Safety, Security and Safeguards. Source: SNL adaptation of graphic by S. DeMuth, Los Alamos National Laboratory (LANL), ASTOR Meeting, Pori, Finland, 2013.

In the case of geological repositories, the difficulty of verification of fuel after final disposal involves the re-design of the safeguards systems with more redundancy, robustness and independence in terms of tampering or failure mode. In fact, once canisters are stored in tunnels, the re-verification of NMA in case of C/S measures failure, is practically impossible. Indeed, deep geological repositories will be unique among nuclear facilities. A geological repository is entirely located underground and then it is never visible in its entirety. Only underground mapping techniques and remote sensing methods (most commonly geophysical methods, including seismic and acoustic monitoring, ground-penetrating radar, etc.) can be used to inspect the repository. Furthermore, unlike other nuclear facilities, the construction of additional emplacement tunnels will continue when emplacement operations will be already started. This makes inspection of a completed facility prior to operation impossible.

Another potential complicating factor is that changes of the design may occur when unanticipated underground conditions (e.g. faults, fractures, etc.) are encountered during construction, involving a change in the design. Such potential variations during construction (and potentially during operations as well), further complicate the ability to verify design information. No other nuclear facility presents such difficulties. The principal safeguards challenges associated with both geological repositories and spent-fuel encapsulation plants include [9]:

- verification of spent fuel at encapsulation plant prior to transport and emplacement;
- assuring that the waste/spent fuel is emplaced as declared;
- assuring that no waste/spent fuel is diverted before or after emplacement, including by excavating a closed and sealed repository;
- detecting such diversion or attempts in a timely manner;
- maintaining the traceability about waste/spent fuel destined for disposal and after disposal;
- verifying repository design information through remote sensing methods and underground mapping, including during concurrent construction and emplacement operations;
- applying effective containment and surveillance (C/S) measures to canisters and to the entire repository (the latter would be accomplished through remote sensing via geophysical methods, aerial and satellite imagery, etc.).

Concerning C/S measures to support the traceability of the fuel, surveillance devices could be used inside facilities to monitor the flow and detect potential undeclared accesses, while tamper-indicating seals could be applied on transport casks to ensure that canisters have not been compromised during transport from the encapsulation plant to the geological repository. However, outside facilities boundaries, copper canisters are more vulnerable to diversion. Therefore, the IAEA and the EURATOM suggested to use a system to provide a unique identity (an identification tag) to each copper canister, in addition to seals on transport casks, as a complementary C/S measure to recover the traceability in case of losses. In contrast to traditional applications in the nuclear field, a tagging system for copper canisters must be designed in compliance with several requirements.

2.2.1 Technical requirements for a tagging system for copper canisters

In general, a tag consists of a pattern that can be used to identify specific items. In the nuclear field, tags must be well shielded against radiations and robust against duplication or counterfeiting. The most important requirements for a copper canister tagging systems are [10]:

1) Large and unique tag memory: the tagging system shall enable fully unique identification of the canister content in a manner consistent with permanent records of the storage or repository.
2) Security against falsification of data, errors/multiple verification: it implies a strong reliability of the tagging system, as well as a strong immunity to falsification or error.
3) Environmental safety: the tagging system shall avoid corrosion effects of canisters which can be induced in the long-term run, thus for instance avoiding leakage of spent fuel components.
4) Non-contact and portable/compact reader system (preferably): each tag shall be readable by a non-contact reader with the aim to preserve the copper canister external surface and above all to protect the reader from the high radiation level of spent fuel.
5) Long operation time: the operating time should be at least to the end of the deposition of the last canister which is estimated to last 45 years.
6) Resistance to harsh environment: the presence of a high radiation level, temperature and humidity could compromise the mode of operation of the tagging system.
7) Cost-effectiveness.
8) Easy implementation and use: the system shall not affect the production chain of copper canisters too much.
9) Minimal human input: the presence of inspectors shall be minimal. The tagging system shall acquire, save and transfer data automatically to inspectors' headquarters.

Traditional tags (engraved, etched, attached, welded) are simple and practical, but may not constitute a unique identifier which could be verified by the IAEA and EURATOM. Moreover, any modification to the outside of the canister may pose a

risk to its long-term integrity and so must be carefully considered [11]. In fact, application of external markings may be restricted if such markings could cause corrosion or otherwise affect the integrity of the canister. Without an external mark, all disposal canisters will be visually identical. Once emplaced and backfilled, canisters will be neither accessible nor visible. Even if recovered from emplacement, these canisters may be largely indistinguishable due to surface corrosion of any distinguishing external markings or other features. Furthermore, a surface treatment often is susceptible to unintentional damage during normal handling, rendering them unusable.

The ability to uniquely identify each copper canisters (identification) is important, but it is also necessary to know that a canister had not been opened and any contents removed or exchanged (authentication). The identification of a canister is the process of clearly distinguishing that canister from the others. The authentication, instead, is the action of proving the originality of a certain canister. In fact, the copper canister external surface is not inherently tamper-indicating and then a tagging system for canisters must be also able to give evidence of counterfeiting or duplication attempts. The most common tagging technologies for nuclear items are described in the next chapter to evaluate to what extent each technique could be used for the identification and authentication of copper canisters.

Chapter 3

Overview on tagging technologies for spent nuclear fuel

A review of conventional tagging technologies in the nuclear field is reported in this chapter. Advantages and disadvantages are illustrated, discussing their relevance for the identification and authentication of copper canisters. [1]

[1]An extended version of this chapter has been published as "Comparison of Tagging Technologies for Safeguards of Copper Canisters for Nuclear Spent Fuel", in *Sensors - Open Access Journal, Volume 8, Issue 4, 2018 [3]*.

3.1 Seals

One of the oldest tagging systems for nuclear waste is the seal [12]. Seals are typically used to provide a unique identity to containers for nuclear items. The integrity of the seal can be verified over time in order to detect potential tampering attempts. The verification of a seal can be implemented with or without removing the seal from the container by checking the identity and integrity. Seals do not provide a physical protection to the sealed item but just give evidence of possible manipulations. Seals can be passive, that do not require any energy source or active, that require power to operate. The most common passive seals are: metal seals, adhesive seals, COBRA seals and ultrasonic seals (Ultrasonic Optical Sealing Bolt (UOSB), Ultrasonic Sealing System Bolt (USSB)).

Metal seals (CAPS) are simple and cheap. The seal consists of two metallic halves (caps), which can be interlocked. The seal is attached by a piece of wire; the ends of the wire are tied inside the seal before closing it. In this way, the loop cannot be opened without cutting (Figure 5). Random scratches and solder smears on the inner surface of the metal cap realize a unique identity. The seal is designed in such a way that any attempt to open it would be detectable. The verification of the seal must be performed at the IAEA and EURATOM's headquarters by comparing the images before installation and after removal.

Figure 5 Metal cap seals.

New developments aim in-situ verification using the laser surface authentication method (to create a unique physical signature on the top and bottom halves of the

metal seal) and the eddy current verification (to verify the wire integrity) [13]. In 2011, the IAEA began the development of a new frangible seal as a replacement for the CAPS seals. It is a two-part glass seal with random coloured patterns throughout the seal body. Upon a tamper attempt, the seal body will break. The intent is that such seals can be verified in-situ for indications of tampering and for authentication.

The adhesive seal is realized with a special material which release evidence of the detachment. For this reason, this kind of seal is intended only for temporary applications and its main advantages is the low price and the low operation, logistics and maintenance train.

The COBRA seal is composed by a fiber-optic loop that is enclosed in a seal and cut in a random way creating unique patterns. After the installation, a reference image of the seal's pattern is recorded. Therefore, during the verification of the seal, it is possible to compare the reference image with the new recorded pattern to detect potential changes [14].

The Ultrasonic Optical Sealing Bolt (UOSB) and Ultrasonic Sealing System Bolt (USSB) are instead stainless-steel seals that involve ultrasound for the detection of a unique fingerprint. The USSB is used primarily for underwater applications, whereas the UOSB is applied on dry storage casks. The USSB is realized by a unique random pattern of metal discs (identity) and a frangible element (integrity) that breaks if the seal is removed from the container (Figure 6). By the ultrasonic reading of the seal, the unique pattern realized by discs and the frangible element can be detected. Patterns recorded during installation are then compared with those obtained during subsequent in situ checks to verify any tampering attempts [15][16].

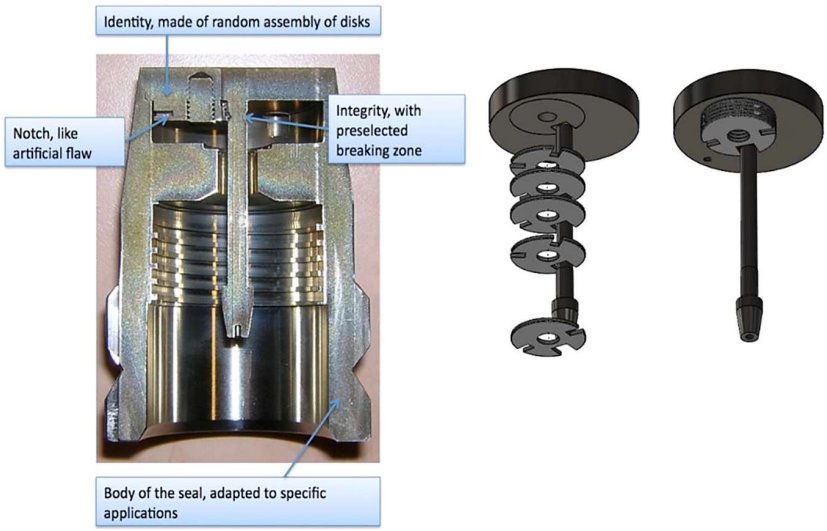

Figure 6 The Ultrasonic Sealing Bolt (USSB) structure composed of an identity and an integrity.

Concerning active sealing systems, the most common used are: the Electronic Optical Sealing System (EOSS), the Remotely Monitored Sealing Array (RMSA) and the Active Optical Loop Seal (AOLS).

The Electronic Optical Sealing System (EOSS) developed by Neumann Elecktronik GmbH is an electronic seal with a fiber-optic loop which provides evidence of opening of the seal once applied on a cask (Figure 7). The reader is realized by a laser source that verifies the integrity of the fiber-optic loop over time. The seal is high reliable and reusable thanks to the "smart" power management system. Moreover, the EOSS can be remotely interrogated and provide information about status, event log, and inspection data [17].

The Remotely Monitored Sealing Array (RMSA) is developed by Mirion Technologies (Canberra) and is used for the identification of a large number of nuclear items. The RMSA is composed by a network of electronic optical seals and a data translator to acquire data from the array. Based upon the Secure Sensor Platform (SSP) technology, the RMSA stores, forwards and communicates data by using a customized data communication protocol over a no-license, low-power radiofrequency link. The data can be stored and transferred remotely and securely (authenticated and encrypted) to the data translator that collects data from all the RMSA seals in a particular location. The seal itself is a reusable device with an expected operative life of four to five years [18].

The Active Optical Loop Seal (AOLS), developed by the Joint Research Centre of the European Commission, is a new type of optical electronic seal that aims to combine the simplicity of a passive seal with the core advantages of electronic seals. It provides a continuous monitoring of the optical fiber wire and simplifies the work of the inspector. The AOLS is the first active seal with an open hardware and software architecture. This allows the inspectorates to more completely assess its security and change functions to meet the wide range of containment requirements [19].

Figure 7 Picture of the EOSS seal connected to the UOSB seal.

Regarding the identification of copper canisters, physical seals cannot be applied if the seal risks compromising the long-term safety performance of the canister, following its emplacement in the repository. Seals could be used as a potential C/S measure for the transport of spent fuel. In fact, seals could be applied on transport casks for copper canisters assuring the traceability of spent fuel during transport and shipment between the encapsulation plant and the repository. In this case, the identification tags on the canisters could be much simpler, since the container seal ensures that the tags could not have been altered.

3.2 Radio Frequency Identification (RFID)

The comprehensive tracking and monitoring of sensitive nuclear materials can be achieved with Radio Frequency Identification (RFID) techniques. These systems not only monitor the condition of the nuclear materials, but also track environmental and physical changes to the packages, sending real-time alerts during storage and transportation. A RFID system generally consists of tags and readers (Figure 8). The tags are attached to the objects to be identified.

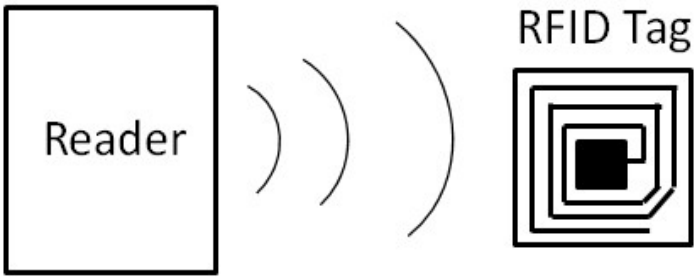

Figure 8 RFID tag and reader.

RFID can be active and passive. Active tags contain a small internal power source to communicate, store and process large amounts of information in the chip. A power source is usually a lithium battery lasting less than 5 years. This makes them unsuitable for use in long-term storages. Passive tags have no battery. In order to provide power and data to the chip, they use the current in the loop antenna which is induced by the interrogating RF signal. Thus, they receive power from the reader's antenna. The reader can be installed inside a truck trailer or storage facility and communicates with the tags through radio waves (UHF, 433.9 MHz, range of transmission up to ≈100 m). When the tag, containing several resonant circuits, enters in the detection zone, the system determines the resonant frequency of each of the resonant circuits and produces a corresponding code. The system tracks the tagged objects and queries their state of health autonomously and continuously [20]. This monitoring system (Figure 9) is then advantageous in terms of streamlined operation, improved record-keeping, enhanced safety, security and safeguards, and cost savings [21]. However, many of the sensitive nuclear materials under surveillance are emitters of neutron and gamma radiation that can impede RFID working correctly.

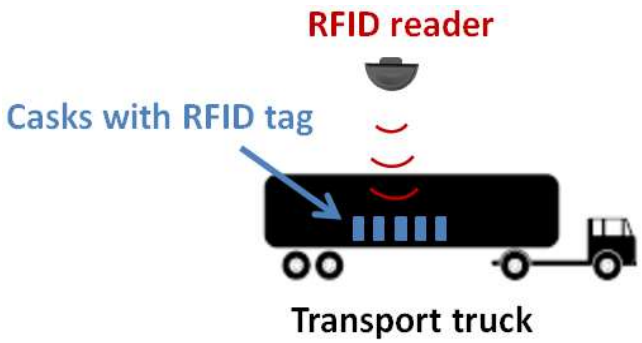

Figure 9 Example of an RFID tracking system.

The implementation of RFID systems for copper canisters identification could be precluded by handling realities. In fact, an exterior affixed tag may be vulnerable to damage during handling. However, a tag on the inside of a canister would not be similarly affected. Consequently, an interior tag would not be as easily subject to intentional tampering. It would have to survive a harsh environment, certainly that from radiation, and would also need to be able to be verified from outside the canister through the thick copper wall (which is not feasible). As a result, RFID tags cannot be used due to copper shielding, but a magnetic-based technology for tagging may be possible.

3.3 Sers-Active Nanoparticle Aggregates

The Surface Enhanced Raman Scattering (SERS) response from SERS-Active Nanoparticle Aggregates (SANAs) provides a unique identifier or signature for tagging applications. SANAs are formed from gold or silver nanoparticles in the 40–80 nm size range. A chemical ‘dye’ is attached to the nanoparticle surface and the nanoparticles are aggregated into ensembles. The dye provides individual identifying information to the aggregate, which is finally coated in a glass layer to provide environmental stability. The completed SANA can be physically embedded in chemically surface-mounted to tag or seal materials. Upon excitation by a laser (Figure 10), a SANA returns a spectroscopic signal unique to the dye, or combination of dyes, absorbed by the SANA metal surface. Depending on the application, the signal can be reduced to a simple barcode, or examined in complex detail to provide a high security signature that is cost prohibitive to replicate.

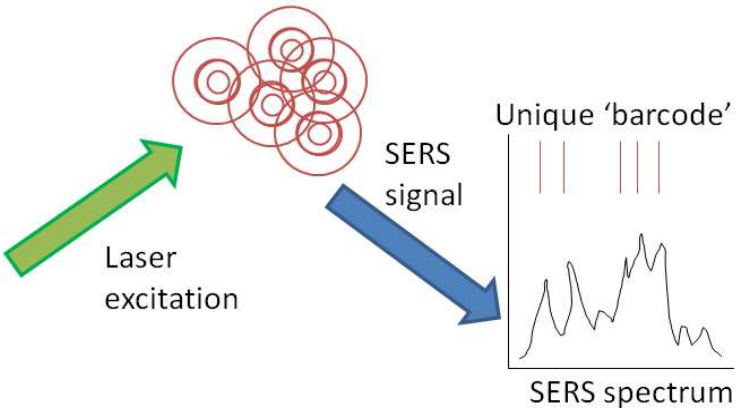

Figure 10 Laser excitation of SANAs to provide a spectroscopic barcode.

SANA-based tags have the fundamental advantages of most passive tagging and sealing technologies. The system is inexpensive due to low material costs for the tags, and shared verification hardware. No on-site power sources or infrastructure is required. In addition, no RF, Wi-Fi, or other networking technologies are required. The SANAs signature can be extensively varied to provide a library of unique tag systems. However, the apparent weakness of this approach is the possibility that the identity of the chemical dye could be determined, leading to the direct preparation of a counterfeit batch of SANAs. Moreover, silver and gold nanoparticles are known to suffer from structural degradation over long periods, or during adverse environmental exposure, then a silica (or glass) coating should be applied to improve the stability of the fingerprint. In order to increase the tag security, SANAs could be integrated with Reflective Particle Tags (RPT) realizing a highly secure, tamper evident and traceable passive tagging system [22] .

The use of SERS-Active Nanoparticle Aggregates for copper canisters identification requires the application of a tag or a seal on the surface of the container. As already discussed for the RFID technology, the presence of an exterior tag could be a problem during handling. However, if the tag only needs to last until final emplacement, then an affixed tag could be used and removed, if necessary, at emplacement.

Moreover, SERS-Active Nanoparticle Aggregates tags cannot be placed inside canisters because the laser used for the reading of the fingerprint cannot penetrate through the 50 mm of copper thickness due to the high attenuation.

3.4 Reflective Particle Tags (RPT)

The Reflective Particle Tag (RPT) is a new generation of tag technology developed with the aim to provide both a unique identifier and visual evidence of tampering. They are resin tags infused with reflective crystals that are placed over sensitive seals. The goal is developing a verification routine based on image processing that verifies the original set of images of an RPT, against a set taken at a later time. Each set contains images taken by illuminating the RPT from several orientations, creating different views due to crystal reflections.

The tag (Figure 11) consists of reflective particles mixed in a transparent adhesive matrix, which is applied to the surface of the item to be identified and then cured. A reader, consisting of a number of lights and some means of recording an image, is used to read the patterns formed by the reflectors in the tag. Comparing images of the tag to images taken when the tag was applied, verifies the identity of the tag and therefore the item [23].

Figure 11 Reflective particles tag on a COBRA seal.

The RPT architecture has proven resistant to counterfeiting and removal without detection. Furthermore, the tag requires no power, and is stable through temperature extremes, rough handling, and years of service.

Concerning the identification of copper canisters, if affixed tags could be used, the reflective particle tag (RPT) may be a possible option. However, locating RPT and SANAs tags inside the canister is not very easy. Furthermore, the reader system suffers from image degeneration and irregular calibrations. Moreover, if the RPT tag

is installed on a seal placed on the surface of a canister, it could trigger a corrosion process, undercutting the long-term stability of the canister structure [24].

3.5 Reflective laser scanning

During transportation and storage of nuclear items, their location and security can be verified by a low power laser scanning system and retro-reflective material used as tags. An identification tag comprises a retroreflective substrate for reflecting incident light beams, and patterned indicia for selectively reducing retro reflectivity of the retroreflective substrate. The unique identity is due to the presence of a non-reflective material on the retroreflective surface of the tag. Tags affixed to the items can be monitored from a fixed observation point by a laser scanning system having a rotating mirror with ultra-precise angular resolution (Figure 12). If a tag is missing or it has moved, the system detects this change.

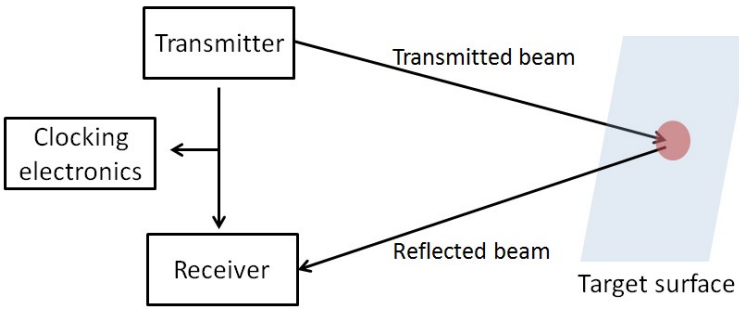

Figure 12 Reflective laser scanning system.

Considering a potential application of this system for the identification of copper canisters, the same set of problems observed for RFID systems can be found. Unlike RFID, this method of information transfer is virtually impossible to intercept or falsify [25]. However, tags could be removed and reattached or even duplicated, without alerting the system. In order to avoid any risks of failure, having redundancy could be effective but also expensive in terms of costs and resources. Moreover, reflective laser scanning is most useful for long-term static storage and not for monitoring during transport of canisters. Indeed, the application of tags on the external surface could be a problem during handling of canisters.

3.6 Tungsten based identifier

The tungsten-based identifier has been specifically developed for the identification of copper canisters for spent nuclear fuel. This method envisages the realization of a series of holes on a tungsten plate, reproducing a unique binary code. The tungsten insert is located inside copper canisters, just underneath the copper lid. The configuration of holes is machined in correspondence of the spent fuel assemblies in order to detect the gamma rays. Because of the strong collimation of gamma rays due to tungsten's high gamma attenuation, the unique code realized on the tungsten plate can be acquired by a gamma rays detector placed above the copper lid. In particular, the change of the gamma-counting rate in the reader gives evidence of the holes' disposition and so giving a unique fingerprint. More than a binary code can be realized on the plate to guarantee redundancy and an ultrasonic transducer can be used to confirm the location of holes on the plate (Figure 13). Depending on the source of gamma rays, this approach can involve passive tags (intrinsic source) or active tags (artificial source). The active tag is realized by α-emitting isotopes with a high energy that create a unique pattern, avoiding non-uniformities of the radiation background.

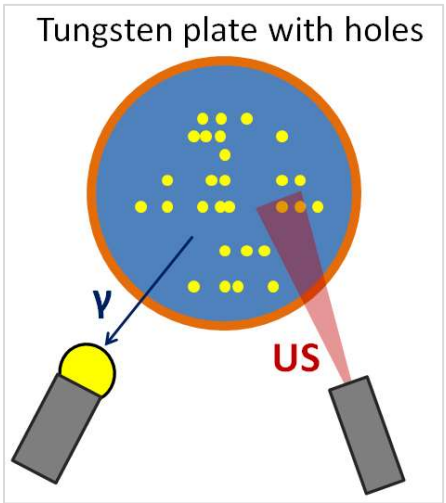

Figure 13 Set-up of the tungsten-based identifier.

Nevertheless, this type of tags is difficult to implement in practice. In fact, the presence of radioisotopes implies the installation of a devoted laboratory at the encapsulation plant and increase the radioactivity level of copper canisters. On the contrary, the implementation of passive tags is more realistic because they need only

the radiation of the spent fuel. This way of identification of the copper cask does not impair the integrity of the cask and it offers a way for the information about the spent nuclear fuel to be read up to a few thousand years. Moreover, differently from the other technologies that involve tags attached on the surface, this method avoids any problems related to canisters handling. Nevertheless, the tag is artificially prepared and then it could be reproduced. The only aspect that can contribute to making this solution secure is the high cost of replication [26][27].

In conclusion, none of the technologies analysed in this chapter can fully meet all the requirements listed in paragraph 2.2.1. In particular, the ability to guarantee security against duplication attempts is the most critical condition to be satisfied. For this purpose, a new method based on ultrasound has been proposed in the coming chapters. The possibility to penetrate copper material by ultrasound allows the recording of particular features, intrinsically contained in the structure of copper canisters. Before presenting the ultrasonic method and the development of a tamper-proof system prototype, it is worth to describe the design and manufacturing process of canisters in order to put in evidence acoustic properties of copper canisters.

Chapter 4

Characterization of copper canisters

In this chapter the geometrical design and the material properties of copper canisters are presented. Then, the description of the manufacturing process is reported, focusing on the Friction Stir Weld (FSW) between the copper lid and tube. Acoustic properties of copper canisters are then investigated, and an optical inspection is accomplished to study the geometry of the internal gap between the lid and the tube, after the FSW process. [1]

[1]Part of the work reported in this chapter has been published as "Innovative Method to Authenticate Copper Canisters Used for Spent Nuclear Fuel Based on the Ultrasonic Investigation of the Friction Stir Weld," in *IEEE Access, Volume 5, 2017 [28].*

4.1 Design and manufacturing

Copper canisters represent the first barrier of the KBS-3 system developed by SKB for the long-term storage of spent nuclear fuel. For the development of a robust tagging system for copper canisters, it is extremely important analysing the geometrical and material properties of the canister, with the aim to identify interesting peculiarities. Each canister is a big cylinder, about 5 m high and 1 m in diameter, composed by a copper shell and a nodular cast iron insert with steel channel tubes for the fuel. The outer shell is composed by a tube, a lid and a base. An exploded view of a canister is illustrated in Figure 14.

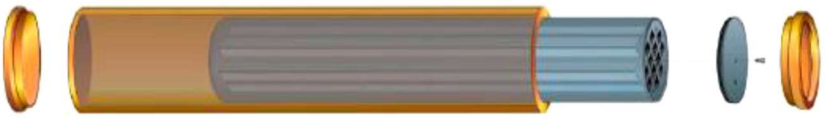

Figure 14 Exploded view of a copper canister for spent nuclear fuel and its components (from the left: copper base, copper tube, insert, steel lid for insert and copper lid).

The dimensions of the copper shell of a canister are illustrated in Figure 15 and detailed in Table 1. All dimensions are specified at a room temperature of 20 °C. The conformity of the reference design to the design premises is analysed in [29]. Copper canisters are designed to provide containment of the spent fuel and prevent the dispersion of radioactive substances over a long period of time. Therefore, a minimal copper thickness of 50 mm, also considering the welds, is imposed [30]. In addition, in order to conform to the design premises regarding the corrosion loads, the copper shell, i.e. tube, lid and base, are made of highly pure copper (> 99.99 %). Concerning the weight of a canister, the maximum total mass, including the fuel, is 24,700 kg for BWR (Boiling Water Reactor) and 26,800 kg for PWR (Pressurized Light-Water Moderated and Cooled Reactor).

Figure 15 Copper tube, lid and base dimensions specified at room temperature, 20 °C.

Table 1 Dimensions of the copper tube, lid and base of a canister with tolerances.

Dimension designation	Copper shell	Nominal value (mm)	Tolerance (mm)
A	Total length	4,835	+3.25/-2.75
B	Outer diameter	1,050	+1.2/-1.2
C	Inner diameter	850	+0.8/-0.8
T	Wall thickness	49	+0.3/-0.3
	Weld thickness*	48.5	+0.7/-0.7
E	Inner diameter	952	+0.5/-0.5
F	Inner diameter	821	+0/-0.5
G	Inner diameter	850	+0.8/-0.8
H	Diameter, lid	953	d8
H	Diameter, tube	953	H8
I	Corner radius	10	-
K	Dimension	35	+0.5/-0.5
L	Dimension	50	+0.2/-0.2
M	Thickness, lid	50	+0.6/-0.6
N	FSW position, top	60	-
P	Dimension	75	+0.3/-0.3
Q	Thickness, base	50	+1/-1
R	FSW position, base	50	-

*The weld thickness differs from the wall thickness since the copper tube surfaces that connect to the lid and the base respectively are further machined.

The geometry of canisters presents very small tolerances because the manufacturing process is very accurate. The production of a canister includes several steps:

- casting of insert in nodular cast iron,
- casting of copper ingot,
- extrusion of copper tube,
- forging of copper lid and base,
- welding by means of Friction Stir Welding (FSW),
- machining,
- final inspections.

The inserts are manufactured from nodular cast iron. The form of the graphite in the nodular cast iron has a major impact on the qualities of the material; this is controlled

through the addition of small quantities of certain substances to the molten metal. The steel lids for the inserts are manufactured from steel plate. The steel tube cassette is manufactured with 12 channels for BWR assemblies or 4 channels for PWR assemblies (Figure 16). The channels are formed with the aid of square-profiled steel tubes, which are welded together to form a cassette. The verification of the straightness of the channel tubes is one of the most important aspects at this stage of the manufacturing, in order to ensure the correct insertion of fuel assemblies.

Figure 16 Part of the machined insert with the notches between the fuel channels and a steel lid (on the left) and a steel tube cassette for hosting fuel assemblies (on the right).

Regarding the copper shell of canisters, SKB has chosen the extrusion method as the reference method for the hot forming of copper tubes. The production of large ingots is normally carried out by means of semi-continuous casting, which creates a cylindrical and solid ingot (Figure 17).

Figure 17 Large copper ingot for the production of a copper tube.

The copper lid/base is also manufactured by continuous casting: the ingot is heated up to a desired temperature and then forged in several different steps by a press until it forms the final lid. After the blank has cooled, it is machined with a simplified geometry suitable for ultrasonic testing.

In the end, the copper lid and base are welded onto the copper tube by Friction Stir Welding (FSW). The weld is performed by a rotating tool, which consists of a probe and shoulder, which is forced down into the joint to be welded and moved along the joint around the entire circumference of the canister. A more detailed description of FSW is reported in the next paragraph.

4.2 The Friction Stir Welding process

Copper welding is usually difficult by conventional fusion welding processes because the copper has a high thermal diffusivity, which is about 10 to 100 times higher than many steel and nickel alloys. The heat input required is much higher than almost any other material, and weld speeds are quite low. To overcome these problems, the FSW is applied to the joining of copper. FSW is a type of friction welding that was invented in 1991 at the Welding Institute in Cambridge, England [31]. FSW is a thermo-mechanical solid-state process, i.e. not a fusion welding method. This means that problems encountered in fusion welding (such as

unfavourable grain structure, grain growth and segregation phenomena) can be avoided. The welding machine at the SKB's Canister Laboratory is designed for welding in air (Figure 18). However, to investigate the effect on the welding process and the weld zone properties, welds in Argon gas have been produced using a provisional gas chamber.

Figure 18 Welding machine at the SKB's Canister Laboratory. Source: SKB.

Before the welding begins, an inspection is made to ensure that the joint surfaces of the base and the tube are not damaged in any way and they are cleaned to reduce the probability of defects and impurities in the weld. The FSW process is used to weld both the lid and the base onto the copper tube. The welding cycle can be divided into several sequences which can be seen in the following Figure 19. At the beginning of the weld, a rotating tool is plunged 75 mm above the weld line between the pieces to be welded (1). When the temperature of the tool has reached a specific level, the welding speed is accelerated to a constant value (2). After the acceleration sequence has been completed and the temperature of the tool has reached the required equilibrium temperature and has become stable, the tool is moved down to the joint line (3). Here, joint line welding is carried out. After a complete rotation (4), the tool is 75 mm moved up where the welding cycle is completed (5) [32]. Both the acceleration sequence and the exit hole are then machined away when the lid is given to its final dimensions.

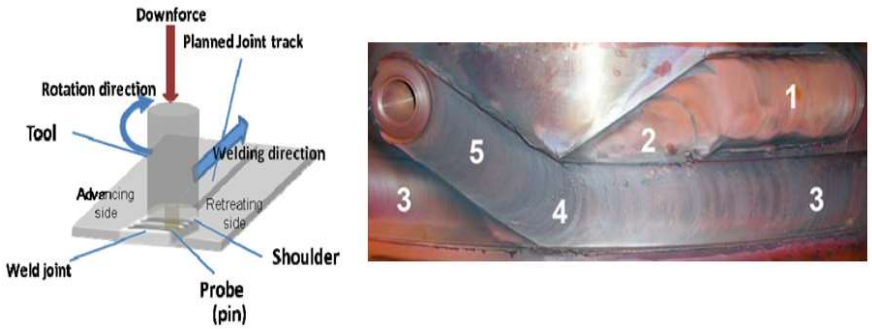

Figure 19 Welding tool rotation and sequences in the welding cycle: (1) acceleration sequence, (2) downward sequence, (3) joint line welding, (4) overlap sequence and (5) parking sequence.

The quality of the weld depends on different factors such as the depth of the shoulder in the metal, the tool temperature, the torque of the spindle motor and the force on the tool in the direction of travel. These parameters should be set with a good precision to reproduce the same welding cycle for each copper canister. In order to guarantee the canister properties and verify the quality of the weld, different inspections are carried out in accordance with established standards developed by SKB. Different Non-Destructive Testing (NDT) methods are employed among which the radiographic examination and the ultrasonic inspection [33][34].

During the FSW process, a copper canister results perfectly welded along the line of welding but beneath it, an air gap between the lid and the tube occurs (Figure 20).

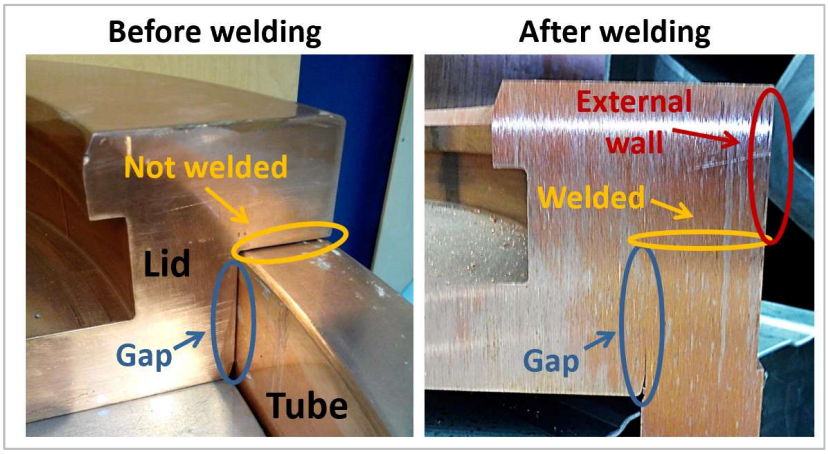

Figure 20 Section view of the lid and the tube before FSW (on the left) and after (on the right); in both cases the internal gap between lid and tube occurs.

According to [35], tolerances for canisters machining should avoid the presence of any excess air gap; in reality, in order to allow the installation of the lid on the tube before welding, a small gap of about 0.3-0.6 mm exists between the two welded components. This gap has a crucial role in the ultrasonic method for the identification and authentication of copper canisters. In fact, the gap represents a discontinuity in the material detectable by ultrasound. Because of the heat produced by the rotation of the shoulder, this gap can be partially filled by copper and then the height of the gap is strictly related to the welding process. Therefore, in order to study the geometry of the gap, an optical inspection is accomplished by a digital microscope.

4.2.1 Optical inspection of the internal gap

In order to analyse the geometry of the internal gap between copper lid and tube, after the FSW process, an optical testing is carried out using a digital microscope. The internal gap of two copper flanges, i.e. slices of a copper lid already welded onto a tube, is investigated. The set-up of measurements is illustrated in Figure 21.

Figure 21 Set-up of measurements for optical inspection by a digital microscope.

The tiny gap between the lid and the canister is barely visible to the naked eye; however, the microscopic inspection could clearly show the microstructure of the interface region in the friction welded joint. Several pictures are acquired by the digital

microscope moving the camera along the entire height of the gap on both flanges (Figure 22).

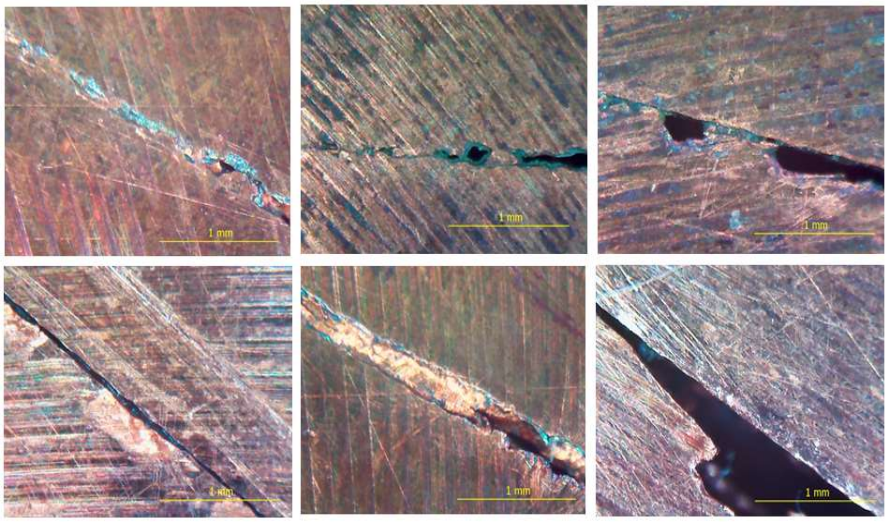

Figure 22 Pictures of the internal gap interface in copper flanges, acquired by the digital microscope.

Observing the images, it is possible to appreciate the presence of air between the lid and the tube. Depending on the side of the flange investigated, the gap appears more or less indented. Moreover, the height of the gap can change depending on how copper grains aggregate during the FSW process.

4.3 Mechanical and acoustic properties of copper canisters

Copper has been selected for a combination of factors, among which good heat transfer and stress handling properties, chemical and corrosion resistance, and stability in pure water. A copper canister, in fact, should withstand corrosion and mechanical loads that could occur in the geological repository. In particular, the copper material used for the production of canisters shall guarantee an elongation >40%, a creep ductility >15%, and an average grain size <800 μm. For this purpose, phosphorus, sulphur and hydrogen are added, in different percentages, to highly pure copper. Regarding the properties that affect the canisters pressure bearing capacity, the canister should withstand an isostatic load of 45 MPa, being the sum of maximum

swelling pressure and maximum groundwater pressure. Indeed, the copper corrosion barrier should remain intact after a 50 mm shear movement at a velocity of 1 m/s for buffer material properties of a 2,050 kg/m3 Ca-bentonite, for all locations and angles of the shearing fracture in the deposition hole, and for temperatures down to 0°C. As reported in the paragraph 4.1, since canisters are designed to provide enough containment of the fuel, the minimal copper thickness of the shell should be 50 mm (considering also the welds). In particular, the design tolerances imposed are 49±0.3 mm for the tube, 50±0.6 mm for the lid and 48.5±0.7 mm for the welds. The microstructure of copper canisters is related to the forging process of copper components. Furthermore, the copper grain size can vary in the weld zone between copper lid and tube. Results of the metallographic examination of the welding area put in evidence that the copper grain size in the welding area is lower than 350 µm in average and can vary from 200 µm to 60 µm on varying of the weld [36]. Among the NDT performed at the end of the FSW process, the inspection by ultrasound is used to verify the presence of defects in the weld (Figure 23).

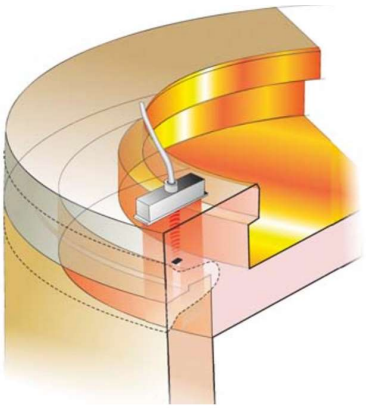

Figure 23 Non-destructive testing of the FSW from the top of the lid using a phase array probe. Source: SKB.

As shown in the picture, the ultrasonic inspection is performed using a phased array located on the top of the welded lid. To ensure that the entire volume is inspected, the ultrasonic testing is carried out before the final machining of the copper canister. Some of the possible defects detectable by ultrasound are joint line hooking and wormholes (Figure 24). The first can occur in the internal part of the weld due to the bending of the vertical joint between the tube and the lid during welding. The detectability of this type of defect is very good with ultrasound, while it cannot be detected by

radiography. The wormholes, instead, can occur in the outer part of the weld as a consequence of welding variables outside the process window. The detectability of this type of defect is good with ultrasound but it can only be detected by radiography in the extreme case when it forms a volumetric defect.

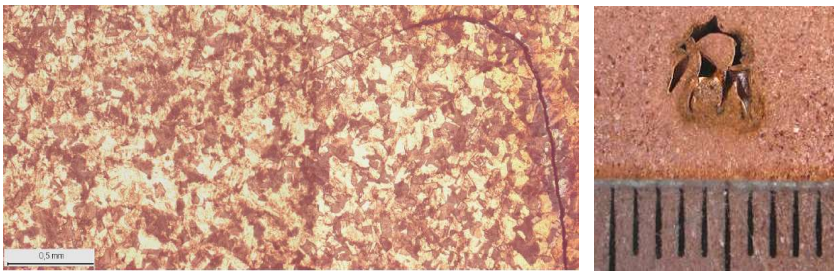

Figure 24 Example of a joint line hooking (on the left) and of a volumetric wormhole (on the right).

The ultrasonic investigation of the welding area allows also the evaluation of copper canisters' acoustic properties. In particular, the velocity of sound in copper canisters is approximately 4660 m/s for longitudinal waves and 2260 m/s for shear waves. The attenuation of sound, instead, can vary depending on the inspection frequency and the copper inner structure: according to [37], the attenuation in copper can vary from 50 to 200 dB/m at 5 MHz, depending on the grain size.

The definition of the speed of sound and the sound attenuation in copper canisters is extremely important for the selection of the most suitable transducer to include in the ultrasonic system for the identification and authentication of copper canisters.

Chapter 5

The Ultrasonic Method: Identification concept

A brief introduction on the ultrasonic method for the identification and authentication of copper canisters is given at the beginning of this chapter. Then, the identification concept is described in detail reporting preliminary studies carried out in laboratory and simulations for the definition of unique configurations of chamfers detectable by ultrasound. In the end, the experimental validation of this approach on a laboratory mock-up is illustrated. [1]

[1]Part of the work reported in this chapter has been published as "Ultrasonic Identification Methods of Copper Canisters for Final Geological Repository" in *ESARDA bulletin, Issue 54, June 2017 [38].*

5.1 Preliminary studies

The ultrasonic method is an innovative approach developed to provide a reliable and robust solution for the identification and authentication of copper canisters. In contrast to conventional tagging systems analysed in chapter 3, this method can not only identify uniquely each container thanks to a code of chamfers realized on the copper lid, but also can verify the authenticity of a canister by the acquisition of a natural fingerprint, strictly related to its material properties and the welding process.

The identification concept is based on the acquisition of the ultrasonic amplitude response of unique configurations of chamfers (notches), artificially realized on the inner surface of copper lids before welding. The ultrasonic beam is reflected whenever encounter a discontinuity in the material. The presence of chamfers introduces a change in the lid geometry, detectable by ultrasound. Originally, instead of chamfers, Flat Bottom Holes (FBHs) were to be drilled on the inner surface of the copper lid in an area where the copper thickness is higher than 50 mm, that is the minimal thickness according to the geometrical design (Figure 25).

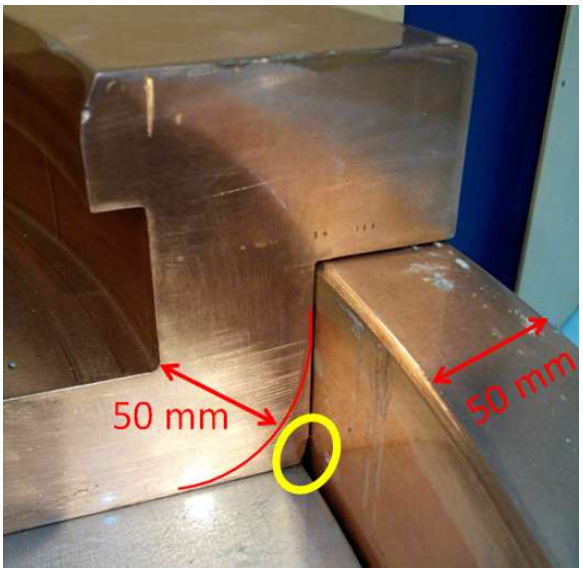

Figure 25 Area (yellow circle) where the thickness of the lid is higher than 50 mm and where a geometry modification can be realized without significantly affecting the copper.

Indeed, the dimension of FBHs should be defined as small as possible to avoid problems related to the integrity of the canister structure. In Figure 26 are reported

two sketches of a copper flange (i.e. a slice of a copper lid already welded onto a tube) created by SolidWorks CAD, where a potential configuration of FBHs is illustrated.

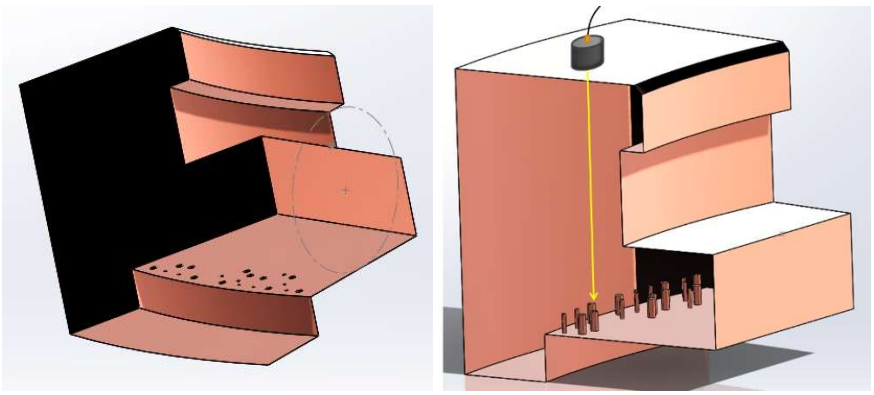

Figure 26 Drawing of FBHs arranged in the area where the copper thickness is higher than 50 mm.

The ultrasonic amplitude response can be acquired by a contact transducer placed on the top of the flange, at a distance from holes of about 135 mm. Depending on the dimensions (diameter and height) of holes, the inspection frequency of the transducer can be different. For example, in the case of inspection of a configuration of FBHs with diameter of 2 mm, 4 mm, and 6 mm, a 10 MHz transducer can guarantee a suitable axial and lateral resolution for the discrimination of each hole [39]. However, because of the anisotropy of copper, whose microstructure changes depending on the investigated portion, the attenuation of ultrasound in a copper canister could be not negligible. Therefore, the selection of the transducer should be realized in order to find a trade-off between resolution and signal to noise ratio.

In order to decrease the effect of the attenuation without loss of resolution, FBHs have been replaced by chamfers, i.e. cuts of the lid edges. As illustrated in Figure 27, chamfers can be arranged all around the lid circumference to create a code, different for each canister.

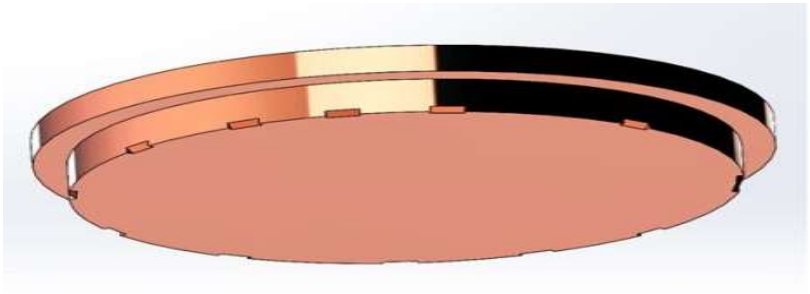

Figure 27 Drawing of chamfers arranged around the copper lid circumference.

As for FBHs, chamfers must be located where copper thickness is more than the minimal thickness "Tmin" of 50 mm. As a consequence, for the acquisition of ultrasonic echoes reflected by chamfers, the probe must be relocated in a different position (Figure 28). In particular, the probe must be kept inclined at fixed height "h", according to Snell's law.

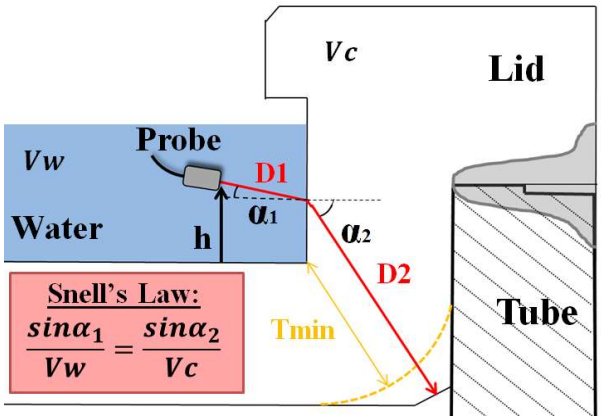

Figure 28 Ultrasonic immersion testing of chamfers. The inclination α_1° of the transducer is chosen in accordance with the slope α_2° of the chamfer, as reported by the Snell's law where Vw is the velocity of sound in water (about 1481 m/s at 20 °C) and Vc is the velocity of sound in copper (4660 m/s).

In this way, the travel path of the ultrasonic beam is reduced and the attenuation too. In addition, the possibility to perform an immersion testing, using water as a couplant, makes the automatic displacement of the probe easier. The ultrasonic amplitude response acquired by a 360° rotation of the transducer around the lid, can represent an identification fingerprint for each canister (Figure 29). This response can be recorded considering the maximum amplitude within a certain time window (programmable

gate): whenever a chamfer is encountered, the amplitude of the echo increases; vice versa, when the chamfer is not present, the amplitude of the echo decreases.

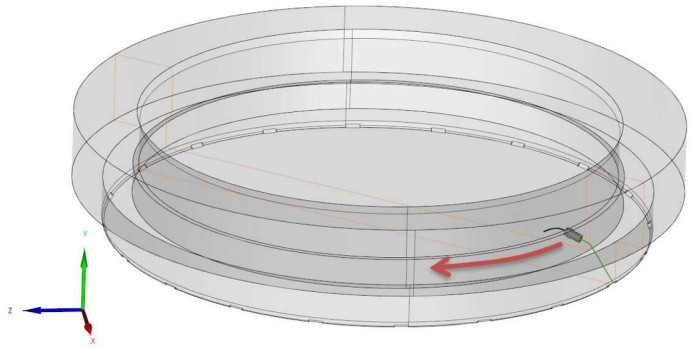

Figure 29 By the rotation of a transducer kept at a fixed height, the unique code realized by chamfers can be detected.

For the definition of the time gate, it is important to calculate the expected time of flight (TOF) of chamfers' echoes following the equation (1). In particular, V_W and V_C are the speed of sound in water (about 1481 m/s at 20 °C) and in copper (4660 m/s) respectively, whereas D_1 and D_2 represent the water path and the geometrical distance between the centre of a chamfer and the impact point of the ultrasonic beam at the boundary between water and copper.

$$TOF = \left[\frac{2 \cdot D1}{Vw}\right] + \left[\frac{2 \cdot D2}{Vc}\right] \quad (1)$$

The identification concept has been validated in the laboratory by performing experimental tests on copper samples.

5.2 Experimental testing in the laboratory

Several static experimental tests have been carried out on copper flanges provided by SKB to our laboratory, to select a suitable ultrasonic probe for the acquisition of the chamfers' response. As already discussed for FBHs, the selection of the transducer is strictly related to the type of discontinuity/defect to be detected. Since the beginning, the use of a phased array probe was discarded for the elevated complexity of the electronics and the high cost of production. According to requirements listed in paragraph 2.2.1, in fact, the tagging system for copper canisters must be cost-effective

and easy to use and implement. Therefore, only single transducers have been considered for the development of the ultrasonic identification system. However, instead of a single probe, a phased array can investigate a wider area and the focus can be adjusted at different depths depending on the surface to investigate.

Following preliminary inspections carried out on copper flanges [40], the identification concept has been validated on a laboratory mock-up with the same morphology of a full-scale lid, except that the diameter, has been ¼ scaled (Figure 30). A configuration of chamfers 50° inclined, 12 mm wide and with 22.5° of angular extension have been machined on the bottom surface of the lid. Cavities have been also included in the design of the mock-up in order to facilitate manufacture in the laboratory. However, in the real case only chamfers are considered for the realization of a unique pattern around the copper lid.

Figure 30 Mock-up of the copper lid with a ¼ scaled diameter but the same thickness of a full-scale lid (on the left). View of the bottom surface of the mock-up where chamfers and cavities are realized.

The ultrasonic testing has been accomplished by an immersion transducer placed 14° inclined in order to receive the signal reflected by chamfers according to the Snell's law. The probe used for the inspection was the Olympus V311 immersion transducer characterized by:

- central frequency: 10 MHz;
- element diameter: 0.5'' (13 mm);
- -6dB bandwidth: 73.36 %;
- spherical focus: 8.4'' (213.36 mm) in water.

The probe was rotated around the sample circumference by a 24 V synchronous motor and the transmission/reception of signals to/from the probe was regulated by an US-Key module (Lecouer Electronique) [41]. The main features of the US-KEY are:

- USB2 High Speed connection;
- ultralow noise preamplifier: 0.74 nV/√Hz;
- - 6 dB bandwidth: 540 kHz to 18 MHz;
- high voltage transmitting pulses (up to 230 V);
- PRF 100 Hz to 20 kHz;
- MTBF 100000 hours;
- digitizer 12 bits at 80 MSPS;
- programmable gain: 0 to 80 dB;

The block diagram of the US-Key is shown in Figure 31. For the inspection of chamfers on the laboratory mock-up, the US-Key was set to the following parameters: 200 V of transmitter voltage, 1 kHz of P.R.F. and 30 dB of receiver gain. The Lecoeur data acquisition software is used to set measurements parameters and display acquired signals.

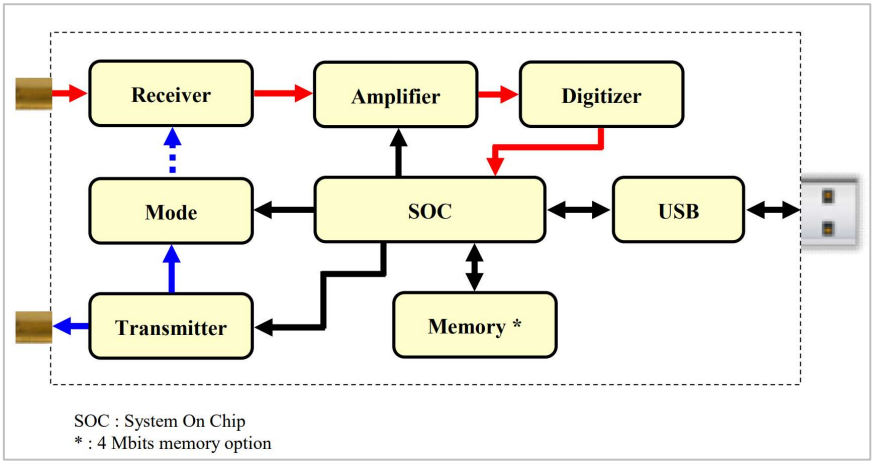

Figure 31 Block diagram of the US-Key module by Lecoeur Electronique.

The ultrasonic reading of chamfers was realized by immersion testing and then a bit of water was poured inside the mock-up before the testing. The set-up of inspection

and the signal acquired by a 360° rotation of the transducer are reported in Figure 32. The amplitude and Time Of Flight (TOF) signals of the maximum peak within a certain time window (gate) are recorded. The uncertainties of measure are about 1.9% for the amplitude and 0.05 μs for the TOF. The gate was set around 62 μs, that is where the echo of chamfers was expected following equation (1) where D1 is 20 mm and D2 about 84 mm.

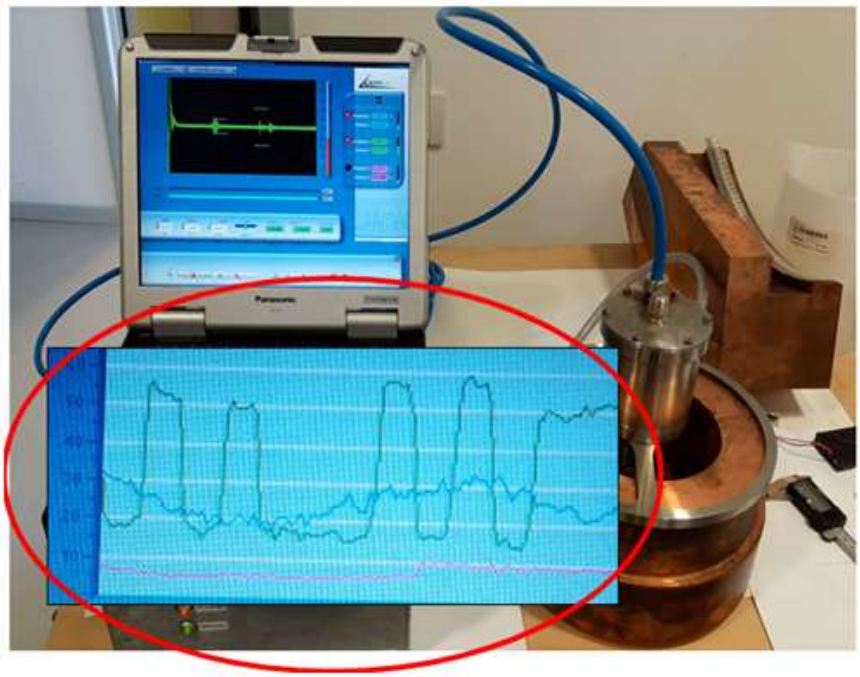

Figure 32 Set-up of measurements for the ultrasonic testing on the laboratory mock-up. In the red circle, the ultrasonic amplitude response of the configuration of chamfers.

As a result, the amplitude response presented several peaks strictly linked to the chamfers' position. The TOF response was also affected by the presence of chamfers, however the variation of the TOF is not as pronounced as the amplitude and it was not considered for the definition of an identification fingerprint. At the end of the acquisition, water was pumped back. This preliminary test on a copper mock-up suggested the possibility to acquire an ultrasonic response from chamfers, rotating an inclined transducer during immersion testing. In particular, the amplitude response of chamfers can represent an identification fingerprint, unique for each canister. Further studies on the identification concept are reported in chapter 7.3. In the real case,

chamfers could be manufactured during the production process of copper lids, before the FSW of the canister. Then, the ultrasonic amplitude response of chamfers could be recorded as a reference fingerprint by ultrasonic testing at the encapsulation plant. In this way, in case of necessity or lack of traceability, the identification fingerprint could be acquired again at the geological repository and compared with the reference to verify if there is correspondence or not. However, the machining of chamfers around the copper lid circumference will introduce an additional step in the manufacturing process of canisters and further research should be accomplished to verify that chamfers do not affect the canister's long-term structure. For this purpose, it is also extremely important to study the best chamfer dimension and layout around the copper lid.

5.3 Design of chamfers

The use of unique configurations of chamfers on copper lids could solve the identification issue for copper canisters. Chamfers should be designed to maximize the ultrasonic beam reflection once investigated by an inclined transducer. Depending on the chamfers slope, the probe orientation must be adjusted in order to keep always the perpendicularity between the chamfer's surface and the transducer. The width of chamfers must be selected in order to not affect the copper too much (the minimum copper thickness must be always 50 mm) and increase the signal to noise ratio during ultrasonic testing (20 dB at least). Moreover, the definition of the angular disposition of chamfers around the lid circumference is important to optimize the identification code. The last part of this paragraph, indeed, is focused on the definition of mechanical tolerances for the positioning of the ultrasonic probe and the study of the temperature influence in the ultrasonic testing.

5.3.1 Width, slope and arrangement

The study of the best chamfer dimensions is carried out by simulations with Extende CIVA software. CIVA is a multiple-expertise software platform for Non-destructive testing (NDT) and comprises different modules among which the Ultrasonic Testing (UT) module [42].

Inspection simulations are implemented on a copper sample with different chamfers having the same inclination of 50° and a different width of 5 mm, 10 mm, 15 mm and 20 mm respectively (Figure 33).

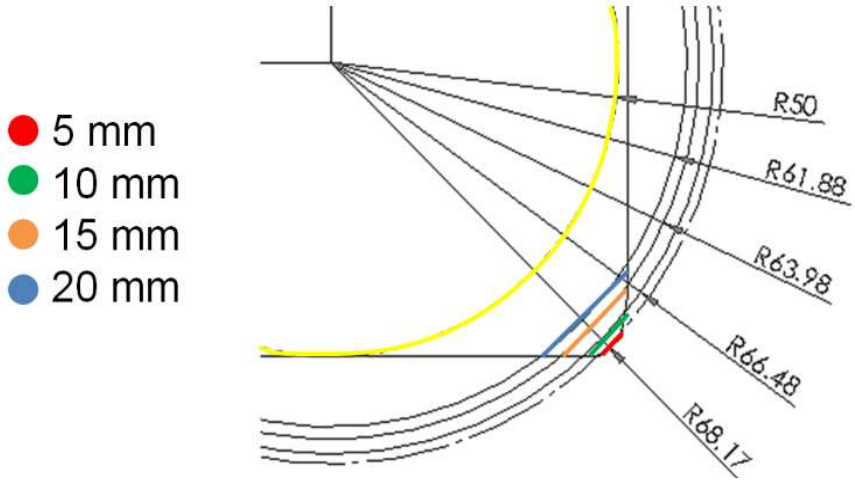

Figure 33 Chamfers geometries used for CIVA simulations.

All the chamfers do not exceed the limit of 50 mm of minimal copper thickness represented by the yellow arc in the picture. Simulations are performed considering an immersion transducer with the same features of the Olympus V311, described in the previous paragraph 5.2. A water path of 20 mm is imposed and the attenuation of ultrasound in copper is neglected. The beam computation of the simulated probe is illustrated in Figure 34. The probe is kept at a fixed height of 18 mm, 14.55° inclined considering the speed of sound in water of about 1500 m/s and in copper of 4660 m/s.

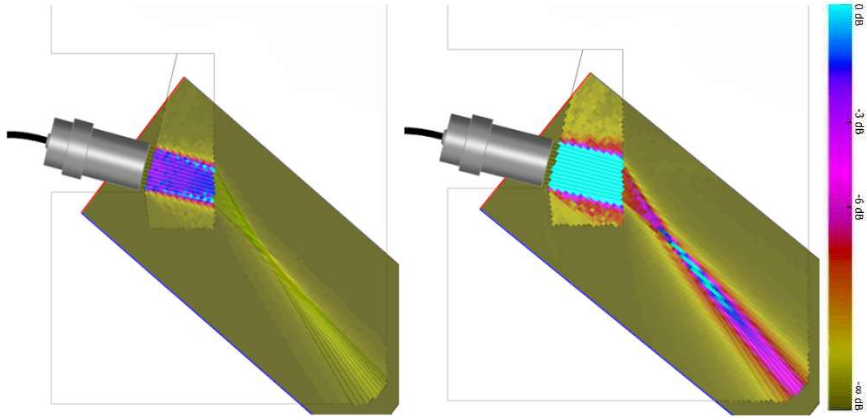

Figure 34 Beam computation of the Olympus V311 immersion probe. On the left, the default beam with 0 dB of dynamic; on the right, the post processed beam with 15 dB of dynamic (gain increased). Sky blue stands for the highest intensity, yellow for the lowest.

As a result of inspection simulations, the chamfer 10 mm wide seems to be the best compromise between the need of having a good ultrasonic echo and not changing the canister geometry too much. In fact, the area to be removed in case of chamfers 10 mm wide is about 20 mm^2, as shown in Figure 35.

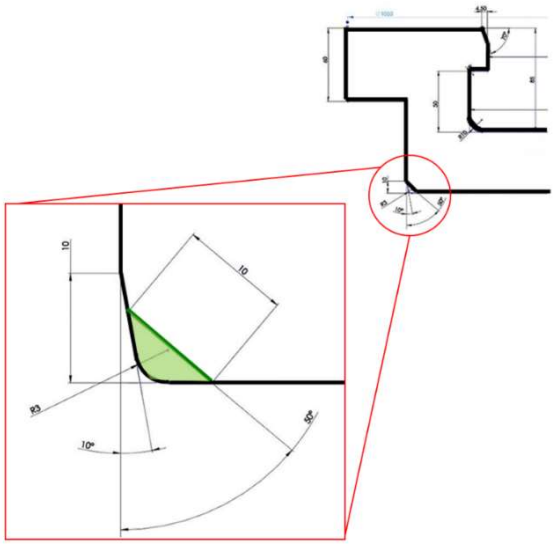

Figure 35 Section view of a copper lid with a zoom showing the area (in green) to be removed in case of machining of chamfers 10 mm wide and 50° inclination.

The disposition of chamfers around the lid circumference is another relevant aspect in the definition of the identification fingerprint for copper canisters. The first designed code was a binary code made of chamfers 6º wide plus a reference chamfer 12º wide (Figure 36). The latter is important to have a reference during the reconstruction of the binary code. This solution would ensure a different unique code for more than 6000 canisters using a maximum number of 14 chamfers, including the reference. This means removing only 130 g of copper out of 708 kg of an entire lid.

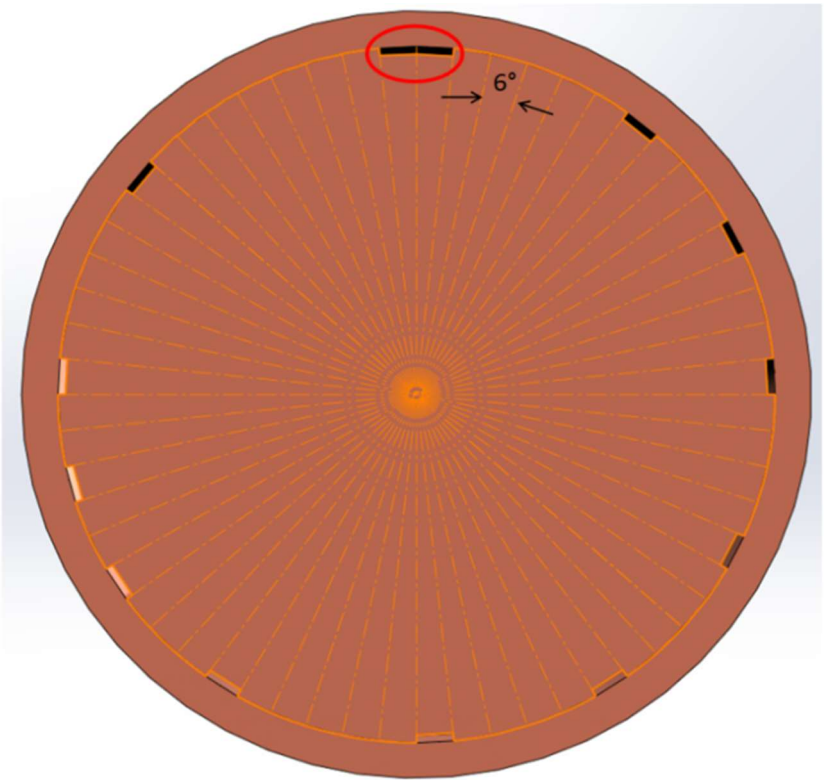

Figure 36 Example of chamfer disposition for the realization of a binary code with chamfers 6° wide and a reference chamfers of 12° (highlighted in red).

The ultrasonic investigation of this type of configuration will generate an ideal amplitude response similar to the one illustrated in Figure 37. The maximum value of amplitude "1" will be just in correspondence of a chamfer, "0" elsewhere.

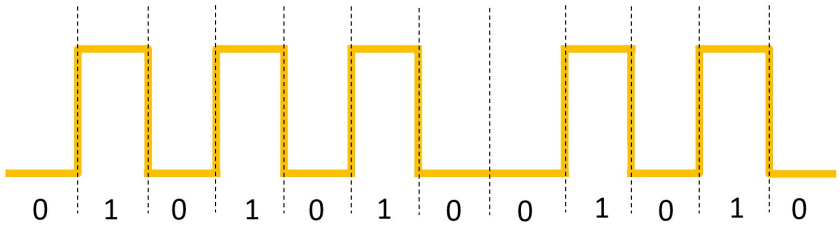

Figure 37 Example of ideal binary code realized by chamfers arranged around the copper lid.

The use of a binary code could be a valid solution for the identification concept. However, the number of chamfers to be machined on the copper lid can become even lower implementing another kind of code. In particular, chamfers 6º wide can be replaced by chamfer 3º wide and then the reference become 6º wide. Moreover, the circumference can be divided into four sections, 27º wide, representing respectively thousands, hundreds, tens and units. In this way, with a maximum of 4 chamfers plus the reference, it is possible to uniquely identify more than 6000 canisters. In addition, only 24 g of copper would be removed from the entire lid (considering chamfers 10 mm wide and 50º inclined); therefore, the copper lid geometry will be little altered. A graphical representation of this new concept is illustrated in Figure 38.

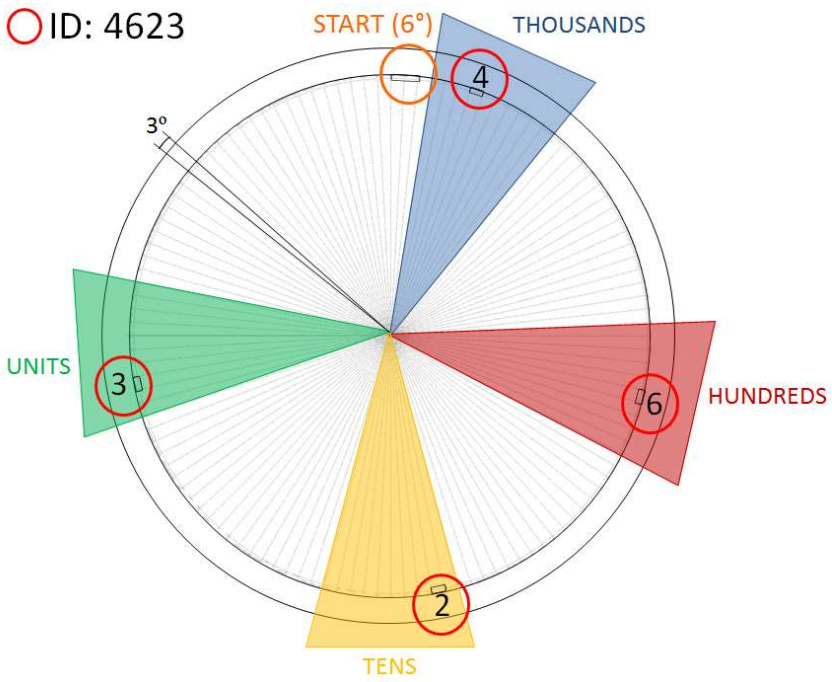

Figure 38 Example of identification code for the canister number 4623, according to the new coding.

This new code offers two main advantages: on the one hand the number of chamfers is drastically reduced, as well as their angular extensions; on the other hand, the splitting of the circumference into sections guarantees the identification of thousands of canisters. Nevertheless, the electronics of the acquisition system should be designed to ensure a constant sampling rate in order to trace chamfer position with precision during scanning. Furthermore, a rotary encoder could be installed to support the software in the definition of the probe position during motion.

5.3.2 Mechanical tolerances

The parametric study is a tool of CIVA software which allows the definition of several varying parameters during inspection simulations. The use of this application is extremely important for the evaluation of measure tolerances during the acquisition of the ultrasonic echo reflected by chamfers. The ultrasonic inspections, in fact, could be affected by temperature variations and a wrong inclination or deflection of the ultrasonic probe during motion. The parametric study is implemented on different 3D

models of the copper lid with and without chamfers. In particular, chamfers 50° inclined with different width (5 mm, 8 mm, 10 mm, 12 mm) are considered and the set-up is adjusted to have a maximum reflection at 40 °C with a probe inclination of 14.55° and no angular deflection. Regarding the mechanical fixture of the probe, the variation of the inclination is varied between 16° and 13° with a step of 0.1°. The probe deflection, instead, is varied from -3° to +3° with a step of 0.6°. Figure 39 and Figure 41 reports some pictures of the ultrasonic beam and the acquired ultrasonic amplitude responses on varying of the probe inclination, while Figure 40 and Figure 42 on varying of the probe deflection. The amplitude reported in charts is a relative value measured in relation with the maximum echo obtained during the simulation.

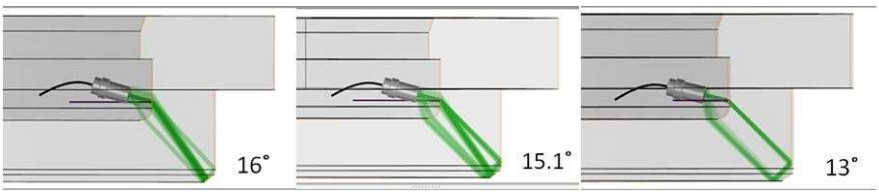

Figure 39 Variation of the ultrasonic beam for different probe inclinations.

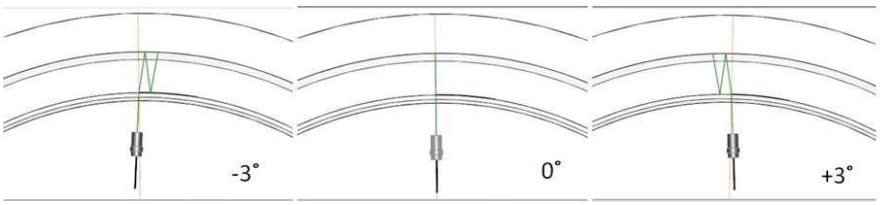

Figure 40 Variation of the ultrasonic beam for different probe deflections.

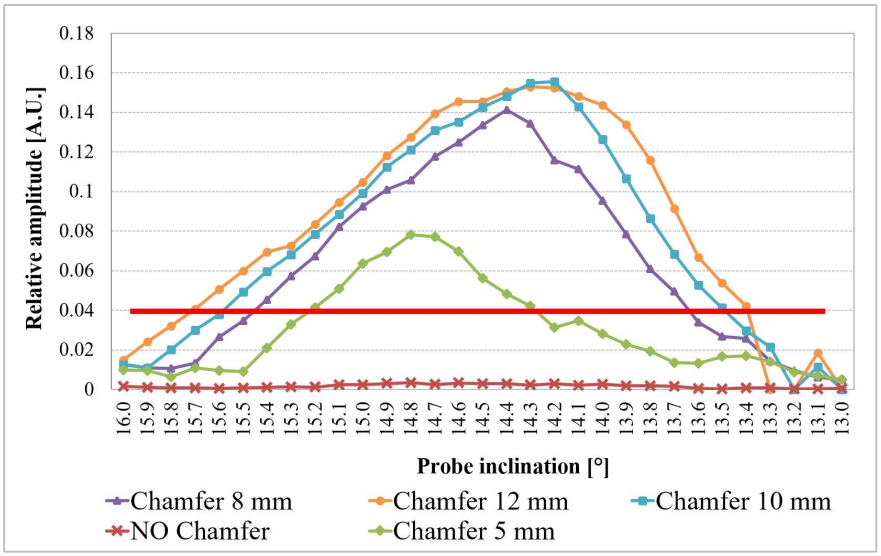

Figure 41 Ultrasonic amplitude response acquired by the investigation of a lid without and with chamfers (5 mm, 8 mm, 10 mm, 12 mm wide), considering a probe inclination varying from 13° to 16° with a step of 0.1°.

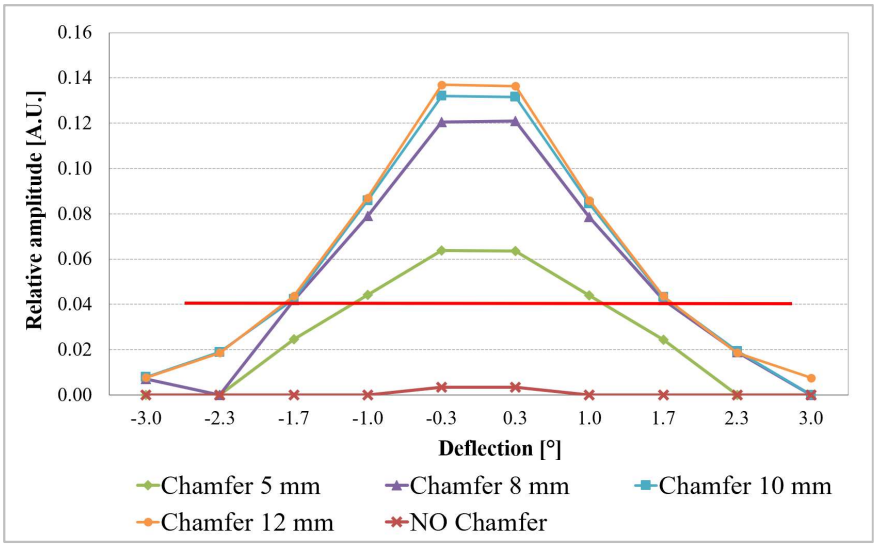

Figure 42 Ultrasonic amplitude response acquired by the investigation of a lid without and with chamfers (5 mm, 8 mm, 10 mm, 12 mm wide), considering a probe deflection varying from -3° to +3° with a step of 0.6°, from the 0° position.

The red line at 0.04 represents the minimum amplitude value to discriminate the presence of a chamfer with a good margin: this amplitude threshold, in fact, is 10 times bigger than the maximum amplitude received in the case without chamfers. The analysis of the results shows that the wider the chamfer, the larger the tolerance for the probe to inclination and deflection.

5.3.3 Operative temperature range

Concerning the influence of temperature in the ultrasonic investigation of chamfers, several parametric studies with CIVA have been implemented to evaluate the variation of the amplitude response on varying of the temperature. Before describing the simulated set-up and related results, it is worth to analyse the temperature changes in copper and water. In general, copper canisters are designed to withstand high temperatures due to the radioactivity decay of the internal nuclear spent fuel [43]. The temperature on the outer surface of the canister is designed to never exceed 100 °C. From the ultrasound point of view, the temperature variation could have a strong impact on the accuracy of the ultrasonic testing. In particular, the velocity of sound in copper and in water could be affected by temperature. As shown in Figure 43, the speed of sound in water increases with rising temperature [44].

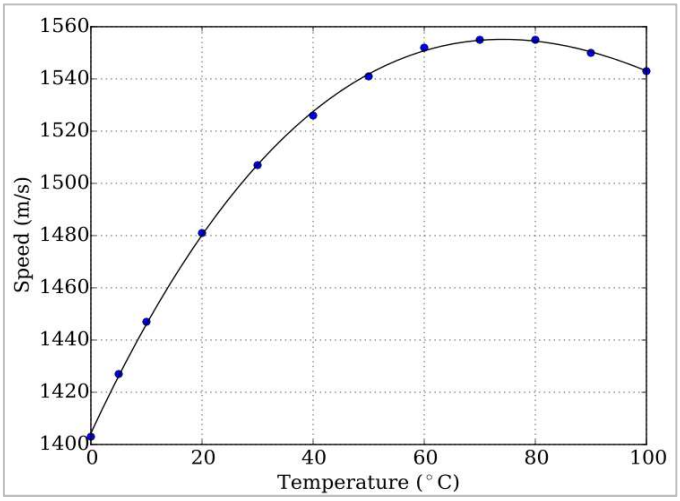

Figure 43 Velocity of sound in water for a temperature between 0°C to 100°C.

The velocity of sound in water could fluctuate from 1403 m/s at 0 °C up to a maximum of 1555 m/s at 74 °C with a percentage variation of about 11%. Ultrasound

travels slower in hotter water after that point. Concerning canisters, the speed of sound in copper depends on the Young's modulus and the density. Canisters are made of pure copper and the content of other elements is limited (phosphorus 30–100 ppm, sulphur < 12 ppm). The variation of the Young's modulus of copper with temperature between 0 °C to 100 °C is roughly 2% while the variation of density in the same range is around 0.5% [45][46]. Therefore, the variation of the sound velocity in copper ΔV_c due to temperature variation (between 0 °C to 100 °C) is illustrated in equation (2):

$$\Delta V_c = \frac{1.02}{1.005} = 1.015 \quad (2)$$

This value is negligible with respect to the variation of the speed of sound in water. Consequently, simulations with CIVA are performed considering only the temperature variation in water. The simulated set-up is the same of the previous case: chamfers 5 mm, 8 mm, 10 mm, 12 mm wide are investigated by a probe placed 14.55° inclined (considering the maximum echo reflection at 40 °C) and ultrasonic echoes are acquired varying the temperature of water from 5 °C to 70 °C. The acquired amplitude responses are illustrated in Figure 44.

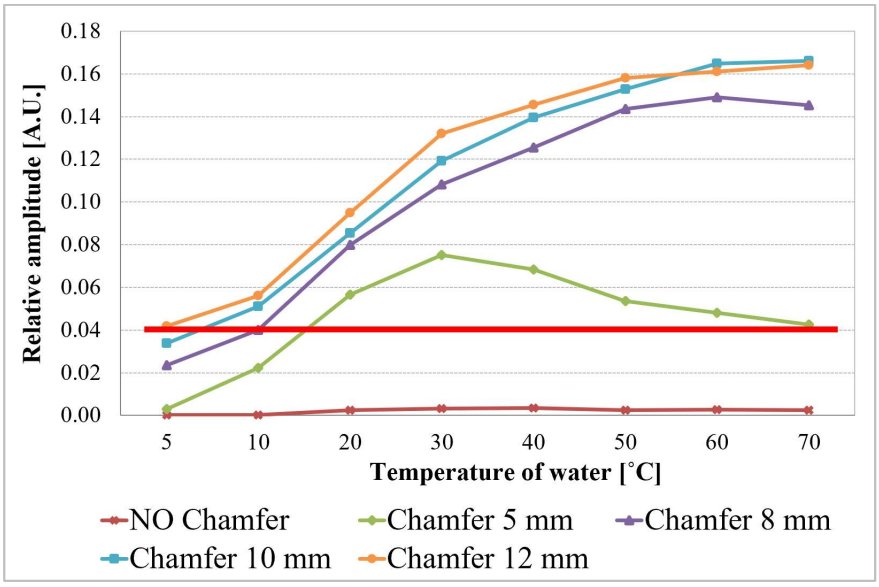

Figure 44 Ultrasonic amplitude response acquired by the investigation of a lid without and with chamfers (5 mm, 8 mm, 10 mm, 12 mm wide), considering a temperature variation from 5 °C to 70 °C.

As in the previous paragraph, a red line at 0.04 represents the minimum amplitude limit to guarantee a reliable acquisition of the chamfers' echo. In general, the amplitude is more or less constant for high temperatures (50 °C - 70 °C) and decreases at lower temperatures, in accordance with the evolution of speed of sound in water reported in Figure 43.

In conclusion, geometrical tolerances for the mechanical fixture of the probe (inclination/deflection) and the operative temperature ranges for the inspection of chamfers are collected in Table 2.

Table 2. Tolerances for the mechanical fixture of the probe and operative temperature ranges defined for chamfer 5 mm, 8 mm, 10 mm, and 12 mm wide.

Chamfers width	**Probe Inclination [°]**	**Probe deflection [°]**	**Temperature variation [°C]**
5 mm	+15.2/+14.3	+1.2/-1.2	+15 / +70
8 mm	+15.4/+13.6	+1.66/-1.66	+10 / +70
10 mm	+15.6/+13.3	+1.66/-1.66	+7 / +70
12 mm	+15.7/+13.4	+1.66/-1.66	+5 / +70

Considering the ranges reported in the Table 2, a chamfer 10 mm wide results to be the best compromise to guarantee a good ultrasonic inspection and not affect the copper canister too much. However, a good anchorage of the transducer could minimize errors during motion. The influence of temperature, instead, could be limited using a temperature sensor devoted to measure temperature variations during the ultrasonic testing. Possible fluctuations could be compensated by a calibration algorithm based on the signal's adaptation on a unique scale.

In conclusion, the identification concept by ultrasound has been successfully validated on a laboratory mock-up and simulations with CIVA software contributed to identify the best chamfer's geometry and position and define the ranges of tolerances in terms of probe inclination/deflection and temperature variations. However, according to paragraph 2.2.1, the tagging system for copper canisters must be tampered-proof, giving evidence of falsification attempts. The identification fingerprint can provide a unique label for each canister but could be potentially duplicated. Therefore, an authentication fingerprint has been proposed. A detailed description of the authentication concept is reported in the next chapter.

Chapter 6

The Ultrasonic Method: Authentication concept

The authentication concept is illustrated in this chapter. The ultrasonic amplitude response of the internal gap between lid and tube after welding is proposed as an authentication fingerprint for copper canisters. Following the description of preliminary studies carried out on copper flanges, the development and testing of two ultrasonic acquisition systems is reported. In the end, the probabilities of correct and false authentication are calculated to verify the efficacy of the ultrasonic method.[1]

[1]Part of the work reported in this chapter has been published as "Ultrasonic Investigation of the Welding Area of Copper Canisters for Spent Nuclear Fuel", in *ESARDA bulletin, Issue 56, pp. 19-27, June 2018* [47].

6.1 Ultrasonic inspection of the internal gap

The authentication concept is based on the research of a natural fingerprint, intrinsically contained into copper canisters and then not falsifiable. As already discussed in paragraph 4.2.1, after the FSW process, an air gap of about 0.3-0.6 mm remains between lid and tube. This gap represents a discontinuity in the material, detectable by an ultrasonic probe kept at a fixed height "h", perpendicular to the welding line, as illustrated in Figure 45. Performing an immersion testing, it is possible to acquire echoes from the interface water/copper, the internal gap and the external wall considering three different time windows (gate 1, gate 2, gate 3). An example of the acquired signal in A-scan mode is illustrated in Figure 46.

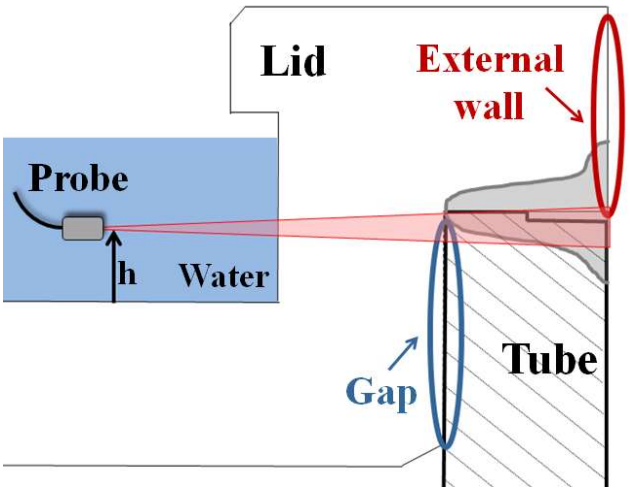

Figure 45 Ultrasonic immersion testing for the investigation of the welding area between the copper lid and tube. The probe is kept at a fixed height, perpendicular to the welding line in order to receive echoes from the internal gap and the external wall.

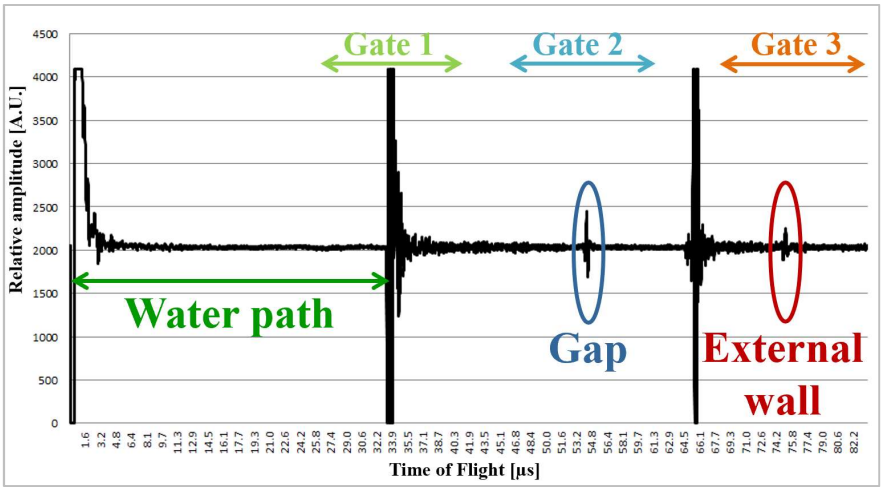

Figure 46 Example of acquired signal in A-scan mode in case of static ultrasonic immersion testing with a probe at fixed height "h". Three gates can be defined for the detection of: the interface water/copper echo (gate 1), the internal gap echo (gate 2) and the external wall echo (gate 3).

Depending on the height "h" of the transducer, the amplitude of the internal gap echo could be lower while the amplitude of the external wall echo could become higher. The variation of these echoes' amplitude is related to the material structure and copper grain size. Since the copper lid is forged and pressed before welding and final machining, its internal structure could be composed by grains with various dimensions that when investigated by ultrasound could attenuate the beam in different ways. In addition, the height of the gap around all the circumference of the lid can vary according to the welding process. Therefore, by rotating the probe around the whole lid circumference, the amplitude response of the internal gap can be variable depending on the material structure after the welding process. This response could be potentially used as an authentication fingerprint for copper canisters. As for the identification fingerprint, the authentication signature can be recorded after the FSW of copper canisters at the encapsulation plant and then can be compared with following acquisitions to verify the presence of counterfeit canisters.

6.1.1 Preliminary tests on a copper flange

In order to study the variations of the internal gap amplitude response along the canister's circumference, preliminary experimental tests have been carried out on a copper flange available in laboratory (Figure 47). The flange, corresponding to a 50° slice of an entire copper lid already welded onto a tube, is inspected moving manually the ultrasonic probe along with the length of the flange. The arc of circumference investigated is approximated to a line 380 mm long and the probe is moved with a step of 10 mm. Several measurements have been performed changing the height "h" of the transducer from 15 mm to 25 mm with a step of 2 mm.

Figure 47 Views of the copper flange investigated by ultrasound.

Following preliminary tests carried out with different probes [28], the Olympus V311 immersion transducer is used for the scan of the flange. Considering a water path of 50 mm, the probe (whose features are described in paragraph 5.2) is focused in copper at a depth about 50 mm, that is exactly where the internal gap is located. Ultrasonic echoes are acquired using the US-Key module whose gain in reception is set to 40 dB. Three gates are also imposed for the detection of the interface water/copper echo, the internal gap echo and the external wall echo expected at 67 μs, 89 μs, and 110 μs, respectively. These values have been calculated using equation (1),

considering a D1 of 50 mm and a D2 of 51 mm for the internal gap and 100 mm for the external wall. The following chart (Figure 48) shows the ultrasonic amplitude responses of the internal gap and the external wall acquired on varying of the probe position and height.

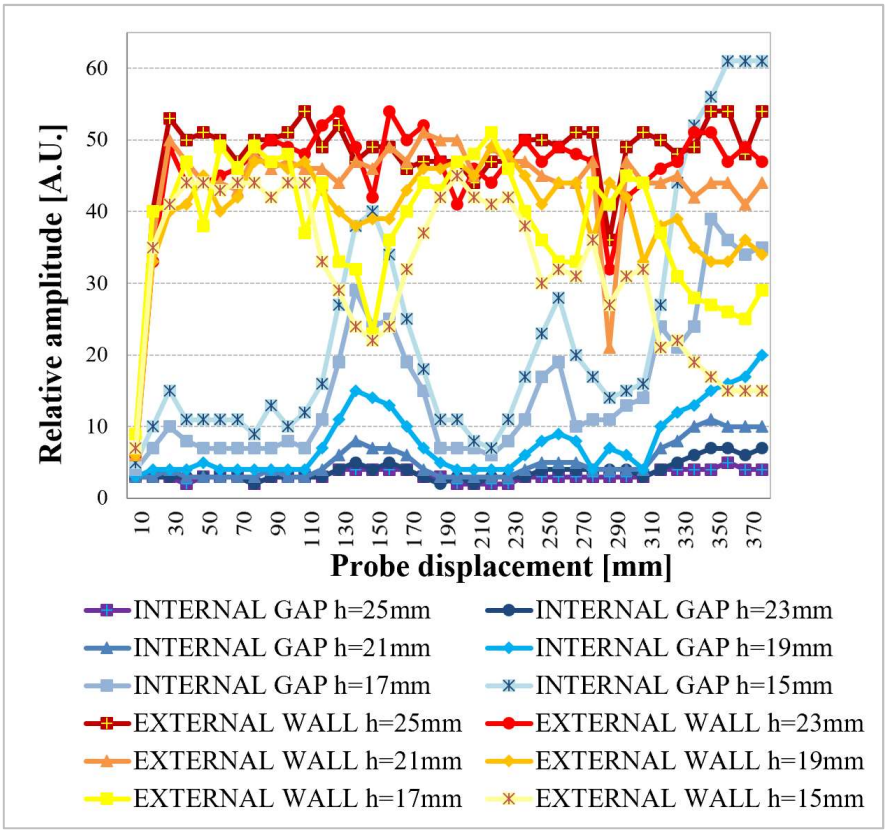

Figure 48 Relative amplitude responses of the internal gap and the external wall echoes acquired on varying of h=15, 17, 19, 21, 23, 25 mm.

The analysis of amplitude responses revealed that around the welding line (at height 25 mm) the amplitude response of the external wall is higher than the amplitude response of the internal gap. Instead, moving down the probe (for example at height 15 mm), the response of the gap become more fluctuating and its amplitude is sometimes higher than the external wall response, such as between 130 mm and 170 mm. It means that depending on the angular position of the transducer, kept at a fixed height, the internal gap can be more or less detectable. The reason of these variations in the amplitude response of the internal gap lies on the variability of the welding

process which can affect the geometry of the internal gap. Therefore, the amplitude response could be potentially used as an authentication fingerprint for each canister. However, further investigations on real copper lids already welded should be implemented. For this purpose, a first automatic scanning system prototype has been developed. The design and testing of such a system are reported in the next paragraph.

6.2 Development of an ultrasonic system prototype

The first ultrasonic system prototype for the acquisition of the amplitude response of the internal gap from copper canisters was called “IDA Reader” (Identification and Authentication Reader). This system is composed of a reader, a control box and a computer (Figure 49). The reader consists of three supporting arms, centred on the lid, and a motor devoted to the rotation of a rod holding the ultrasonic transducer (Olympus V311, described in paragraph 5.2). The probe is kept perpendicular to the side of the lid surface and its distance from the lid can be adjusted from 50 mm to 25 mm, while the height “h” from 35 mm to 14 mm from the top surface of the lid. The rotation of the probe is ensured by a synchronous motor which allows a complete rotation of the transducer in about 4 minutes. The control box includes a 220 V to 24 V AC inverter to power the motor and the US-Key module to regulate ultrasonic inspections. Lastly, the box is connected to a computer where a new dedicated user interface, different from the Lecoeur software interface, is included for the signal processing and the display of collected data.

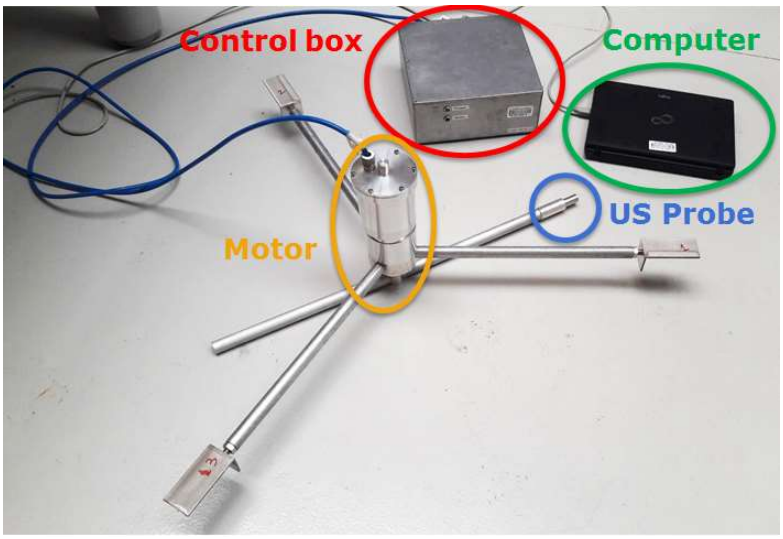

Figure 49 First ultrasonic system prototype: the IDA Reader.

The software interface is made of four different tabs: *Main Menu*, *Gap acquisition*, *Ascan echoes* and *Correlation*. The first tab allows the setting of the main measurement's parameters including the position of three gates of interest, where echoes are expected. The second and third tabs are then focused on the acquisition of the internal gap fingerprints. Two charts display the maximum amplitude response within the three gates and the acquired echoes in A-scan mode. The last tab is instead dedicated to the calculation of the Pearson's correlation index ρ between two fingerprints selected from the database; this index is calculated according to equation (3) where *cov* is the covariance, σ_X is the standard deviation of curve X and σ_Y is the standard deviation of curve Y.

$$\rho_{X,Y} = \frac{cov(X,Y)}{\sigma_X \sigma_Y} \tag{3}$$

Two fingerprints can be considered correlated in case of correlation indexes above 0.9. Below this value, additional tests should be implemented to verify the correspondence between the two fingerprints. This threshold has been imposed since it has already been used for the comparison of ultrasonic fingerprints of bolt seals applied on nuclear storage casks. For a more accurate definition of the threshold, a statistical analysis should be implemented on a significant number of canisters (50 for

example) in order to verify the uniqueness of the ultrasonic fingerprint on varying of the threshold. Calculating the correlation index between fingerprints acquired from different canisters, it is possible to evaluate the most suitable value of threshold to discriminate two canisters. The probability of correct authentication or false authentication can be then obtained on varying of the threshold. A more detailed description of this concept is reported at the end of paragraph 6.3.

6.2.1 The testing in laboratory on copper flanges

Before testing the reader on a real welded lid, a first experimental test is carried out in laboratory on copper flanges arranged around a circumference reproducing the same geometry of an entire copper lid already welded on a tube (Figure 50). The aim of this preliminary test is verifying if the IDA Reader can acquire the ultrasonic response of the internal gap with a good repeatability before performing the test on full-scale welded lids. Once flanges are carefully fixed around the circumference to ensure the stability of the set-up, the entire configuration is put underwater and the IDA reader is placed above as shown in Figure 51. The three arms of the reader are perfectly aligned at the same height to keep the probe perpendicular to the lid surface during revolution.

Figure 50 Copper flanges arranged around a circumference in order to reproduce the full copper lid geometry.

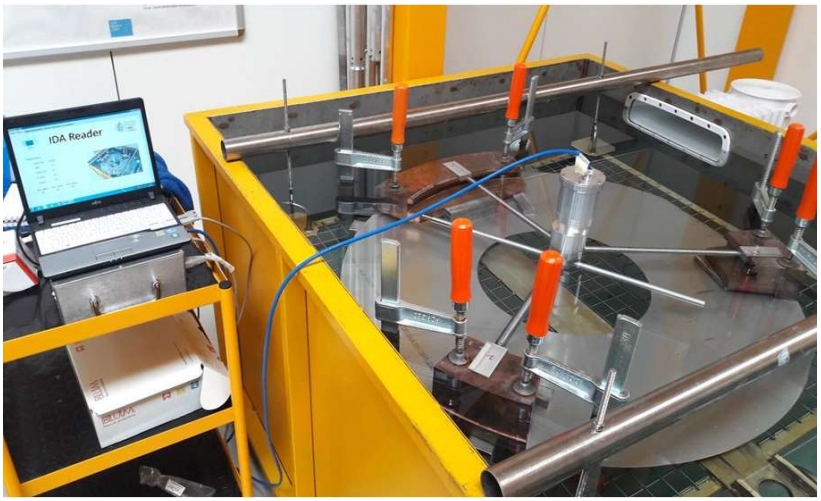

Figure 51 Set-up of measurements for the investigation of the internal gap in copper flanges with the IDA Reader.

Before starting the test, the temperature of the water is measured by an infrared digital thermometer and the probe distance and height are evaluated thanks to a calliper and then regulated (Figure 52, Figure 53). Depending on the temperature and the probe position, the three gates can be adjusted to ensure a good reception of the ultrasonic echoes.

Figure 52 Evaluation of temperature of water before testing.

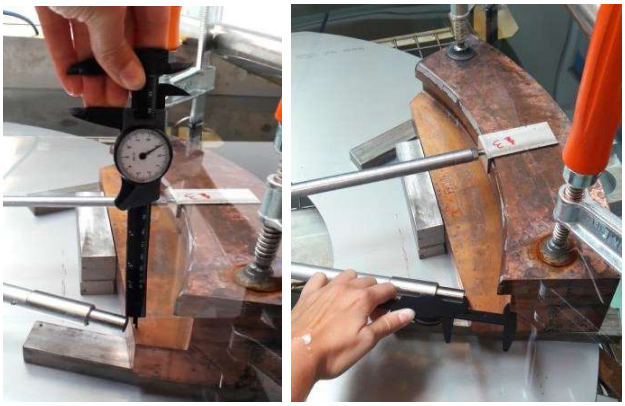

Figure 53 Verification of probe height and distance from the surface of the copper lid.

From the *Main Menu* (Figure 54) of the user interface it is possible to set the three gates for the acquisition of echoes from: the interface water/copper (gate 1: 60 µs - 75 µs), the internal gap (gate 2: 80 µs - 95 µs) and the external wall (gate 3: 105 µs - 120 µs). The gain in reception is set to 35 dB and the scan time is defined of about 4 minutes that is the time employed by the motor to complete a 360° rotation. According to the speed of the motor and the sampling frequency, a sample is acquired each 0.2°.

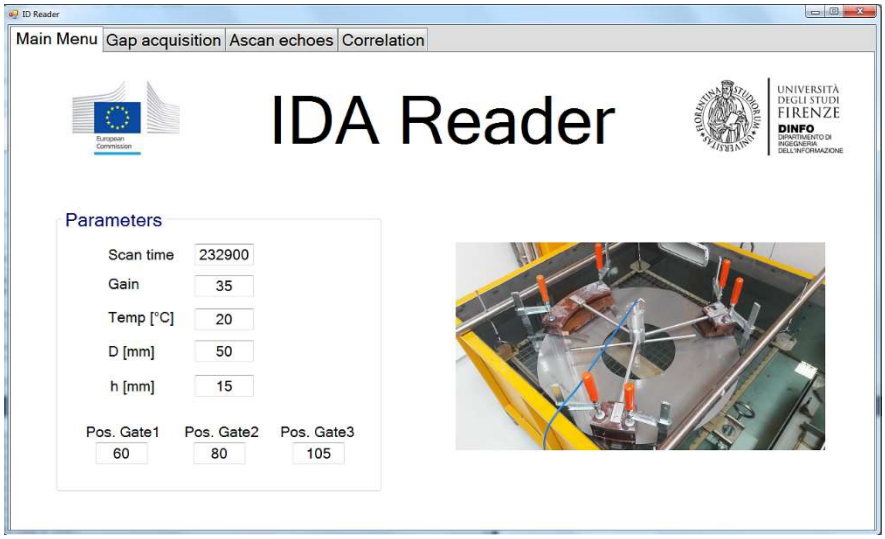

Figure 54 Main menu of the software interface.

By clicking the button on the *Gap acquisition* tab, the test starts. Once completed, the chart within the tab displays the maximum amplitude within each gate on varying

of the probe displacement (gate 1 in blue, gate 2 in green, gate 3 in pink). An example of acquired signal is shown in Figure 55, where three main reflections corresponding to the three flanges can be seen. Spurious reflections with other surfaces of the set-up are neglected. In addition, all the acquired echoes can be seen in A-scan mode in the *Ascan echoes* tab (Figure 56).

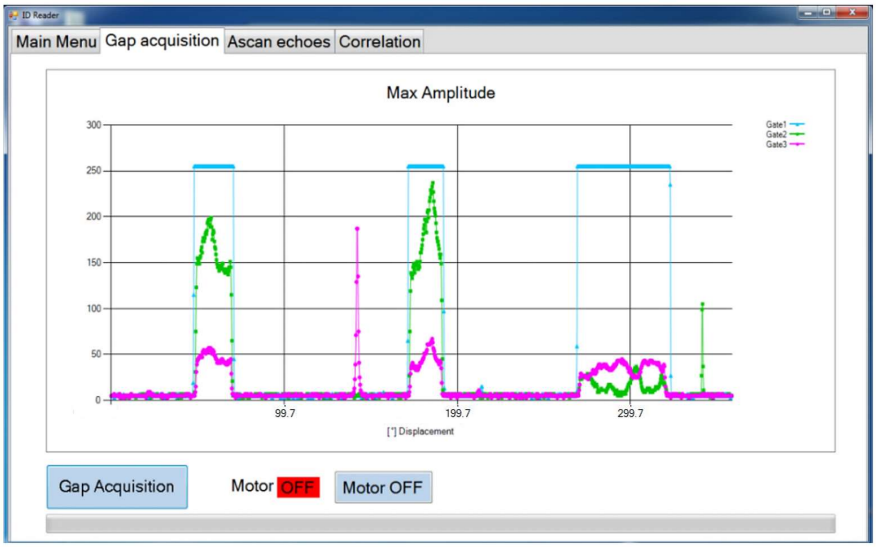

Figure 55 Example of amplitude responses acquired within each gate during the transducer rotation. In blue gate 1 (interface water/copper), in green gate 2 (internal gap echo), in pink gate 3 (external wall echo).

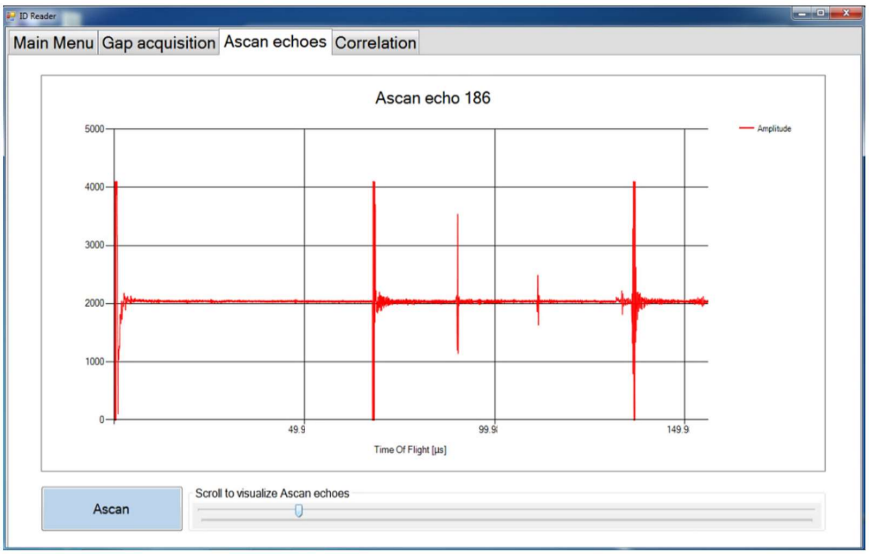

Figure 56 The Ascan echoes tab allows the visualization of all the A-scan signals recorded during the probe rotation.

Several tests are carried out changing the position of the reader arms above flanges in order to verify the repeatability of measurements. The correlation indexes between internal gap fingerprints acquired in different tests were always above 0.9 demonstrating the repeatability of the measurements. An example of the correlation index calculated between different acquisitions carried out changing the arm position above the flanges, is show in the *Correlation tab* illustrated in Figure 57. The two fingerprints are resampled on a same number of elements and then displayed on a chart, overlapped and shifted. The C# code implemented for the correlation of fingerprints is reported in Appendix A.

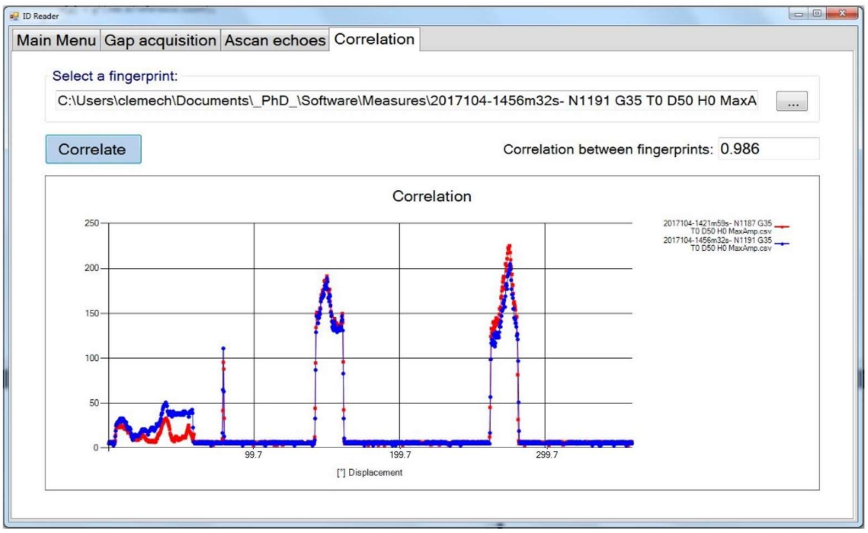

Figure 57 The correlation index reported in this picture is related to two different acquisitions carried out changing the arms position above the flanges.

6.2.2 Experimental tests at the SKB's Canister Laboratory

Preliminary tests on copper flanges produced encouraging results. Afterwards, the reader prototype has been tested on two copper lids already welded onto tubes at the SKB's Canister Laboratory. The SKB's Canister Laboratory, situated in Oskarshamn (Sweden), is the centre for the development of technologies that will be used for the encapsulation of spent nuclear fuel in copper canisters. The aim of this testing campaign was verifying if the ultrasonic response of the internal gap could be used as an authentication fingerprint for copper canisters [48]. The uniqueness of the authentication fingerprint could not be demonstrated since the number of samples available for the inspection was not sufficient to implement a statistical analysis. Because of the high cost of the FSW process, only two welded lids (FSWL 121, FSWL 122) were available for tests; in addition, the geometry of the two original lids were slightly different, as illustrated in Figure 58.

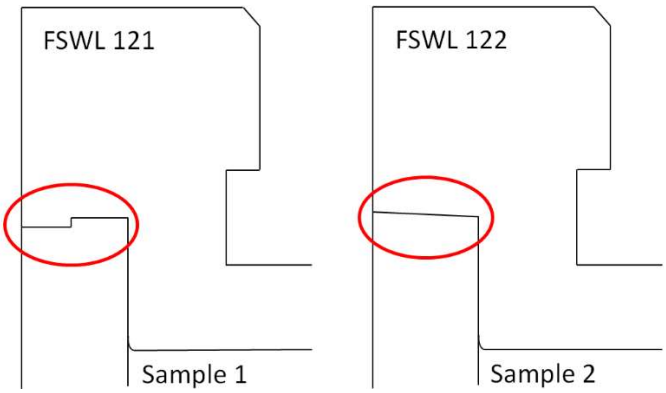

Figure 58 Section view of the FSWL121 and FSW122.

In order to perform ultrasonic immersion tests, copper samples are placed in a tank with water and four labels are arranged at 90° from each other on the upper surface of the lid to create a reference pattern for measures. Several acquisitions have been carried out changing the arms positions around the circumference. The sequence of implemented measurements is shown in Figure 59.

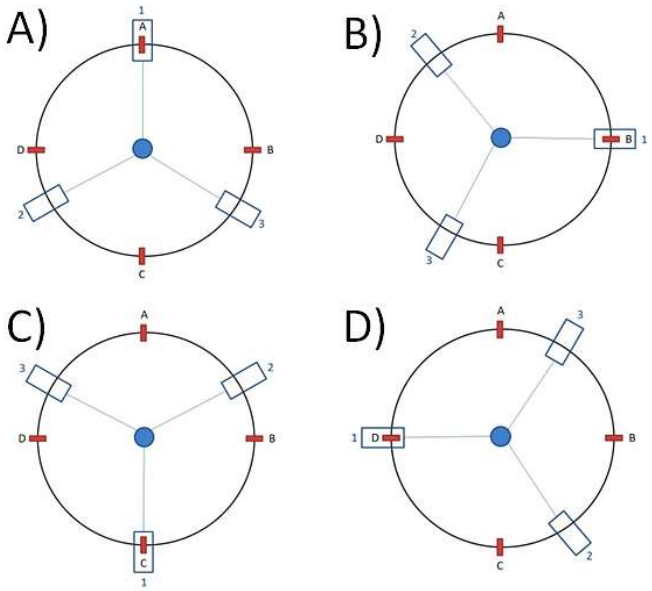

Figure 59 Sequence of measurements implemented on copper samples.

For each position A, B, C, D, the height of the transducer is changed from 15 mm to 21 mm with a step of 2 mm. Through the variation of the reader position, it is possible to verify the reader ability to perform repeatable measurements. The adjustment of probe heights, instead, aims to detect which is the variation of the ultrasonic amplitude response along the circumference. The temperature of water during the test is 18 °C, the probe distance 50 mm and the gain of the receiver is set to 37 dB. The set-up of measurement is illustrated in Figure 60.

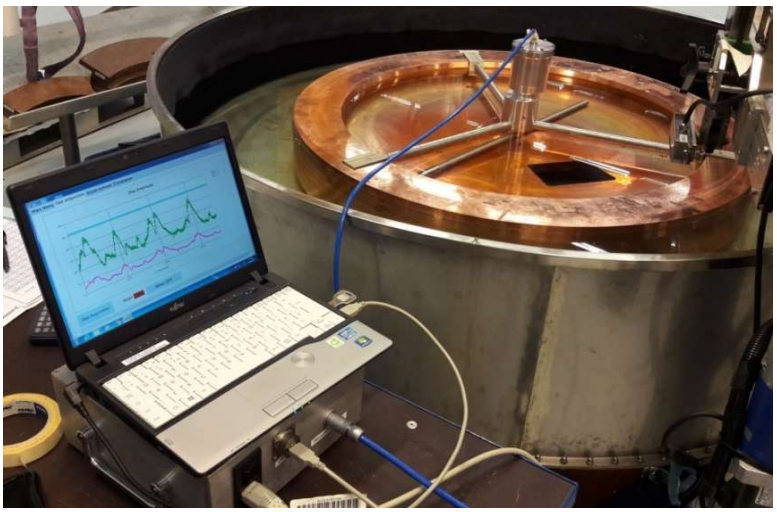

Figure 60 Experimental testing of the IDA reader prototype at the SKB's Canister Laboratory.

Three gates are imposed for the acquisition of the interface water/copper (gate 1: 60 µs – 75 µs), the internal gap (gate 2: 80 µs – 95 µs) and the external wall echoes (gate 3: 100 µs – 115 µs). The acquired amplitude responses are collected in a database for further processing. The analysis of results has revealed that the amplitude response of the internal gap is fluctuating in both investigated samples. The variation of this signal can be related to the different grain size in the material that generates various attenuation patterns around the lid circumference. On varying the probe height, the amplitude of the internal gap echo decreases or increases according to the geometry of the weld. For example, in the FSWL 122, at height 15 mm (10 mm below the welding line), the internal gap echo appears clearly detectable; as shown in Figure 61, in blue is reported the internal gap echo on varying of the angular position of the transducer and in purple its double reflection. In fact, this second echo is temporally

located within the same time window of the external wall echo and replicate the same evolution of the internal gap echo.

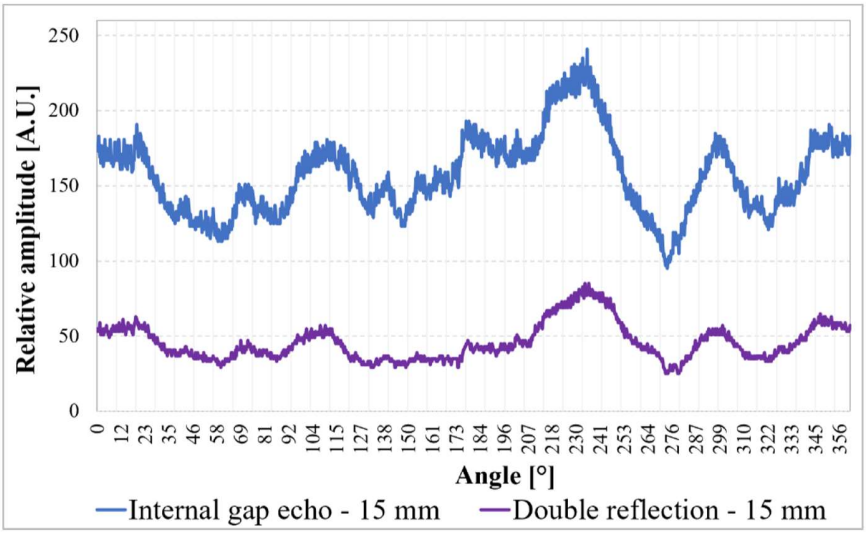

Figure 61 Ultrasonic amplitude response of FSWL 122 at height 15 mm.

The amplitude of received echoes is relative to the reference voltage of 5V of the A/D converter; acquired data are digitized on 255 levels (8-bit resolution). In order to verify that the echo in purple is exactly the repetition of the internal gap, an inspection simulation with CIVA software is implemented. As a result (Figure 62), the simulated A-scan exhibits three main echoes: the first related to the interface water/copper, the second due to the reflection on the internal gap (highlighted in blue) and then a second reflection whose features (amplitude and time of flight) agrees with the measured echo (purple trace).

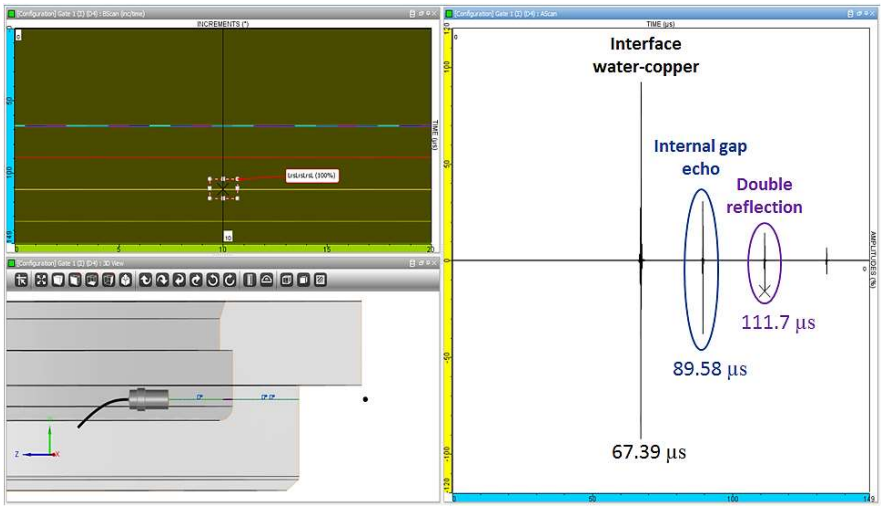

Figure 62 Inspection simulation implemented by CIVA software for the verification of the time of flight of the double reflection on the internal gap.

Moving the probe up, the response of the internal gap changes and the echo of the external wall appears. Figure 63 shows the ultrasonic response of the internal gap (in blue) and the external wall (in red), acquired at height 19 mm.

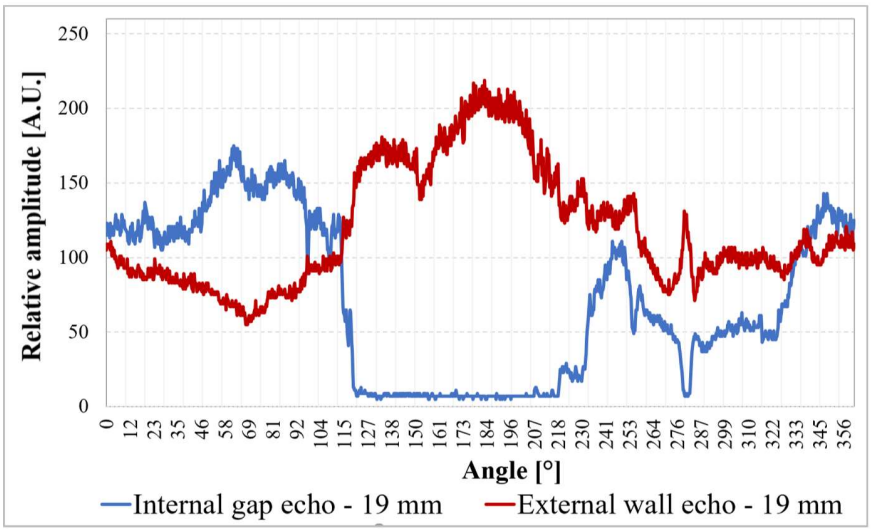

Figure 63 Ultrasonic amplitude response of FSWL 122 at height 19 mm.

The pattern of signals in this chart is particularly interesting. In fact, there is an arc of about 100º, from 115º to 230º, where the internal gap echo is practically zero. It means that in this area lid and tube are welded and ultrasound can penetrate in copper without reflections up to the last interface that is the external wall of the canister. However, the presence of this trend could be also related to an incorrect alignment. In addition, at around 210° there is another signal inversion, which corresponds to the point where the welding tool passes twice during the welding process (point 4 of Figure 19).

The ultrasonic investigation of the second sample, FSWL 121, has generated similar results as shown in Figure 64 and Figure 65. In particular, at height 17 mm the internal gap echo and its double reflection can be detected; whereas at height 21 mm the echo of the external wall appears. In addition, as observed in the previous case, at about 69º, an inversion of signals reveals the crossing point of the welding tool.

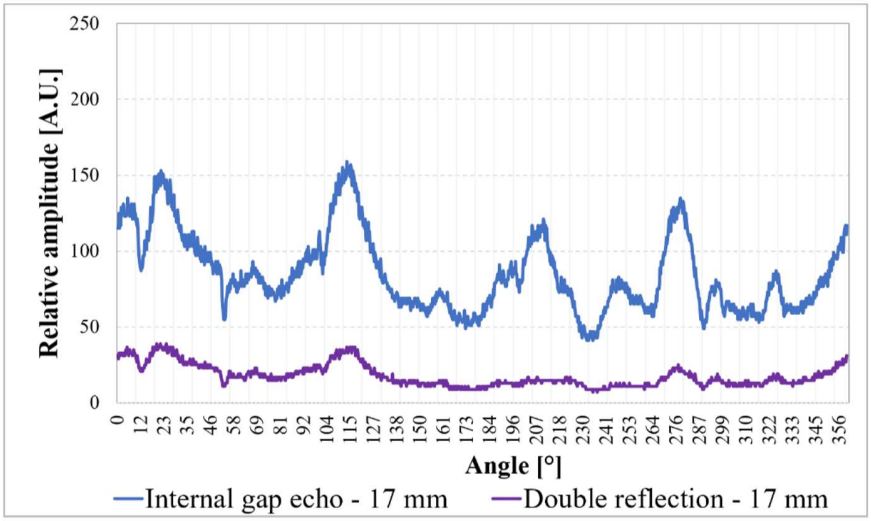

Figure 64 Ultrasonic amplitude response of FSWL 121 at height17 mm.

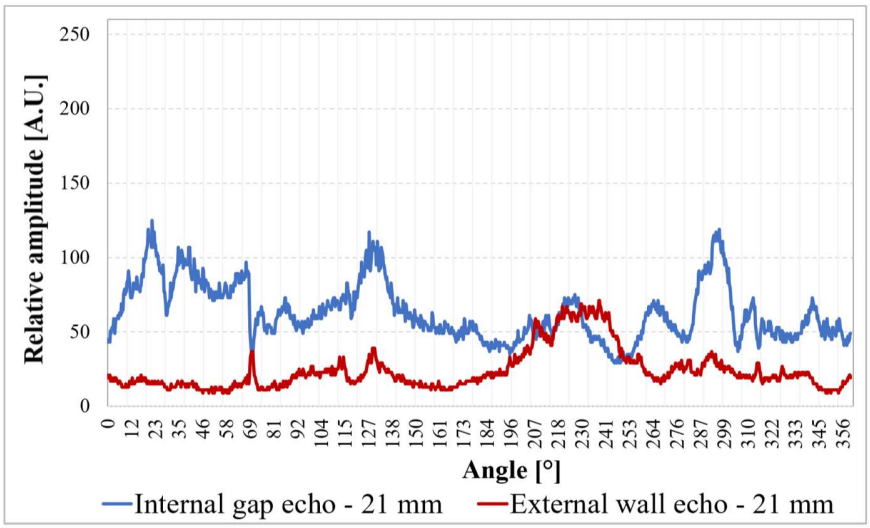

Figure 65 Ultrasonic amplitude response of FSWL 121 at height 21 mm.

The investigation of the two welded lids at the SKB's Canister Laboratory put in evidence that the ultrasonic amplitude response of the internal gap presents different peculiarities which can be detected at different heights depending on the type of lid geometry. However, the IDA reader presents some problems related for example to the fixed speed of rotation of the synchronous motor that limit the experimental tests in terms of acquisition time. In addition, the reader presents a difficult mechanism to change the probe height and needs a socket to power the motor. For this purpose, a new optimized acquisition system has been developed.

6.3 Optimization and testing of the ultrasonic system prototype

The optimization of the IDA Reader consisted in the re-design of the reader and the control box, including also new features in the software acquisition tabs. The design of the new rotating reader is similar to the previous one: it includes three angular arms spaced at 120° to center the system above the lid and a rotating bar to hold the Olympus V311 immersion transducer (Figure 66). However, the height of the transducer can be finely adjusted by a threaded shaft which simplifies the old

mechanism where the shaft was locked with a transverse positioned grub screw. The synchronous motor is then replaced with a NEMA 17 stepper motor (minimum motor step with gearbox is 0.0112º). In this way, the rotation speed of the probe can be adjusted to verify if it would be possible to speed up the acquisition without losing in resolution.

Figure 66 Ultrasonic acquisition device placed above a copper sample for inspections.

The stepper motor and the ultrasonic probe are connected to a control box where new components have been included. The block diagram of the new control box is in Figure 67. For the control of the motor, an Arduino UNO connected to a motor stepper driver (DRV8855) is introduced. Moreover, a LiFePO4 battery pack (12V, 3.5Ah) is adopted to remove the need of a fixed socket to power the motor. The US-Key module is used for the excitation of the probe and the acquisition of ultrasonic echoes. The software interface is also upgraded to include the button for the start/stop of the motor and the adjustment of the rotation speed.

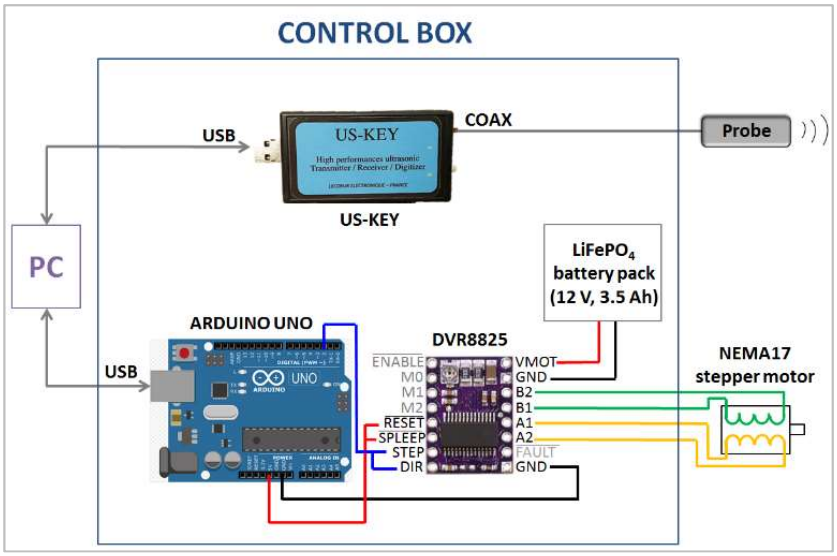

Figure 67 Block diagram of the control box onboard on the ultrasonic acquisition device.

The new acquisition system prototype has been tested at the SKB's Canister Laboratory where two welded samples where available: a welded lid (FSWL130) and a welded base. According to the ultrasonic method, only the lid would be investigated for the detection of authentication fingerprints. However, since the base is welded onto the tube by the same welding process of the lid, the investigation of these samples is useful to learn further information about the amplitude responses of the internal gap and the external wall after welding. As in the previous case, the two samples are deposited on a tank with water at 18 °C and four stickers are applied around the circumference to define some reference points 90º angularly spaced: A, B, C and D (Figure 68). The position of label A is not random but corresponds to the starting point of the weld joint (point 0º), i. e. where the tool crosses twice during the welding process. This point is highlighted because, in the previous testing campaign, a remarkable variation of the ultrasonic amplitude response was observed.

Figure 68 FSWL130 with reference stickers A, B, C, D, separated from each other by 90°.

Several experimental tests are carried out changing the height of the ultrasonic probe from 14 mm to 26 mm with different steps and starting the acquisition from a different position between A, B, C and D as shown in Figure 69.

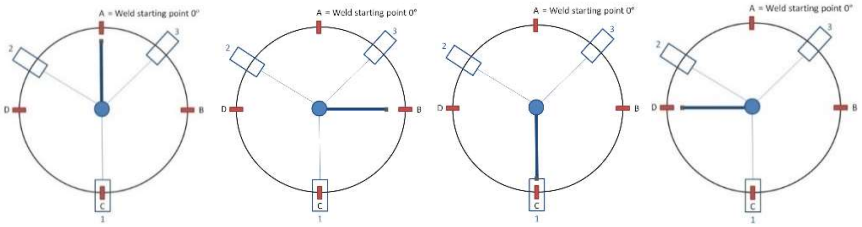

Figure 69 Starting positions of the transducer: A, B, C, and D, from left to right. The acquisition device is kept at a fixed position with the arm 1 in correspondence of point C.

This inspection sequence is performed for both the welded lid and the welded base. It is also worth to underline that the geometry of the base is slightly different from the lid (Figure 70) and then, for the inspection of the base, the three supporting arms of the reader are replaced with another version which better fits onto the base geometry. Regarding the acquisition time, the majority of acquisitions are carried out considering a sampling frequency of about 5 samples/s and a motor speed of 125 steps/s that means acquiring one sample each 0.3°. Some tests are also performed increasing the motor speed and results of acquisitions are compared.

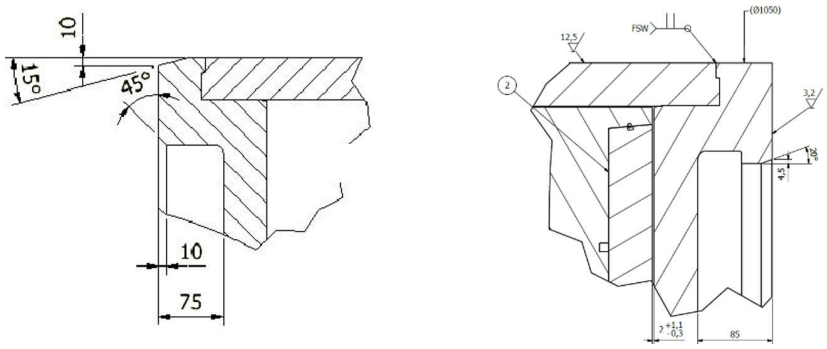

Figure 70 Geometry design of the copper base (on the left) and the copper lid (on the right).

The analysis of echoes acquired on the welded lid reveals that raising the height of the transducer, the amplitude response of the internal gap decreases; vice versa the amplitude response of the external wall increases. In addition, several peculiarities can be observed in the amplitude responses of the internal gap (blue signal) and the external wall (red signal) acquired at heights 14 mm, 17 mm, 19 mm and 21 mm; these signals present a zone where the amplitude echo of the gap decreases sharply. As shown in Figure 71, for example, at height 17 mm, the internal gap amplitude echo remains low from 229° and 275°, except for a small peak around 255°. This is a curious behaviour, probably because the gap is extremely narrow in that zone and ultrasound can be transmitted to that interface. Otherwise, it could be that a defect is included in that area of the lid circumference. In addition, in contrast to the FSWL121 and FSWL122 previously investigated, the internal gap response of the FSWL130 appears more oscillating.

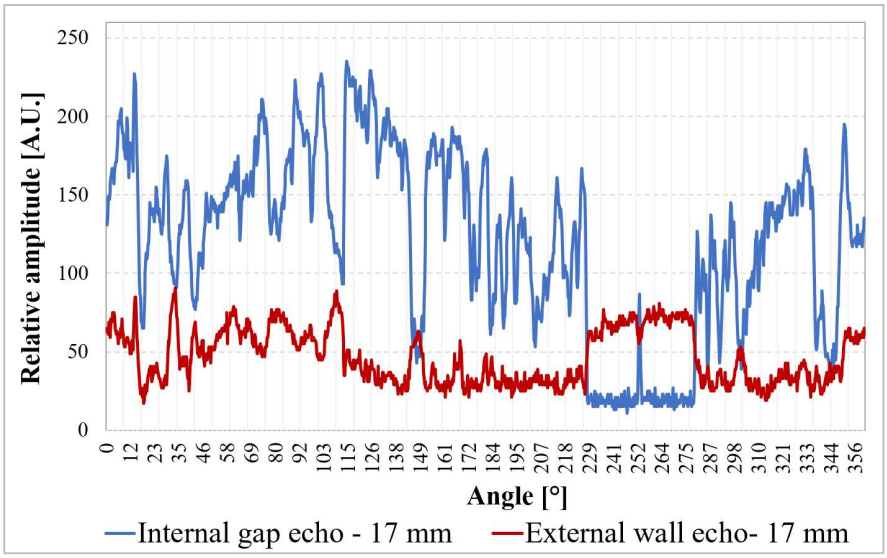

Figure 71 Ultrasonic amplitude response of the internal gap (in blue) and the external wall (in red) at height 17 mm starting the acquisition from position A (see Figure 69).

Analysing the amplitude responses acquired at heights 22 mm, 23 mm, 24 mm and 26 mm, instead, it is possible to appreciate that the point where the welding tool crosses twice during the welding cycle, is detectable. An example is reported in Figure 72; in correspondence of position A (at about 90° - 100° from the starting position D), there is an inversion of the signals trends that is linked to the point 4 of the welding sequence. Moreover, it is worth to observe that around 110° there is a peak in the internal gap amplitude echo probably related to presence of a discontinuity maybe developed by the welding process. However, the nature of this peak is still under study.

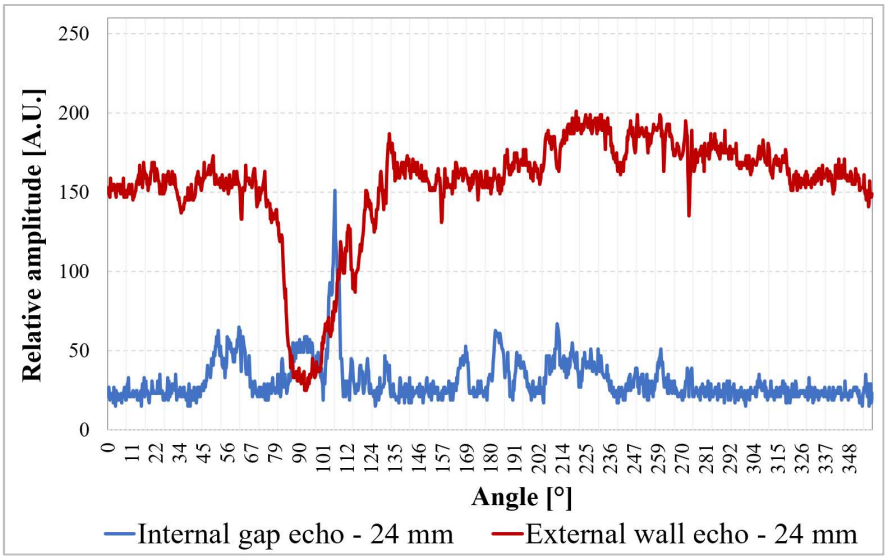

Figure 72 Ultrasonic amplitude response of the internal gap (in blue) and the external wall (in red) at height 24 mm starting the acquisition from position D.

In the end, some tests are performed doubling the rotation speed of the motor from 125 steps/s to 150 steps/s. The two amplitude responses acquired with different rotation speed are then compared. In the following Figure 73 is shown the correlation index between the amplitude responses of the internal gap, acquired at height 14 mm with a different speed of the motor. As a result, the correlation index between curves is about 0.97. It means that potentially the ultrasonic investigation of the welding area can be realized with a doubled speed of the motor without losing the content of acquired echoes.

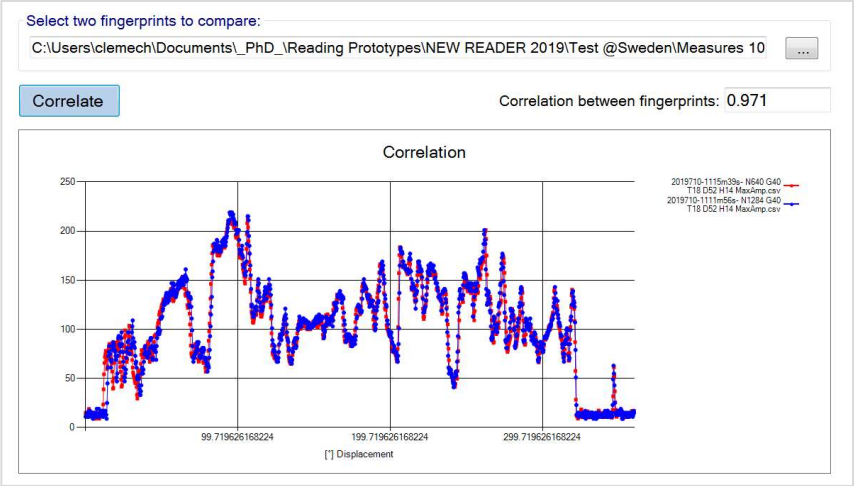

Figure 73 Calculation of the correlation index between the amplitude responses of the internal gap acquired at height 14 mm with a motor speed of 125 steps/s (in blue) and 150 (in red).

Concerning the analysis of echoes acquired by the investigation of the copper base it is possible to state that the variation of the internal gap amplitude is not quite as marked as in the copper lid. In this sample, it is also clearly detectable the inversion of signals which is correlated to the crossing area of the welding tool. An example can be seen in Figure 74, at about 180° from position C, where there is an inversion of signals trends.

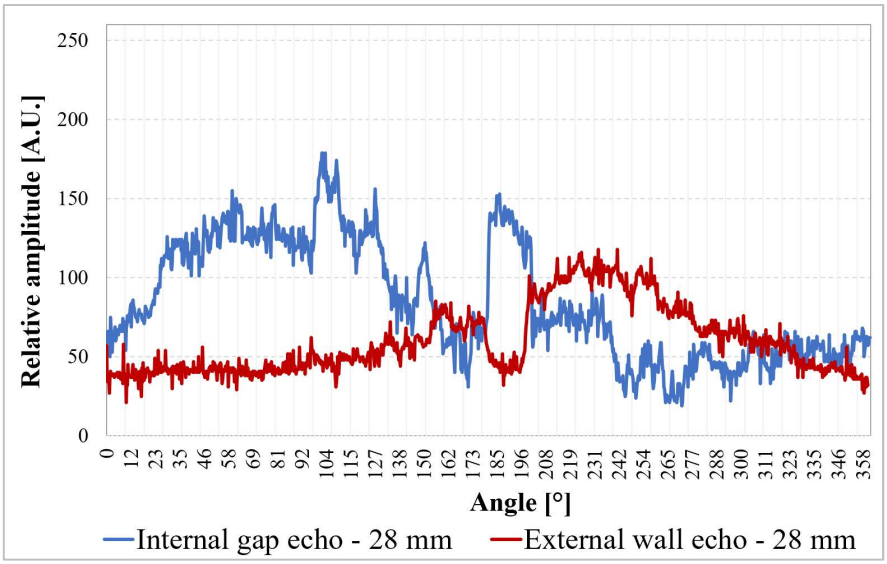

Figure 74 Ultrasonic amplitude response of the internal gap (in blue) and the external wall (in red) at height 28 mm starting the acquisition from position C.

Another interesting aspect regards the height of the weld joint line. In contrast to the FSWL130, the weld joint line seems to be around a height of 30 mm and not 25 mm, as foreseen by the geometry design. In fact, the amplitude of the external wall echo become higher than the amplitude of the internal gap echo only above 32 mm (Figure 75).

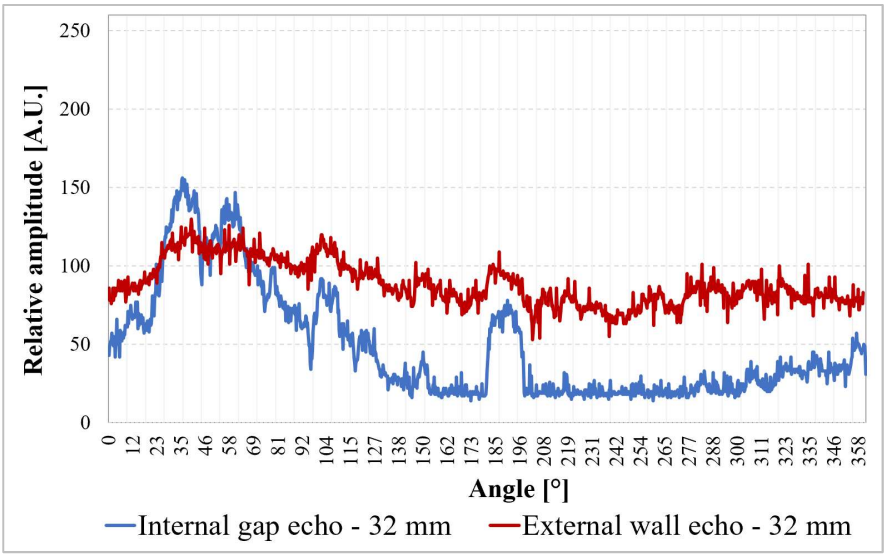

Figure 75 Ultrasonic amplitude response of the internal gap (in blue) and the external wall (in red) at height 32 mm starting the acquisition from position C.

The analysis of ultrasonic echoes acquired by the new acquisition system contributed to collect further information about the shape of the internal gap after the welding process. The response of the internal gap echo changes, on varying of the height of inspection, not only in terms of amplitude, but also in terms of time of flight. Depending on the presence of the gap or not, the phase of ultrasound can vary. For this purpose, the possibility to use the phase changes of the ultrasonic beam as an authentication fingerprint for canisters has been investigated. According to the preliminary results reported in Appendix B, this solution has been discarded.

The ultrasonic amplitude response of the internal gap can be used for the authentication of copper canisters: if the correlation index between two ultrasonic responses acquired from a canister is above a certain threshold, the canister is correctly authenticated. Instead, comparing two fingerprints acquired from two different canisters, the correlation index should be below a certain threshold, otherwise a false authentication occurs.

Considering two authentication fingerprints A1 and A2 from a canister “A” and two from a canister “B”, B1 and B2, it is interesting to calculate the probability of correct authentication (True Positive, TP) and the probability of false authentication (False Positive, FP). When the correlation indexes between A1 and A2 or B1 and B2 are

above the threshold, the authentication is correct, otherwise a false negative (FN) occurs. Differently, a true negative (TN) appears when the correlation index between A1 and B1 or B2, and between A2 and B1 or B2, are above the threshold. Depending on the threshold imposed, the probability of having a TP and a FP can vary. In Figure 76 are illustrated A1, A2, B1 and B2 on varying of the number of samples. Each amplitude response is composed by 1150 samples acquired at the same height (h=19 mm) for canister A and canister B.

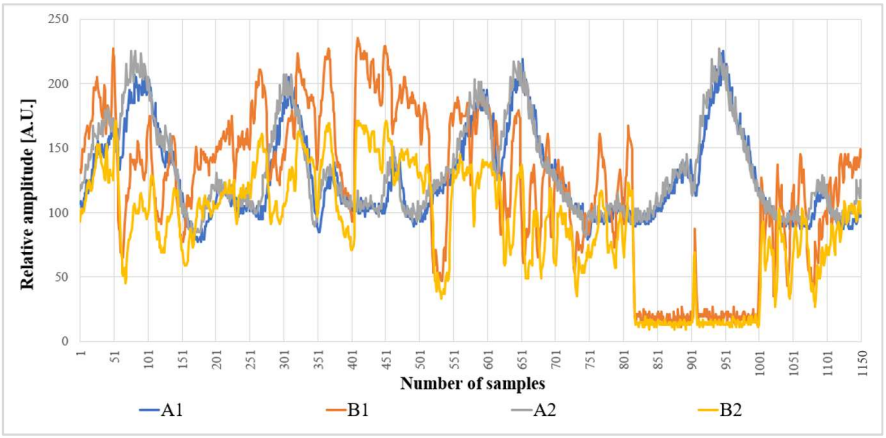

Figure 76 Ultrasonic amplitude responses of the internal gap of a canister A (A1 in blue and A2 in grey) and a canister B (B1 in orange and B2 in yellow).

The correlation index between A1 and A2, and B1 and B2 is 0.95 while the correlation index between A1 and B1 or B2 is 0.03 and the correlation index between A2 and B1 or B2 is 0.02. Considering a threshold of 0.9, as suggested by the ultrasonic method, canister A can be authenticated and well distinguished from canister B. However, in order to increase the number of data and verify which threshold is more suitable for the authentication of canisters, the probabilities of TP, FP, TN and FN can be evaluated dividing each fingerprint into 10 sections (of 115 samples each one) and 5 sections (of 230 samples each one) as illustrated in Figure 77.

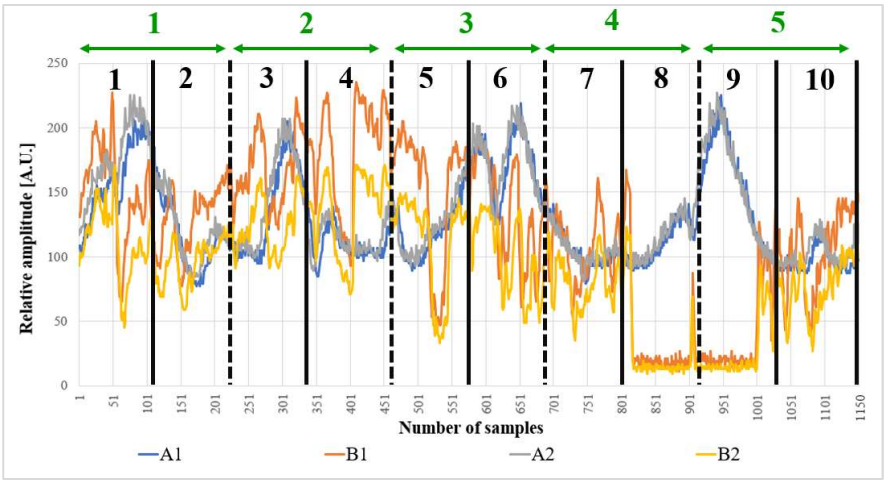

Figure 77 The division of A1, A2, B1 and B2 into 10 sections (black lines) and 5 sections (dashed black lines).

The probabilities of TP and FN are then calculated comparing sections of fingerprints acquired from the same canister: A1 with A2 and B1 with B2. Depending on the number of sections and the imposed thresholds "Th" (Th= 0.9, 0.8, 0.7), different values of TP and FN are obtained. Results of this study are reported in Figure 78. Figure 79 shows instead the probabilities of TN and FP calculated comparing sections of fingerprints acquired from different canisters: A1 or A2 with B1 or B2.

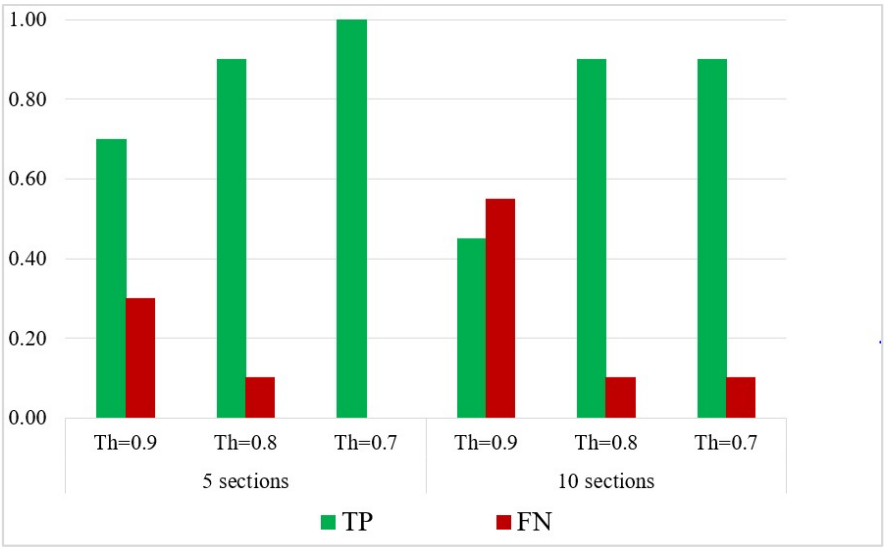

Figure 78 Probability of TP (in green) and FN (in red), in case of partition of fingerprints into 5 sections of 230 samples and 10 sections of 115 samples, on varying of threshold Th: 0.9, 0.8 and 0.7.

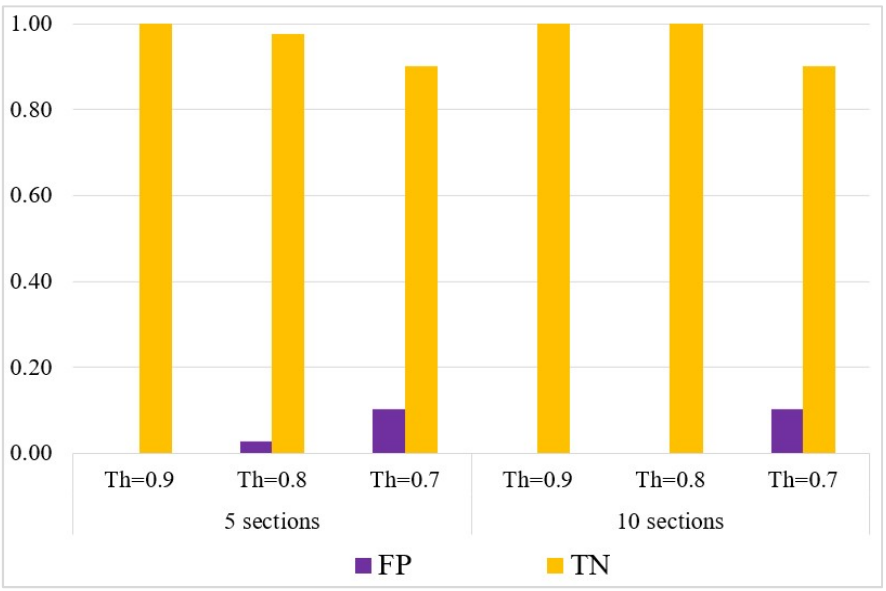

Figure 79 Probability of FP (in purple) and TN (in yellow) in case of partition of fingerprints into 5 sections of 230 samples and 10 sections of 115 samples, on varying of threshold Th: 0.9, 0.8 and 0.7.

The analysis of results revealed that, being equal the threshold, considering a higher number of samples for each section, the probability of correct authentication increases. In addition, a threshold of 0.9 is suitable for the correct authentication of a canister since the probability of FP is zero. Nevertheless, in case of partition into 10 sections, the threshold must be lower than 0.9 to avoid the presence of FN. However, a statistical analysis on many copper canisters could verify if this value of threshold is really the best solution for the discrimination of canisters. Moreover, the stability of the authentication fingerprint in the long-term, is extremely important to ensure the correct authentication of each canister over time. Further studies on these two aspects should be performed to make the ultrasonic method reliable and secure.

Chapter 7

The ultrasonic system to identify and authenticate copper canisters

In the first part of this chapter, the angular matching between the identification and the authentication fingerprint is illustrated. The development and testing of a new acquisition system prototype including a single probe and a beam splitter is then reported. In the end, the integration of the Seal Fingerprint Acquisition Device within the ultrasonic system is proposed as a valid option to improve the performances of the electronics.[1]

[1]Part of the work reported in this chapter has been published as "Development of an Innovative Ultrasonic Reader for the Authentication and Identification of Copper Canisters for Spent Nuclear Fuel", in proc. *IEEE International Ultrasonics Symposium, October 2019, Glasgow (UK)* [49].

7.1 An angular matching between fingerprints

Following the experimental validation of both the identification and the authentication concepts, a third fingerprint can be used to improve the security of the ultrasonic method. In particular, the angular matching between the identification and authentication fingerprints can generate a third signature, unique and more difficult to replicate (Figure 80). This new fingerprint can be obtained simply connecting the crossing points between the authentication fingerprint and the rising and falling edges of the identification fingerprint. As shown in Figure 81, in fact, depending on how the fingerprints are overlapped, the third signature could be different; therefore, in case of duplication of both the identification and the authentication fingerprints, implementing the angular matching between them, it is possible to detect a falsification attempt.

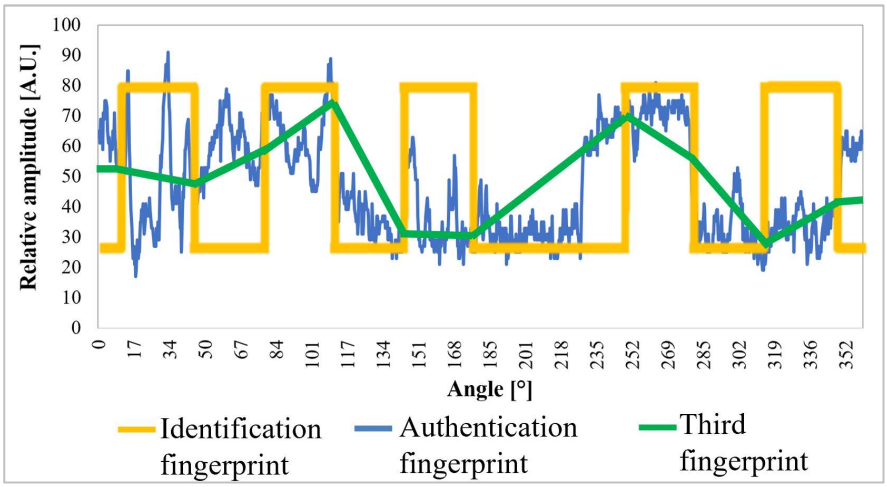

Figure 80 The angular matching between identification (in yellow) and authentication (in blue) fingerprints creates a new fingerprint (green line) that is unique and robust against falsification.

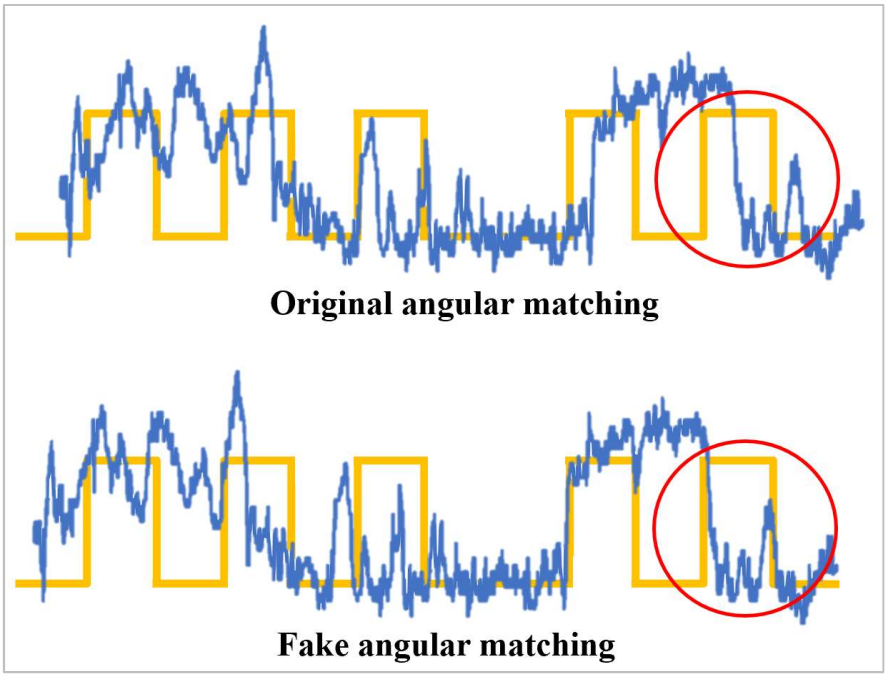

Figure 81 Comparison of an original angular matching (on the top) and a fake (on the bottom).

The combination of the two fingerprints is then important in increasing the robustness and reliability of the method. The acquisition of the identification and the authentication fingerprints can be realized by two immersion probes. Originally, the ultrasonic acquisition system (Figure 82) for the collection of fingerprints has been conceived as a big cylinder including a water container for the immersion testing, the control electronics and two probes: the first, inclined, for the detection of the chamfers' code (identification fingerprint) and the second for the acquisition of the amplitude response of the internal gap (authentication fingerprint). By a 360º rotation of the whole structure, the two identification and authentication signatures could be recorded and saved for the post processing. The angular matching between signals could be then implemented at the end of measurements [50].

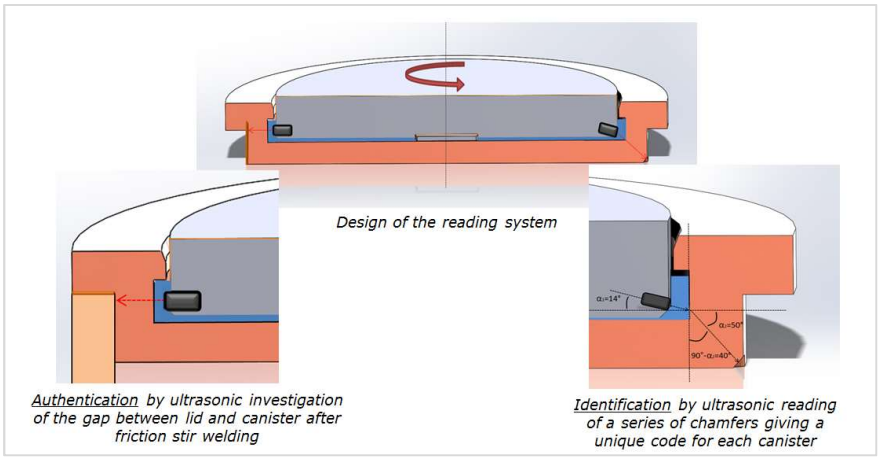

Figure 82 Original design of the ultrasonic system for the acquisition of identification and authentication fingerprints by two ultrasonic immersion transducers.

The acquisition of fingerprints could be performed at the encapsulation plant, after the radiographic inspection of the weld. The idea is to produce a reading system which could be remotely put in place by a crane or robotic arm and automatically centred on the lid (Figure 83). Once in place, water included in the tank can be released and poured on the external concave part of the lid, making an ideal and easy solution for the ultrasonic probe coupling. After a 360° inspection, the two curves are registered, stored or sent wirelessly to a control station.

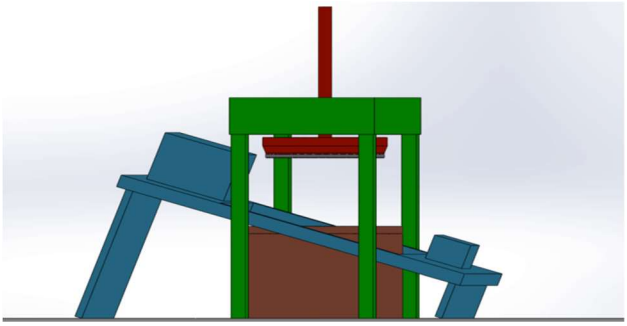

Figure 83 Drawing of a potential set-up for the implementation of the ultrasonic acquisition device at the encapsulation plant. Reference fingerprints could be acquired after the radiographic inspection of the weld (radiographic station in blue) thanks to the deposition of the ultrasonic acquisition device (in red) above the lid by a crane (in green).

7.2 Integration of a beam splitter in the ultrasonic acquisition system

The acquisition of the identification and authentication fingerprints can be implemented using two probes or a single probe with adjustable inclination to carry out a double inspection. In both cases, the electronics requires a complex structure and the time for acquisition and processing of data could be long. For this purpose, another measurements set-up consisting of a single probe and a beam splitter has been proposed. According to this new configuration, the ultrasonic beam can be split in two directions for the inspection of both the chamfers and the internal gap. As shown in the following picture (Figure 84), the ultrasonic probe is kept with a fixed inclination thanks to a stainless steel holder having a sloping surface which acts as a mirror for ultrasound. In this way, the split ultrasonic beam can be directed both to chamfers and to the internal gap.

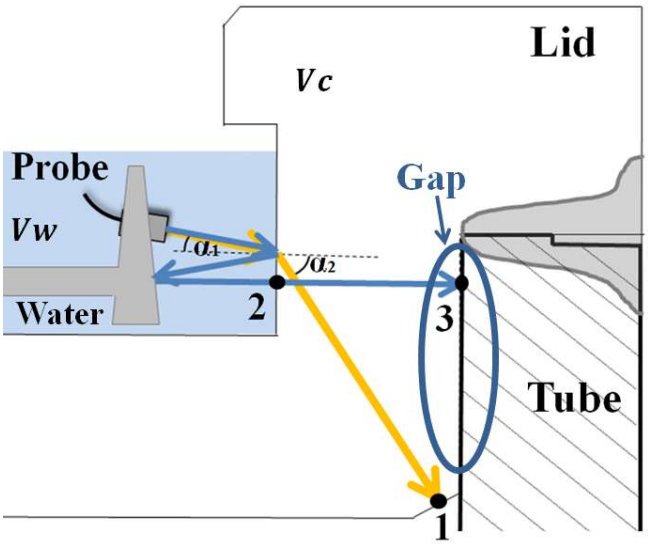

Figure 84 Ultrasonic acquisition of the identification and authentication fingerprints by a single probe and a beam splitter. The echoes from chamfers (point 1), interface water/copper (point 2) and internal gap (point 3) can be acquired by the transducer in immersion testing.

This new solution offers simple control electronics for the transmission/reception of data to/from a single ultrasonic transducer and an excellent temporal and spatial correlation between these two reflection signals. This way, the selection of the most suitable probe and the choice of its position, in terms of height, become crucial for the

success of the ultrasonic investigation. In fact, the lateral and axial resolution of the probe should be enough to detect the presence of a chamfer but also to reveal changes in the internal gap. In order to identify the best solution, the new set-up of measurements has been simulated with CIVA software and results are analysed. Simulations pointed out the possibility to realize an ultrasonic inspection of chamfers and the internal gap simultaneously, keeping a water path of 20 mm and a probe height of 24 mm. The speed of sound considered for simulations was 1481 m/s in water and 4660 m/s in copper; in this first analysis, the attenuation of ultrasound has been neglected to study only the propagation direction of the ultrasonic beam with the beam splitter. The probe used in the simulation was the V311 immersion transducer. As reported in (Figure 85), the A-scan view of simulated echoes shows three main peaks at different times of flight (TOF) corresponding to the echo of the chamfer (TOF_1), the echo of the interface between water/copper (TOF_2) and the echo of the internal gap (TOF_3).

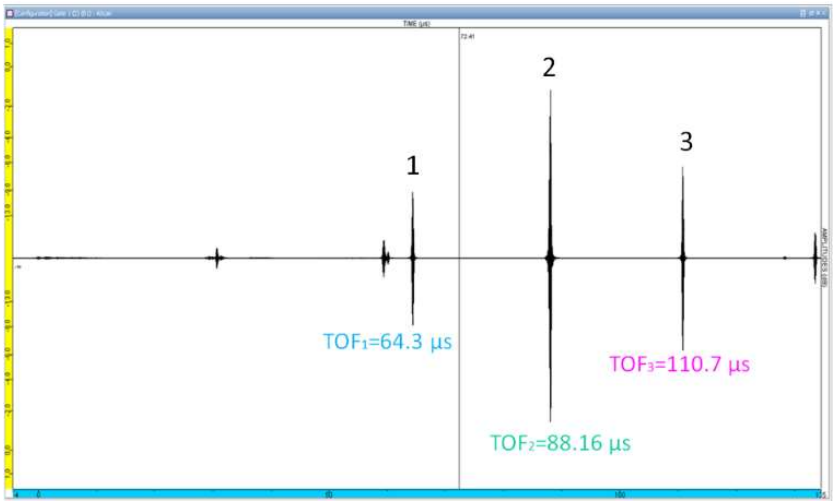

Figure 85 A-scan view of the inspection simulation carried on a copper flange with a probe and the beam splitter on a time window of 135 µs. Three peaks are clearly detectable at the time of flight of 64.3 µs, 88.16 µs, and 110.7 µs correspondent to chamfers, interface water/copper and internal gap respectively.

Therefore, by rotating the ultrasonic probe with the beam splitter around the canister circumference, it could be possible to collect the identification and authentication fingerprints in only one scan, preserving the spatial and temporal coherence of the data. Afterwards, the two fingerprints can be angularly overlapped, and a third unique fingerprint can be realized.

The ultrasonic system prototype developed for the acquisition of the authentication fingerprint is then modified to include a new support for the transducer. In particular, the new probe support consists of a stainless steel block with a 15° inclined hole to host the probe and a 7.5° inclined surface which acts as a beam splitter for ultrasound (Figure 86, Figure 87). The inclination of the probe allows the inspection of chamfer with a slope of 55˚.

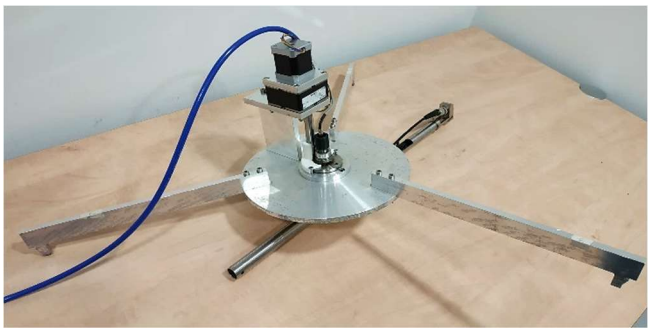

Figure 86 Ultrasonic reader prototype for the recording of both the identification and the authentication fingerprints.

Figure 87 Probe holder with a 15° inclined hole to host the transducer and a 7.5° inclined surface, to split the ultrasonic beam into two directions.

7.3 Experimental testing on a laboratory copper flange with chamfers

Following preliminary tests carried out in [51], the acquisition of both the identification and the authentication fingerprints is carried out using a single probe and a beam splitter. The experimental test is implemented by a modified version of

the ultrasonic system prototype where the probe holder is re-designed to host an inclined mirror to split the signal. A copper flange with chamfers is used as a sample to perform the test in laboratory.

7.3.1 Simulation and Manufacturing of Chamfers on a Copper Flange

Before testing the new ultrasonic acquisition system, it is interesting to describe the design, simulation and final manufacturing of chamfers. Considering a copper flange corresponding to a 50° section of a full-scale welded copper lid, seven chamfers can be machined: C1, C2, C3, C4, C5, C6 and C7. The 3D drawing of chamfers has been realized with SolidWorks and a configuration is reported in Figure 88. Chamfers are arranged in the inner surface of the copper lid and present the same slope but a different width and angular extension. The different chamfers' geometry has been done on purpose to verify which is the most suitable for a good identification code. All chamfers are 55° inclined and their width is 10 mm, except for chamfers C3 and C4 which have a width of 6 mm and 8 mm, respectively. Indeed, chamfers C1, C2 and C7 are extended 1°, 2°, and 6° respectively, whereas all the others are 3°.

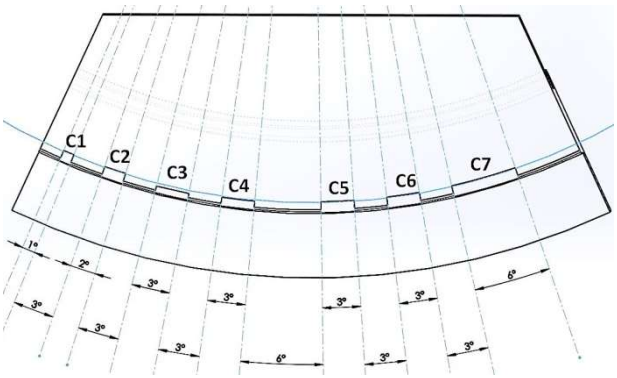

Figure 88 Drawing of seven chamfers C1, C2, C3, C4, C5, C6 and C7 on a 50° slice of copper lid already welded.

According to the coding proposed in 5.3.1, the minimal distance between two adjacent chamfers is 3°. Before machining the pattern of chamfers on the copper flange, CIVA simulations are performed to verify that such configuration of chamfers

is clearly detectable by an ultrasonic probe, 15° inclined, according to Snell's Law. A scanning of 50° is imposed to the probe and ultrasonic echoes are examined on variations of the displacement. According to the probe direction, C1 is the first chamfer encountered. The outcome of the inspection simulation is illustrated in Figure 89.

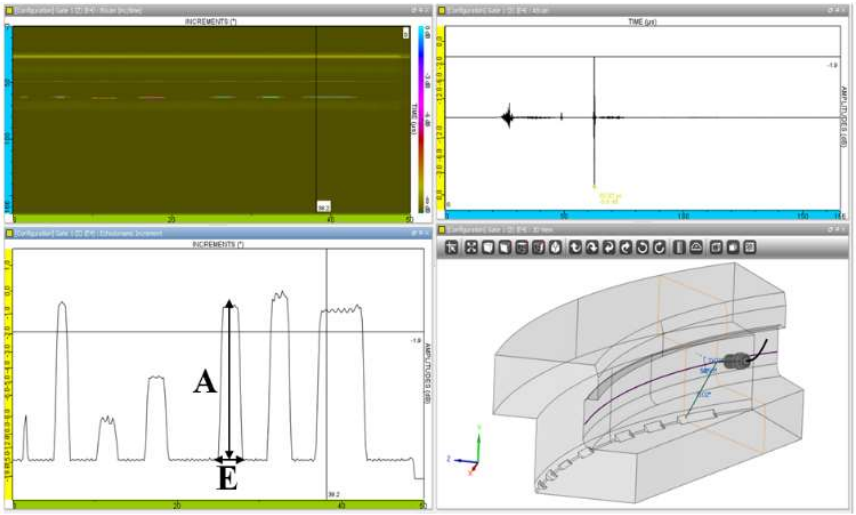

Figure 89 On the left, top to bottom, the B-scan view and the amplitude response on varying of the probe displacement is shown. On the right, the A-scan view and the 3D drawing of the simulated set-up are reported. A is the peak's amplitude of each chamfer whereas E is the angular extension.

As illustrated in the picture, the chart of the amplitude response of chamfers presents seven peaks corresponding to the seven chamfers; all chamfers can be clearly detected by the ultrasonic probe and the peaks' amplitude is correlated to the corresponding width and angular extension. As shown in Table 3, for the same width, the amplitude of the relative peak is proportional to the angular extension of the chamfer. The amplitude values reported in the table are negative since in CIVA the strongest echo resulted from a simulation is set to 0 dB and then the amplitude of all the other echoes is relative to this reference.

Table 3 Simulated values of the peak's amplitude "A" and angular extension "E" of the ultrasonic echo of chamfers.

Chamfers	A [dB]	E [°]	Width [mm]
C1	-7.9	0.8	10
C2	-0.6	2.2	10
C3	-7.9	2.8	6
C4	-4.6	3	8
C5	-0.6	3	10
C6	-0.3	3.2	10
C7	-0.6	6.4	10

Following simulations, the manufacturing of chamfers has been accomplished by a CNC (Computer Numerical Control) milling machine (model C.B.Ferrari B13). Since the lid was already welded onto the tube in the flange, the manufacturing process involved the removal of a part of the tube for the successful realization of chamfers (Figure 90).

Figure 90 Manufacturing of chamfers on a copper flange by a CNC machine.

In the real case, the chamfers should be machined on the inner surface of the copper lid before the FSW process. However, because of the high cost of the welding process, the heavy weight of an entire copper lid and the limited availability of welded samples,

the test of the new ultrasonic acquisition device has been implemented in the laboratory on a copper flange where chamfers have been machined afterwards.

7.3.2 Set-up of measurements and results of the test

The test of the ultrasonic device on the copper flange with chamfers is carried out using the V311 immersion transducer, inclined with $\alpha_1° = 15°$ and fixed at height of 24 mm. As shown in the previous Figure 50, the flange with chamfers has been positioned at 120° from the other two flanges, in order to replicate an entire lid. The investigation of the copper flange is performed by immersion testing considering a water path of about 21 mm. The collection of the identification and authentication fingerprints is implemented establishing three different time windows (gates) for the acquisition of the chamfers echo, the interface water/copper echo and the internal gap echo. The temperature of water during the test was 23 °C. The maximum amplitude echoes acquired within the three gates on variations of the probe displacement are shown in Figure 91.

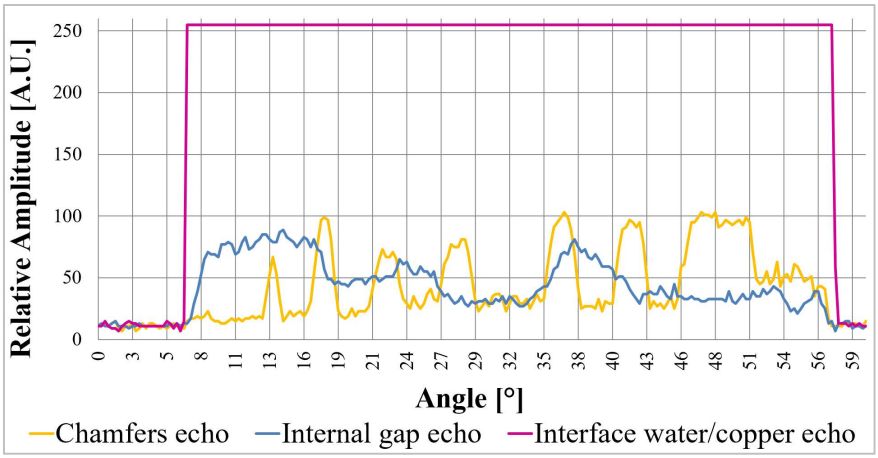

Figure 91 Ultrasonic amplitude responses of chamfers (in yellow), the interface water/copper (in pink), and the internal gap (in blue) on variations of the transducer's angle of displacement.

The seven chamfers are clearly detectable: the amplitude response of chamfers presents seven peaks whose amplitude and angular extensions are in accordance with the geometry of each chamfer. In particular, the measured peak's amplitude values and the angular extensions are reported in Table 4. In agreement with simulations

where the width is equal, the higher the angular extension of the chamfer, the higher the peak of amplitude is.

Table 4 Measured values of the peak's amplitude "A" and angular extension "E" of the ultrasonic echo of chamfers.

Chamfers	A [a.u.]	E [°]	Width [mm]
C1	127	1.2	10
C2	213	2.1	10
C3	145	3	6
C4	178	2.9	8
C5	208	3.2	10
C6	208	2.9	10
C7	213	6	10

Concerning the internal gap echo, the acquired amplitude response should be compared with the amplitude response acquired by a probe kept perpendicular to the welding area. In particular, this signal is examined in contrast to the internal gap amplitude echo acquired before chamfers machining, by a probe with 0° of inclination placed at height of 15 mm. In this way, it is possible to demonstrate that the authentication fingerprint could be acquired not only by a probe perpendicular to the welding area, but also by the inclined probe with the beam splitter. As reported in Figure 92, the Pearson's correlation index ρ between the two curves is 0.9. As a result, the new version of the ultrasonic acquisition device, thanks to the adoption of a single probe and the beam splitter, allows not only the detection of a chamfers code, but also a complete acquisition of the internal gap echo.

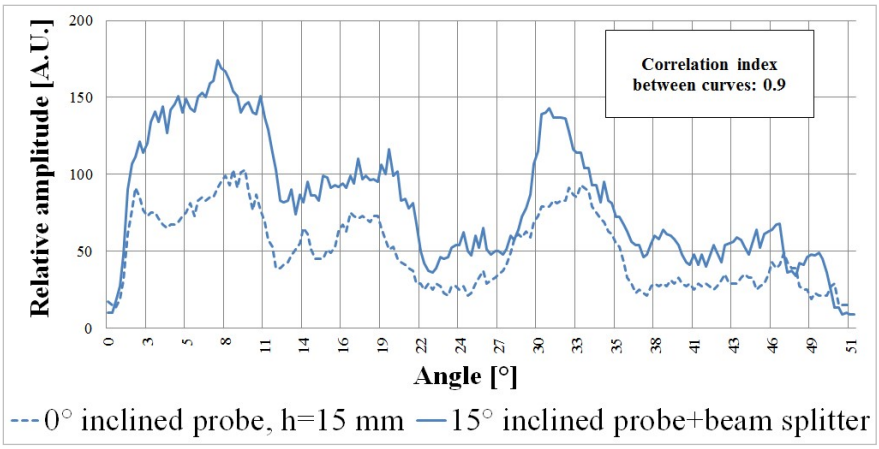

Figure 92 Comparison between the amplitude response of the internal gap acquired by a 15° inclined probe (continuous line) and a 0° inclined probe (dashed line).

As performed for the internal gap, the amplitude response of chamfers has been compared with the response acquired by the same probe inclined at 15° with the same height, water path and temperature, before the machining of chamfers on the flange. As expected, considering the maximum amplitude within the same time window (gate 1), the amplitude response acquired is almost flat due the absence of chamfers (Figure 93). In order to verify the presence of a chamfer or not, an amplitude threshold can be considered. In particular, if the amplitude of the ultrasonic response in gate 1 is above 100, a chamfer can be detected, otherwise not. Observing the amplitude responses of each chamfer, the chamfer which provides the best compromise to do not affect the copper too much and ensure a robust chamfer detection pattern, is the chamfer C3, 6 mm wide and with an angular extension of 3°.

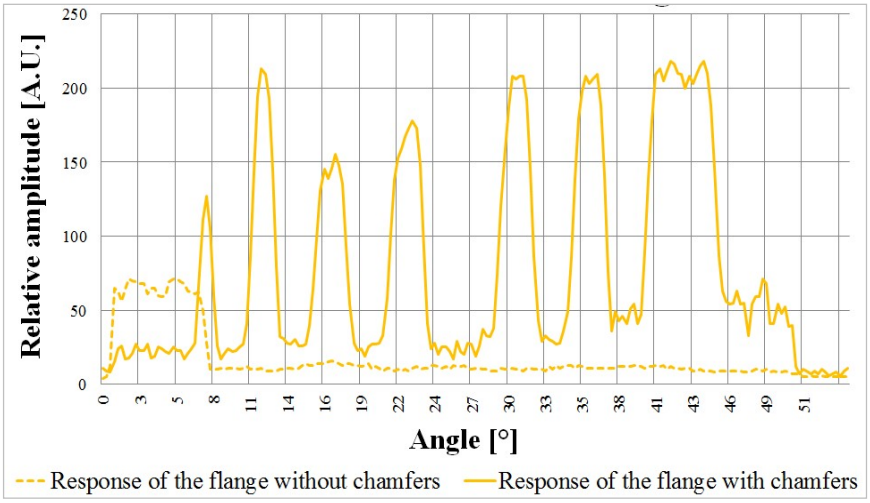

Figure 93 Comparison between the amplitude response within gate 1 acquired by a 15° inclined probe before and after the realization of chamfers on the flange. The dashed line represents the response before chamfer machining and the continuous line of response after chamfer machining.

The testing of the ultrasonic acquisition device points out the possibility to acquire both the identification and the authentication fingerprints simultaneously. Moreover, the angular matching between the two curves can be obtained by simply connecting the intersections points between them. The third fingerprint is obtained by the merging of the other two as illustrated in Figure 94.

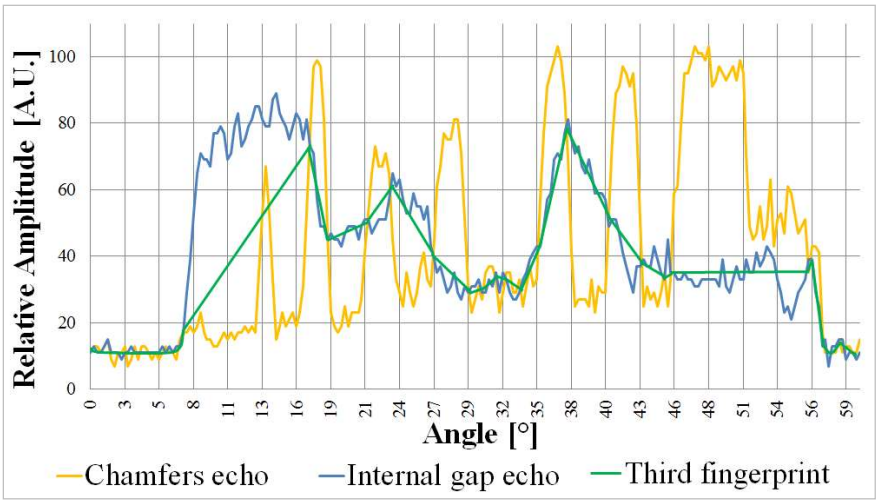

Figure 94 Angular matching between the identification code (yellow signal) and the authentication fingerprint of the internal gap (blue signal). A third unique fingerprint (green curve) can be realized by simply combining the two signals.

Following the test of the new device on a copper flange with chamfers, the potential integration of the Seal Fingerprint Acquisition Device (SFAD) within the ultrasonic acquisition system is discussed. This device could optimize some features of the existing system for a potential implementation in the field.

7.4 Introduction of the Seal Fingerprint Acquisition Device (SFAD)

The Seal Fingerprint Acquisition Device (SFAD) is an innovative customized system able to quickly perform ultrasonic testing and send acquired fingerprints to a remote-control unit. The device, requested by the Joint Research Centre, has been developed by the University of Florence, with the aim of upgrading a currently used reading system for the ultrasonic acquisition of fingerprints from stainless steel seals. However, the device architecture allows a flexible use for different type of acquisition that require different ultrasonic probes, different motors (stepper, synchronous AC), different data storage (wireless transmission, local memory card) and software user interface. This flexibility is obtained by programming the firmware of the two microcontrollers and the touch screen processor. The portability of the device is

obtained by arranging the various system components in a custom plastic case realized with a 3D printer (PLA) with a maximum side dimension of 180 mm and a weight of 2.3 kg, including the rechargeable LiFePO battery (Figure 95). Moreover, the device can be wirelessly connected to a PC where it is possible to set the main parameters of the ultrasonic inspection, control the start and stop of the motor and process received data. On the local display it is possible to monitor the progression of the ultrasonic test and system failure messages.

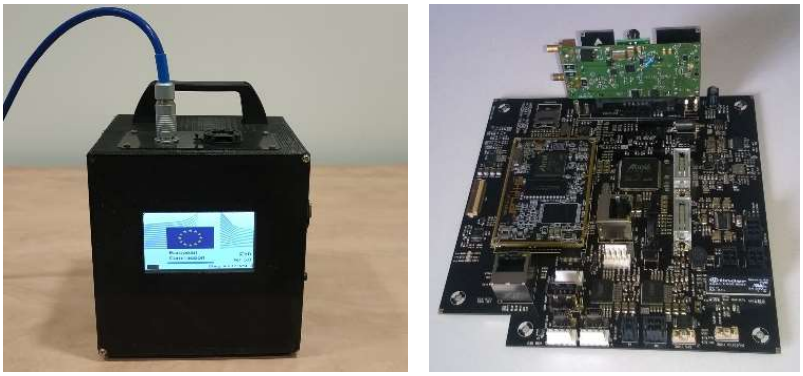

Figure 95 Pictures of an assembled SFAD with 180 mm of side length (on the left) and the designed electronic control board (on the right). IP64 external connectors and touch screen can be used for on-site testing (for example in a geological repository).

The architecture of the SFAD includes different blocks (Figure 96). The core of the device is represented by two ATMEL processors (the ATSAMA5D44A for the software and the ATSAM4E16E for the firmware) for the control of an asynchronous or a synchronous AC motor, the management of the power consumption, the transmission of signals via wireless connection and the storage of data in an external SD card. The power source is represented by a $LiFePO_4$ battery pack (12V, 3.5Ah) which guarantees a minimum operating time of five hours. The ultrasonic testing is regulated by the US-SPI module (Lecoeur Electronique) which presents a SPI high speed connection for the transmission/reception of data.

Therefore, in contrast to the US-KEY, the US-SPI allows the acquisition of a larger amount of data in a reduced time.

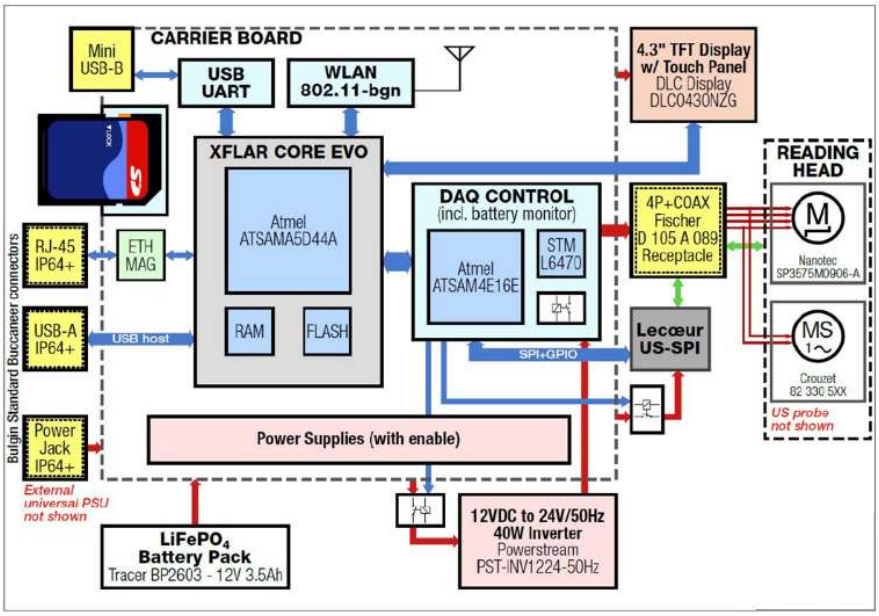

Figure 96 Architecture of the SFAD ultrasonic portable reader.

For sake of simplicity, some tests have been performed on stainless steel seals to verify the replication of the fingerprints acquired with SFAD. An example of ultrasonic response acquired by the currently used JRC reading system (in red) and by the new SFAD (in blue) is reported in (Figure 97).

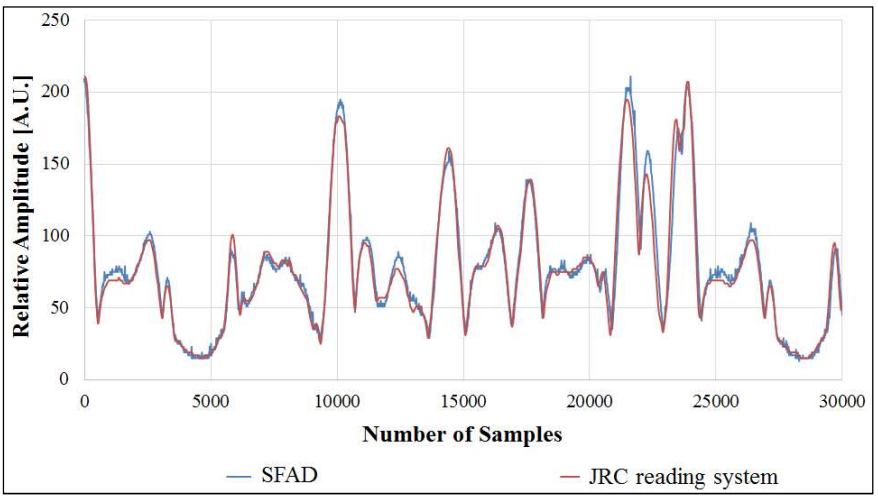

Figure 97 Comparison between the acquisition of a seal fingerprint by the current JRC reading system (in red) and the new SFAD (in blue).

The Pearson's correlation index between the two fingerprints is 0.9 and then it has been demonstrated that the SFAD can replicate the same performances of the JRC reading system even providing new functionalities [52].

The adoption of the SFAD within the ultrasonic acquisition system for copper canisters will introduce new functionalities that satisfy the needs required for the implementation of the device on the field (reported in paragraph 2.2.1). In particular, the presence of inspectors could be avoided and the ultrasonic acquisition could be completely controlled remotely. Thanks to the transmission of data through a SPI bus, the acquisition time could be reduced up to four times, executing a complete round in only 1 minute instead of 4. In addition, the use of the SFAD could contribute to providing a portable solution which is more suitable in the case of inspections in the geological repository.

Chapter 8

Conclusions

This chapter summarizes the main contributions of the thesis, discussing the novelties introduced by the ultrasonic method for the identification and the authentication of copper canisters. Finally, some recommendations for future research on the topic are suggested.

8.1 Summary of Contributions

At the present time, according to the nuclear safeguards' authorities, there are no methods to keep the traceability (Continuity of Knowledge) of spent nuclear fuel during transport and disposal of copper canisters in the Swedish geological repository. In this thesis, an innovative ultrasonic method for the identification and authentication of copper canisters is illustrated. The validation of the method and the development of an innovative ultrasonic acquisition system are presented. The proposed solution, based on a single probe and a beam splitter, results to be an efficient system for the simultaneous acquisition of the identification and authentication fingerprints. In summary, the principal contributions of this thesis are:

a) The implementation of a literature research to analyse to what extent traditional tagging technologies for nuclear items could be used for the identification and authentication of copper canisters.
b) The definition of a new method based on the ultrasonic acquisition of two fingerprints: the ultrasonic amplitude response of a series of chamfers machined on the copper lid (identification fingerprint) and the amplitude response of the internal gap between lid and tube after welding (authentication fingerprint). By the angular matching of the two amplitude responses, a third more robust fingerprint is also obtained.
c) The design of an innovative ultrasonic system for the identification and authentication of copper canisters considering the requirements imposed by the nuclear safeguards' authorities.
d) The development and testing of an innovative ultrasonic acquisition system prototype based on a 10 MHz single probe and a beam splitter for the simultaneously acquisition of the identification and authentication fingerprints.

Regarding my contributions in the research project, I dealt with the optimization of the ultrasonic method by introducing the angular matching between the identification and the authentication fingerprint. I also designed the ultrasonic system prototypes for the acquisition of fingerprints and my colleagues from the mechanical workshop helped me for the practical realization of the devices. Then I tested all the prototypes performing ultrasonic tests in laboratory with the aim to define the best parameters for the acquisition of ultrasonic echoes from copper samples. For this purpose, I also upgraded the software on board of the control box in order to include a GUI interface for the setting of measurements parameters, the processing of data and the displaying of fingerprints.

8.2 Direction of Future Work

The ultrasonic method for the identification and authentication of copper canisters has been validated in laboratory but further researches should be implemented to improve the study.

Concerning the identification fingerprint, ultrasonic inspections should be performed on a full-scale welded lid with chamfers to test an algorithm for the decoding of the chamfers' code. In addition, structural studies should be performed to calculate to what extent the presence of chamfers on the lid could impact its stability in the long-term.

Regarding the authentication fingerprint, the uniqueness of the amplitude response of the internal gap has not yet been demonstrated since enough samples were not available to investigate. Therefore, a statistical analysis on several welded copper lids should be implemented to verify the uniqueness of authentication fingerprints. In case of positive results, the identification fingerprint realized by chamfers could be potentially ignored.

Furthermore, additional ultrasonic tests for the acquisition of both the identification and the authentication fingerprints should be performed to verify the stability of fingerprints in a time frame of 45 years, that is the expected period for the deposition of canisters in the geological repository.

Bibliography

[1] IAEA, “International safeguards in the design of nuclear reactors”, Vienna (Austria), IAEA Energy Series, Tech. Rep. No. NP-T-2.9, 2014.

[2] L. Hildingsson, C. Andersson, R. Fagerholm, “Safeguards aspects Regarding a Geological Repository in Sweden,” presented at the IAEA Symposium on International Safeguards: Linking Strategy, Implementation and People, paper CN-220-166, Vienna (Austria), 20-24 Oct. 2014.

[3] C. Clementi, F. Littmann, L. Capineri, “Comparison of Tagging Technologies for Safeguards of Copper Canisters for Nuclear Spent Fuel,” Sensors 2018 18(4) 929, Mar. 2018. Online. Available: https://doi.org/10.3390/s18040929.

[4] Storage and Disposal of Radioactive Waste, accessed on Oct. 11, 2019. Online. Available: http://www.world-nuclear.org/information-library/nuclear-fuel-cycle/nuclear-wastes/storage-and-disposal-of-radioactive-wastes.aspx.

[5] L. Cederqvist, M. Johansson, N. Leskinen, U. Ronneteg, “Design, production and initial state of the canister,” Swedish Nuclear Fuel and Waste Co., Stockholm, Sweden, Tech. Rep. TR-10-14, Dec. 2010. Online. Available: https://www.stralsakerhetsmyndigheten.se/contentassets/88649a119efd4011b85372a616afae73/canister-production-report.pdf.

[6] J.M. Benz, J.E. Tanner, H.A. Smartt, M.R. MacDougall, “Maintaining Continuity of Knowledge (CoK) of Spent Fuel Pools: Tool Survey”, Pacific Northwest National Laboratory, Richland, WA, USA, 2016. Online. Available: https://www.pnnl.gov/main/publications/external/technical_reports/PNNL-25663.pdf.

[7] R.S. Bean, D.S. Blair, C.A. Pickett, “Attaining and maintaining a continuity of knowledge to draw safeguards conclusions with confidence,” ESARDA Bulletin No. 51, pp. 51-57, 2014.

[8] D. H. Hanks, “Managing Safety, Security, and Safeguards (3S) Relationship: A National Regulatory Authority Perspective United States Nuclear Regulatory Commission”, U.S. Nuclear Regulatory Commission Office of Nuclear Material Safety and Safeguards, 54th Annual Meeting, 20-24 July 2013, Atlanta, Georgia, USA.

[9] R. Mongiello, R. Finch, G. Baldwin, “Safeguards Approaches for Geological Repositories: Status and Gap Analysis”, Sandia National Laboratory (SNL), Tech. Rep., June 2013.

[10] D. Chernikova, “A New Approach to Environmentally Safe Unique Identification of Long-Term Stored Copper Canisters presented at the IAEA International Safeguards Symposium: Linking Strategy, Implementation and People, Vienna (Austria), 20–24 Oct. 2014.

[11] IAEA, “Model Integrated Safeguards Approach for a Geological Repository”, 03-SG-PR-1306, Department of Safeguard, Vienna (Austria), 2011.

[12] IAEA, “Sealing of Underground Repositories for Radioactive Wastes”, Tech. Rep. N.. 319, 1990.

[13] IAEA, “IAEA Safeguards Techniques and Equipment”, International Nuclear Verification Series No.1 (Rev. 2) Section 4, Vienna (Austria), 2011. Available online: http://www-pub.iaea.org/MTCD/Publications/PDF/nvs1_web.pdf (accessed on 05/01/2018).

[14] P. Jansson, “Technologies Potentially Useful for Safeguarding Geological Repositories”, ASTOR Group Report, May 2017.

[15] Y. Lahogue, F. Littmann, S. Synetos, J. Lupo, V. Piron, and M. Sironi, “Developments in the deployment of ultrasonic bolt seals at the storage ponds of a large reprocessing plant”, in Proc. Symp. Int. Safe-guards, Linking Strategy, Implement. People, Vienna (Austria), Oct. 2014, p. 120.

[16] M. Chiaramello, M. Sironi, F. Littmann, P. Schwalbach, and V. Kravtchenko, “JRC Candu sealing systems for Cernavoda (Romania) and upcoming developments”, ESARDA Bulletin, No. 44, pp. 29-39, June 2010.

[17] “Electronic Optical Sealing System (EOSS)”, Datasheet, Camberra Mirion Technologies. Online. Available: http://www.canberra.com/products/safeguards_surveillance_seals/pdf/EOSS-SS-32701.pdf.

[18] B.D. Schoeneman, “The development and application of the remotely monitored seal array (RMSA)”, in Proc. Symp. Int. Safeguards, Vienna (Austria), Nov. 2010.

[19] IAEA, “Development and Implementation Support Programme for Nuclear Verification 2016–2017”, Tech. Rep. STR-382 Vienna (Austria), Febr. 2016.

Online. Available: https://www.iaea.org/sites/default/files/16/05/development_and_implementation_support_programme_for_nuclear_verificatio.pdf.

[20] K. Chen, H. Tsai, Y.Y. Liu, “Development of the RFID system for nuclear materials management”, Annual Meeting of the Institute of Nuclear Materials Management (INMM), Nashville, TN (United States), 13-17 July 2008.

[21] M. C. O'Connor, “U.S. Department of Energy Employs RFID to Safeguard the Country”, RFID Journal, Apr. 20, 2009. Online. Available:https://www.rfidjournal.com/purchase-access?type=Article&id=4786&r=%2Farticles%2Fview%3F4786#back-from-modal.

[22] L.O. Brown, S.K. Doorn, P.B. Merkle, “SERS-Active Nanoparticles as a Barcoding Technology for Tags and Seals”, in Proc. of the 50th INMM Meeting, Tucson, (USA), July 2009.

[23] K.M. Tolk, “Reflective Particle Technology for Identification of Critical Components”, in Proc. of the 33rd Annual Meeting on Institute of Nuclear Materials Management, Orlando, FL, USA, July 1992.

[24] B.J. Hill, E. M. Dressel, R.I. McCann, R.E. Cabeen, A. Wright, “Tagging RDT and E Volume 1 - Technology Assessments and Development Reports”, Albuquerque International, Albuquerque, NM, USA, 1994.

[25] M. Laughter, “Safeguard Application Options for the Laser-Based Item Monitoring System (LBIMS)”, Oak Ridge National Laboratory, Oak Ridge, TN, USA, 2008.

[26] D. Chernikova, K. Axell, A. Nordlund, H. Wirdelius, “Novel passive and active tungsten-based identifiers for maintaining the continuity of knowledge of spent nuclear fuel copper canisters”, Ann. Nucl. Energy 2015, 75, 219–227.

[27] D. Chernikova, K. Axell, “A unique radioisotopic label as a new concept for safeguarding and tagging of long-term stored items and waste”, arXiv 2013, arXiv:1312.1985v2.

[28] C. Clementi, L. Capineri, F. Littmann, “Innovative Method to Authenticate Copper Canisters Used for Spent Nuclear Fuel Based on the Ultrasonic Investigation of the Friction Stir Weld,” IEEE Access 2017, 5. doi:10.1109/ACCESS.2017.2694878.

[29] L. Cederqvist, M. Johansson, N. Leskinen, U. Ronneteg, “Design, production and initial state of the canister,” Swedish Nuclear Fuel and Waste Co., Stockholm, Sweden, Tech. Rep. TR-10-14, Dec. 2010.

[30] C.G. Andersson, “Development of fabrication technology for copper canisters with cast inserts” SKB Tech. Rep. TR-02-07, Sweden, Apr. 2002.

[31] W.M. Thomas, K.I. Johnson, C.S. Wiesner, “Friction Stir Welding – Recent Developments in Tool and Process Technologies”, Advanced Engineering Materials 2003, 5, No.7, pp.485-490.

[32] K. Savolainen, “Friction Stir Weldability of Copper Alloys”, M.Sc. Thesis., Helsinki University of Technology, Laboratory of Engineering Materials., 2004, 115 p + 3 Appendices.

[33] J. Krautkrämer, H. Krautkrämer, “Ultrasonic Testing of Materials”, Springer-Verlag, 4th fully revised Edition, 1990.

[34] U. Ronneteg, “Friction stir welding of copper and its NDT - From novelty to highly-developed,” 12th European Conference on Non-Destructive Testing, Gothenburg, 11-15 June 2018.

[35] T. Purhonen, “State of the Art of the Welding Method for Sealing Spent Nuclear Fuel Canister Made of Copper, Part 1 – FSW”, Working Report 2014-22, Posiva Oy, May 2014.

[36] A. Forsström, S. Bossuyt, Y. Yagodzinskyy, K. Tsuzaki, H. Hänninen, “Strain localization in copper canister FSW welds for spent nuclear fuel disposal”, Journal of Nuclear Materials, 523, pp. 347-359, doi: 10.1016/j.jnucmat.2019.06.024.

[37] T. Stepinski, M. Engholm, T. Olofsson, “Inspection of copper canisters for spent nuclear fuel by means of ultrasound Copper characterization, FSW monitoring with acoustic emission and ultrasonic imaging,” Swedish Nuclear Fuel and Waste Co., Stockholm, Tech. Rep. TR-09-28, Aug. 2009.

[38] C. Clementi, F. Littmann, L. Capineri, C. Andersson, U. Ronneteg, “Ultrasonic Identification Methods of Copper Canisters for Final Geological Repository”, ESARDA bulletin No. 54, pp. 75-80, June 2017.

[39] C. Clementi, M. Calzolai, L. Capineri, F. Littmann, “Ultrasonic Identification of Copper Canisters to be used for long term geological repository,” IEEE International Ultrasonic Symposium, Tours, France, 18-21 Sept. 2016. Online. Available: https://ieeexplore.ieee.org/document/7728561.

[40] C. Clementi, F. Littman, L. Capineri, “Ultrasonic identification and authentication of copper canisters”, Tech. Rep. JRC114202, European Commission, Ispra (Italy), 2018.

[41] Lecoeur Electronique, “US-Key-New generation of High performances Ultrasonic device”, Datasheet, Chuelles (France), June 2010. Online. Available: http://www.lecoeur-electronique.net/wa_files/us-key_r4_0.pdf.

[42] G. Holmer, W. Daniels, T. Zettervall, “Evaluation of the simulation software CIVA for qualification purpose,” Swedish Radiation Safety Authority, Stockholm, Sweden, Tech. Rep. 2017:29, 2017.

[43] IAEA, “Design of Fuel Handling and Storage Systems for Nuclear Power Plant’”, Safety Guide No. NS-G-1.4., Vienna, (Austria), August 2003.

[44] Engineering ToolBox, “Speed of Sound in Water”, 2004. Online. Available: https://www.engineeringtoolbox.com/sound-speed-water-d_598.html.

[45] R. P. Reed and R. P. Mikesell, “Low Temperature Mechanical Properties Of Copper and Selected Copper Alloys,” NBS Monograph 101, Institute for Materials Research, National Bureau of Standards, Boulder, Colorado 80302.

[46] F. Tesfaye Firdu, P. Taskinen, “Densities of Molten and Solid Alloys of (Fe, Cu, Ni, Co) - S at Elevated Temperatures - Literature Review and Analysis”, Aalto University, Publications in Materials Science and Engineering, Aalto, Espoo 2010.

[47] C. Clementi, F. Littmann, L. Capineri, “Ultrasonic Investigation of the Welding Area of Copper Canisters for Spent Nuclear Fuel”, ESARDA bulletin No. 56, pp. 19-27, June 2018.

[48] C. Clementi, L. Capineri, F. Littmann, “Ultrasonic method to keep the Continuity of Knowledge of spent nuclear fuel from the Encapsulation Plant to the Geological Repository”, IAEA International Conference on the Management of Spent Fuel from Nuclear Power Reactors, 24-28 June 2019, Vienna, Austria.

[49] C. Clementi, F. Littmann, L. Capineri, “Development of an Innovative Ultrasonic Reader for the Authentication and Identification of Copper Canisters for Spent Nuclear Fuel”, 2019 IEEE International Ultrasonics Symposium, 6-9 October 2019, Glasgow, Scotland (UK).

[50] F. Littmann, C. Clementi, L. Capineri, “Ultrasonic Identification & Authentication of Copper Canisters”, INMM 59th Annual Meeting, 16-20 July 2017, Indian Wells, California USA.

[51] C. Clementi, L. Capineri, F. Littmann, “An Authentication and Identification System of Copper Containers for Spent Nuclear Fuel by means of an Ultrasonic Probe with a Beam Splitter”, 2017 IEEE International Ultrasonics Symposium, 6-9 September 2017, Washington, D.C., USA.

[52] L. Capineri, “Seal fingerprint acquisition device,” Final Tec. Rep. Task 1, Contract JRC/IPR/2015/E.8/0051/NC, Feb. 2016 (unpublished).

Appendix A

The correlation algorithm

```
//Correlation function based on Pearson’s correlation formula

        private   double   Correlate(List<Double>   data1,   List<Double>
reference, out int shiftValue)
        {
            shiftValue = 0;

            if ((data1 == null) || (reference == null))
            {
                return -5;
            }

double SumXY, SumX2, SumX, X, Y, SumY, SumY2, CxCorr;
            double Result = -3; // -3 is an invalid value
            int ShiftMax = 0;
            int i, j;

            List<Double> data2 = reference.ToList();
            // the 2 curve should have the same dimension
            if (data1.Count != data2.Count)
            {
                Debug.WriteLine("ERROR: The two data set do not have the
same length");
                return -3;
            }

            int DimMes = data1.Count; //For loop length

            X = 0;
            Y = 0;
            CxCorr = -2; //-2 is an invalid value for CxCorr

// move one curve (data2) over data1 to obtain the best correlation
            for (j = 0; j < DimMes; j++)
            {
                SumX = 0;
                SumX2 = 0;
                SumY = 0;
                SumY2 = 0;
                SumXY = 0;
```

```
                // Compute Pearson correlation parameters
                for (i = 0; i < (DimMes - 1); i++)
                {
                    X = (double) data1[i];
                    Y = (double) data2[i];

                    SumX = SumX + X;
                    SumY = SumY + Y;
                    SumX2 = SumX2 + (X*X);
                    SumY2 = SumY2 + (Y*Y);
                    SumXY = SumXY + (X*Y);
                }

                if ((SumX2 != (SumX*SumX)/DimMes) &&
                    (SumY2 != (SumY*SumY)/DimMes))
                {
                    // Compute correlation
                    Result = (SumXY - ((SumX*SumY)/DimMes))/
                             Math.Sqrt((SumX2                          -
((SumX*SumX)/DimMes))*(SumY2 - ((SumY*SumY)/DimMes)));
                }
                else
                {
                    Result = -2;
                }


                // update correlation and shift
                if (Result <= 1 && Result > CxCorr)
                {
                    CxCorr = Result;
                    ShiftMax = j;
                }

                // shift first sample to the end of data2
                double tmp = data2[0];
                data2.RemoveAt(0);
                data2.Add(tmp);
            }

            shiftValue = ShiftMax;
            return CxCorr; //in out the correlation index CxCorr
        }
```

Appendix B

Study of phase changes in canister welds

The experimental tests described in paragraph 6.3 have been carried out using a broadband pulse excitation for the probe. Usually, this type of measurements ensures a good signal-to-noise ratio but the resolution is quite limited. Therefore, additional studies are carried out using a narrow band excitation for the ultrasonic transducer. Depending on the presence of the gap and its shape, the phase of the received ultrasonic echo could change around the circumference of the lid (Figure A-1). The aim of the study reported in this appendix is verifying if the variation of the ultrasonic echoes' phase could represent an authentication fingerprint for copper canisters; the phase, in fact, is less sensitive to environmental changes such as temperature variations. Moreover, a narrowband excitation of the probe is more sensitive to small changes of the internal gap. However, depending on the inspection frequency and the velocity of sound in the material, the phase can vary in a different way and the attenuation of the ultrasonic beam could be not negligible.

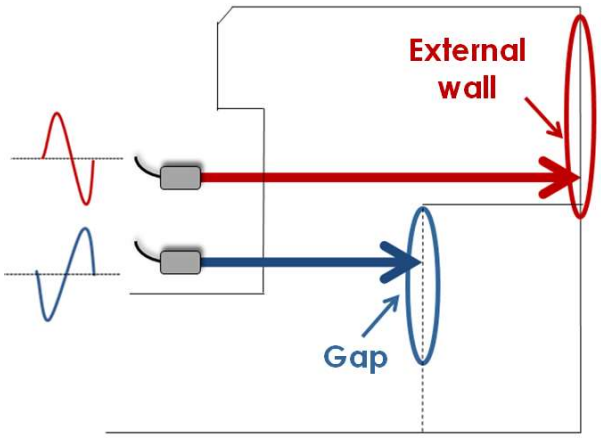

Figure A-1 Investigation of phase changes across the welding area of copper canisters: depending on the interface encountered, the phase could be different in relation with the transmitted signal.

Considering the excitation of the ultrasonic transducer with a sinusoidal burst, the change of phase between the transmitted and the received voltage signals could be evaluated in different ways using the oscilloscope. An option (Figure A- 2) is displaying the two signals as function of time. The phase difference ψ between two channels' phases, θ_1 and θ_2, can be measured following equation (A-1):

$$|\psi| = |\theta_2 - \theta_1| = 360° \left(\frac{t_d}{T}\right) \quad \text{(A-1)}$$

where t_d is the smallest time difference between occurrences of the feature on the two waveforms and T is the period between repeats, related to the frequency of inspection.

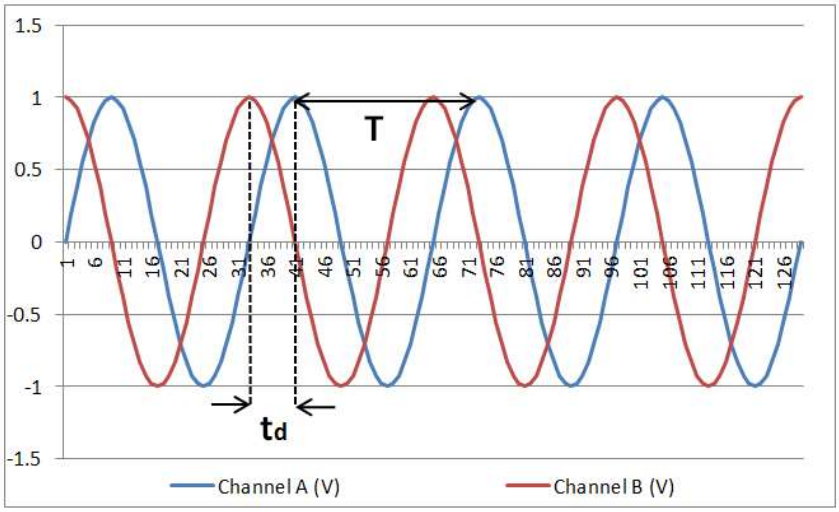

Figure A- 2 Evaluation of phase difference between two signals A (in blue) and B (in red) plotted as function of time. t_d is the smallest time difference between occurrences of the feature on the two waveforms and T is the period between repeats.

The sign of ψ can be determined depending on which signal is leading to the left of the other. For example, in the picture channel B leads to channel A and then ψ is positive. This approach can also be used to calculate phase differences in non-sinusoidal waveforms. Another method is setting the oscilloscope in the XY mode in order to display the voltage of one channel vertically and the other channel horizontally, realizing a Lissajous figure. In this case, the phase difference ψ can be then calculated as in equation (A-2):

$$|\psi| = \arcsin\left(\frac{B}{A}\right) \tag{A-2}$$

where A and B are illustrated in the following picture (Figure A- 3). If the top of the ellipse is in Quadrant II, to calculate the module of ψ it must subtract 180º to the value obtained with the previous formula. The sign of ψ cannot be calculated with this method because in case of opposite sign, the ellipse will look exactly the same. The use of Lissajous figures for the evaluation of the phase difference between two signals is very easy and does not imply measuring time scales. However, it can be used only with sinusoidal waveforms.

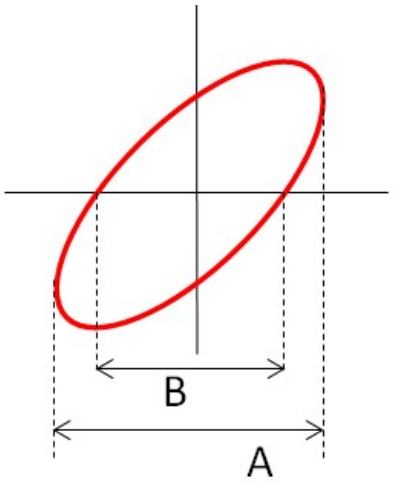

Figure A- 3 Lissajous figure for the evaluation of phase difference between two waveforms.

In case of investigation of copper canisters, it is possible to evaluate the phase difference between the transmitted burst and that one received in correspondence of the internal gap and the external wall interfaces, considering two different time windows. The change of phase difference along with the circumference of the lid could be used as a fingerprint to authenticate each canister. Depending on the inspection frequency, the value of ψ could be more or less affected by the geometrical arrangement of the transducer during acquisitions. For example, exciting the probe with a sine burst at 10 MHz of frequency, the phase complete one cycle of 360º for each wavelength that is about 466 µm in copper. Since the internal gap size could vary from 300 µm to 600 µm, the evaluation of the same value of ψ between different acquisitions could be complicated. In fact, little variations in the probe positioning could give a really different value of ψ. Therefore, lower is the inspection frequency, wider is the wavelength and then more constant will be the value of ψ calculated in repeated tests.

The detection of phase changes in the welding area of canisters is realized following the set-up of measurements illustrated in Figure A- 4.

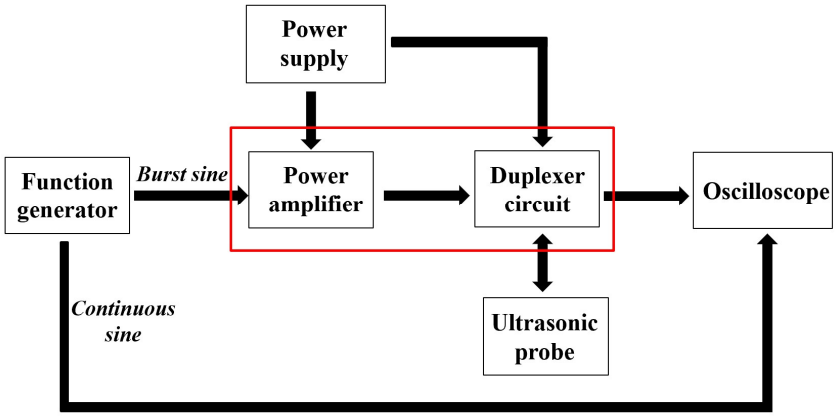

Figure A- 4 Block diagram of the set-up of measurement for the detection of phase changes.

The function generator is used for the transmission of two signals: the first is a sine burst with a frequency and a number of cycles selected according to the probe features and the distance between the probe and the discontinuity to be detected; the second is a continuous sine with the same frequency and phase of the first, used as a reference for phase comparisons. Because of a limited dynamic of the function generator available in our laboratory, a power amplifier is placed upstream the duplexer circuit to ensure a suitable excitation for the ultrasonic probe. The duplexer circuit is then used to transmit/receive a signal to/from the ultrasonic transducer. The received signal is 26 dB amplified and then displayed on the oscilloscope.

Regarding the probe adopted for the phase inspection, preliminary tests with a narrow band excitation of the Olympus V311 immersion transducer revealed that this probe behaves as a high-pass filter, attenuating the burst at the steady-state in reception. This is due to the wide bandwidth of the probe. Therefore, the Olympus V309 immersion transducer is also used for the investigation of the phase. The main features of this transducer are:

- central frequency: 5 MHz;
- element diameter: 0.5'' (13 mm);
- unfocused.

The sequence of tests performed on a copper flange is illustrated in Figure A- 5. The probe is kept at height 15 mm, 25 mm and 35 mm with a water path of 20 mm. First investigations are performed using the V309 transducer excited with a sine burst

characterized by 10 Vpp, 5 MHz of frequency, 10 ms of repetition period and burst duration of 2 μs.

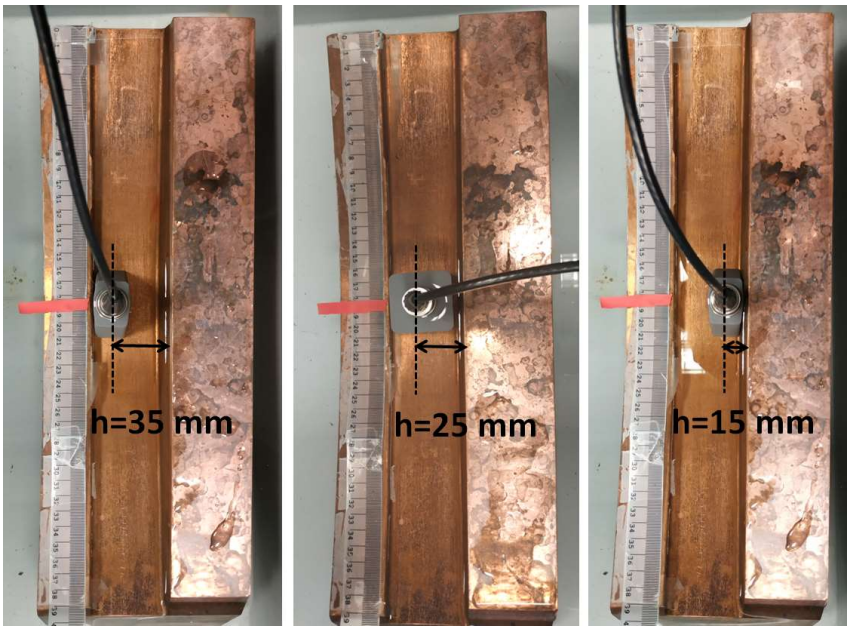

Figure A- 5 Ultrasonic testing on a copper flange with the probe fixed at heights 15, 25 and 35 mm (from right to left).

The signal acquired at height 15 mm is shown in Figure A- 6. The burst echo of the interface water/copper is detectable at 26.4 μs while the internal gap echo is detectable at 48.4 μs with amplitude of about 1.6 mVpp. The phase difference between the burst echo of the internal gap and the reference is calculated using the time-domain mode and Lissajous figures. In both cases, the value of $|\psi|$ is about 138º. However, slightly rotating the probe or the connection cable, the time shift between the two curves changes, affecting also the phase difference $|\psi|$. The ultrasonic tests carried out at heights 25 mm and 35 mm confirmed the difficulties in the calculation of the phase shift which resulted to be inaccurate and not precise.

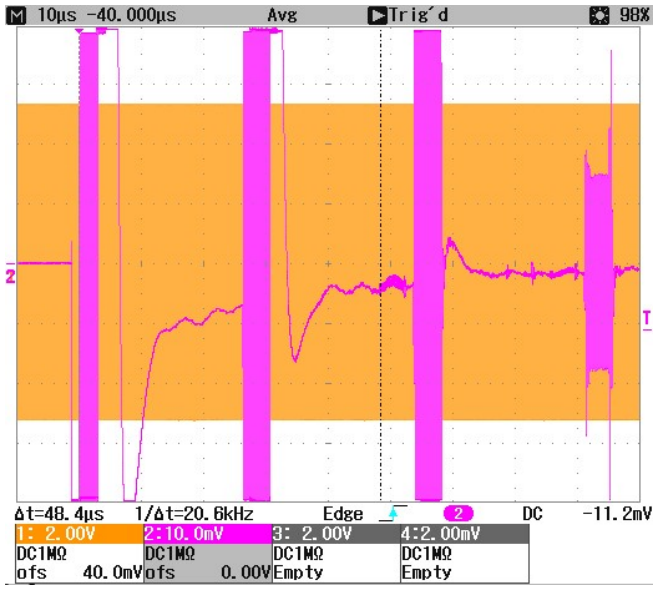

Figure A- 6 In orange (channel 1) the reference (phased with the transmitted burst at 5 MHz) and in pink (channel 2) the signal received by the ultrasonic probe located at height 15mm. The burst echo of the internal gap is detectable at 48.4 µs.

The same investigations are replicated using the V311 immersion transducer but, as expected, the burst echoes reflected by the internal gap or the external wall were such attenuated that further calculations on phase differences were not feasible.

The ultrasonic investigation of the welding area on copper flanges with 10 MHz and 5 MHz immersion probes revealed that the evaluation of phase differences between transmitted and received signals for the definition of an authentication fingerprint is not feasible. In fact, on the one hand, the attenuation of ultrasounds in copper materials affects the integrity of the burst echo; on the other hand, slightly movements of the transducer have an impact on the repeatability of measurements.

In conclusion, the narrowband excitation of the transducer has been implemented to verify if phase changes in the welding area of copper canisters could be better used as authentication fingerprints to be included in the ultrasonic method. However, results of preliminary tests performed on a copper flange with different transducers (Olympus V309 and V311), put in evidence that received burst echoes are strongly attenuated. In addition, the evaluation of the phase shift $|\psi|$ is extremely sensitive to the probe

positioning and then it is difficult to have repeatable measurements. For these reasons, the study of phase changes in the welding has been abandoned.